isvr Institute of Sound and Vibration Research

Evaluating the Dynamic Performance of Seats without Using Human Subjects

L. Wei, C.H. Lewis and M.J. Griffin

ISVR Technical Report No 286

April 2000

University of Southampton

SCIENTIFIC PUBLICATIONS BY THE ISVR

Technical Reports are published to promote timely dissemination of research results by ISVR personnel. This medium permits more detailed presentation than is usually acceptable for scientific journals. Responsibility for both the content and any opinions expressed rests entirely with the author(s).

Technical Memoranda are produced to enable the early or preliminary release of information by ISVR personnel where such release is deemed to the appropriate. Information contained in these memoranda may be incomplete, or form part of a continuing programme; this should be borne in mind when using or quoting from these documents.

Contract Reports are produced to record the results of scientific work carried out for sponsors, under contract. The ISVR treats these reports as confidential to sponsors and does not make them available for general circulation. Individual sponsors may, however, authorize subsequent release of the material.

UNIVERSITY OF SOUTHAMPTON

INSTITUTE OF SOUND AND VIBRATION RESEARCH

HUMAN SCIENCES GROUP

Evaluating the dynamic performance of seats without using human subjects

by

L. Wei, C.H. Lewis and M.J. Griffin

ISVR Technical Report No. 286

April 2000

Authorised for issue by
Professor MJ Griffin
Group Chairman

Contents

ABSTRACT 1

1 INTRODUCTION 3

2 PREDICTING SEAT TRANSMISSIBILITY FROM THE IMPEDANCE OF A SEAT AND THE HUMAN BODY APPARENT MASS 5

2.1 Introduction 5

2.2 Mathematical model for the apparent mass of the seated human body exposed to vertical vibration (Wei and Griffin 1998a) 5

2.2.1 Previous experiment results 5

2.2.2 Seated person mathematical models 6

2.2.3 Discussion 7

2.2.4 Conclusions 7

2.3 Predicting laboratory measured seat transmissibility from measures of seat and foam impedance (Wei and Griffin 1998b) 8

2.3.1 Experiments 8

2.3.2 Seat model 9

2.3.3 Discussion 10

2.3.4 Conclusions 10

2.4 The influence of contact area, vibration magnitude and static force on the dynamic stiffness of polyurethane seat foam (Wei and Griffin 1997) 10

2.4.1 Experimental conditions 10

2.4.2 Discussion 11

2.4.3 Conclusions 12

2.5 The influence of seat cushion inclination on subject apparent mass and seat transmissibility (Wei and Griffin 1998c) 13

2.5.1 Hypotheses 13

2.5.2 Experiment conditions 13

2.5.3 Results and Discussion 13

2.5.4 Conclusions 13

2.6 Seated human-body mathematical model with different vertical vibration magnitudes (Wei and Griffin 2000) 14

2.6.1 Hypothesis 14

2.6.2 Experimental conditions 14

2.6.3 Discussion and conclusions 14

2.7 Human body dynamic properties on a hard and a soft seat with vertical vibration 15

2.7.1 Hypothesis 15

2.7.2 Experiment conditions 16

2.7.3 Subject model on hard seat and soft seat 16

2.7.4 Model fitting results 17

2.7.5 Comparison of prediction results 18

2.7.6 Discussion 18

2.7.7 Conclusions 19
2.8 Modelling the effect of backrest angle on the vertical apparent masses of seated subjects (Wei and Griffin 1999) 21
2.8.1 Hypothesis 21
2.8.2 Experimental conditions 21
2.8.3 Discussion and conclusion 21
2.9 Predicting seat transmissibility measured in vehicles 22
2.9.1 Experimental measurements 22
2.9.2 Prediction results 23
2.9.3 Sensitivity of seat-person model parameters 26
2.9.4 Revised seat-person model and its function 29
2.10 Conclusions 31
3 MEASURING SEAT TRANSMISSIBILITY USING MECHANICAL ANALOGUES OF SEATED HUMANS 34
3.1 Introduction 34
3.1.1 Performance requirements 35
3.2 Development of a Passive Anthropodynamic Dummy 36
3.2.1 Required complexity 36
3.2.2 Contribution of the damper to apparent mass response 37
3.2.3 Predicting the response of a single degree-of-freedom dummy 44
3.3 Car seat tests using prototype dummy and subjects 47
3.3.1 Road tests using prototype dummy and subjects 47
3.3.2 Laboratory seat tests using prototype dummy and subjects 49
3.3.3 Development of an improved prototype dummy 54
3.4 Development of an active anthropodynamic dummy 55
3.4.1 Advantages of active control 55
3.4.2 Description of a prototype active dummy 55
3.4.3 Predicting the apparent mass of the active dummy 56
3.4.4 Dynamic response of first prototype using VP4 actuator 57
3.4.5 Requirements for actuator performance 58
3.4.6 Apparent mass measurements using M50 actuator 63
3.4.7 Alternative apparent mass characteristics 67
3.4.8 Development of a practical active dummy 69
3.5 Conclusions 69
4 ACKNOWLEDGEMENTS 71
5 REFERENCES 72
APPENDIX A. LABORATORY METHOD FOR PREDICTING SEAT TRANSMISSIBILITY 76

Abstract

The transmission of vertical vibration through a seat is dependent on the mechanical impedance of the human body supported on the seat: the seat and the body act as a coupled dynamic system. Current procedures for quantifying seat transmissibility and seat vibration isolation efficiency (e.g. SEAT values) therefore employ human subjects in vehicles or on laboratory simulators. The use of human subjects is costly and time-consuming and can involve a range of safety and ethical problems. The research described in this report was conducted to develop test procedures for evaluating the vibration isolation efficiency of seats without using human subjects.

Two alternative methods of determining seat performance without human subjects have been developed: (i) the mathematical prediction of seat transmissibility from the separately measured dynamic characteristics of seats and the human body, and (ii) the use of mechanical dummies having dynamic characteristics representing those of the human body.

The mathematical prediction method investigated the use of a single degree-of-freedom model and a two degree-of-freedom model of the human body. It was found that while both provided good predictions of measurements of seat transmissibility without a backrest, the two degree-of-freedom model had the advantage of predicting the second resonance often seen in measurements around 8 Hz. It was found that modifications to these models, to allow for variations in vibration magnitudes and backrest contact, could give improved predictions of seat transmissibility for practical situations. The encouraging results suggest that the method will be useful for the prediction of seat dynamic performance. The currently proposed method of prediction is defined in an appendix.

The applicability of a mechanical dummy has been investigated using two forms of mechanical dummy. One type of dummy employed passive elements to represent the mass, damping and stiffness of the human body. It is shown that mechanical dummies tend to suffer from non-linear responses that differ from the non-linear response of the human body and that careful testing of a dummy is required to ensure that the response is appropriate. A prototype single-degree-of-freedom dummy has been developed with an appropriate response at frequencies up to about 20Hz. Tests in the laboratory and in cars shows that this single-degree-of freedom dummy is sufficient to provide useful measures of seat transmissibility. However, optimisation of the interaction of such a dummy with the backrest of a seat requires further investigation.

The second type of mechanical dummy employed an active actuator to provide the damping and some of the stiffness of the dummy. It is shown that the apparent mass of an appropriate single degree-of–freedom system could be reproduced and controlled at frequencies up to 20 Hz. This active dummy has various potential advantages, including the adjustment of characteristics by computer control and minimisation of difficulties associated with the non-linearity of a passive dummy and the different non-linearity of the human body.

1 Introduction

The objective of the research described in this report is to establish seat test procedures for evaluating the vibration isolation efficiency of seats without using human subjects.

There are various empirical methods for quantifying the dynamic performance of a seat and its overall isolation efficiency, such as seat transmissibility and SEAT values. However, these methods mostly involve the measurement of a seat with subjects sitting in the seat, because the transmission of vibration through a seat is dependent on the mechanical impedance of the body supported on the seat: the seat and the body act as a coupled dynamic system. In cars, tests with subjects are time-consuming and give variable results according to the subjects used. Laboratory motion simulators can be used, but suitable simulators are expensive to operate and there are inherent risks to exposed persons giving rise to the need for a range of medical and ethical precautions. It would be desirable to predict the dynamic performance of a seat without exposing subjects to vibration.

The seat having the optimum dynamic properties is the seat that minimizes the unwanted vibration responses of the occupant in the relevant vibration environment. Three factors combine to determine the seat dynamic efficiency: the vibration environment, the seat dynamic response and the response of the human body. The optimum seat for one vehicle may not, therefore, be the optimum seat for another vehicle. The 'tuning' of a seat to an environment consists of adjusting the dynamic response of the seat in order to minimize the most important adverse effects of the vibration. This can only be achieved if the environment is known and there are adequate methods of predicting human response to the complex vibration that occurs on seats.

Two alternative methods of determining seat performance without human subjects have been developed: (i) mathematical prediction from the dynamic characteristics of the seat and the human body, and (ii) the use of a mechanical 'dummy' having dynamic characteristics representing those of the human body.

The mathematical prediction method is a development of a technique first investigated by Fairley and Griffin (1986). The method is based on separate measurements of the impedance of the seat and the impedance of the human body. An advantage of the mathematical method of prediction is that it encourages the development of a better understanding of the dynamic performance of seat components (e.g. suspensions, foams, and covers). Eventually, with a full understanding of the role and dynamic performance of each seat component it may be possible to predict seat dynamic

performance from the physical and chemical construction of the various seat parts. By these means a mathematical model could be used to identify the desired dynamic properties of a seat and the method of achieving this performance could also be predicted. For example the required mix of foam ingredients might be predicted. The research to develop a standard means of applying this method is described in Section 2. The currently proposed standard method is defined in Appendix A.

Two forms of mechanical dummy have been developed in the studies. One type of dummy uses passive elements to represent the mass, damping and stiffness of the body (see Section 3.2). The second type of dummy uses an active actuator to provide the damping and some of the stiffness of the dummy. This active dummy has various potential advantages, as described in Section 3.4.

2 Predicting seat transmissibility from the impedance of a seat and the human body apparent mass

2.1 Introduction

The prediction of seat dynamic involves two main parts: (i) the measurement and modelling of seat dynamic properties, and (ii) the measurement and modelling of human body apparent mass.

Preliminary studies confirmed that it was possible to obtain reasonably accurate predictions of the transmissibility of foam from separate measures of the impedance of the foam and the human body (Wei, 1995). However, there were many limitations, such as subject posture (no backrest), input vibration spectrum (flat random vibration), vibration magnitude (0.5 m/s^2 r.m.s.), and foot support condition, etc.

The factors that might affect prediction results may be listed as follows:

- Seat impedance – seat test method, pre-load, contact area, input spectra, vibration magnitude and seat inclination.
- Human body apparent mass – subject posture, input spectra, footrest condition, vibration magnitude, hard or soft seat, seat inclination and seat backrest angle.

The study commenced with the formation of basic seat and seated person mathematical models. The influence of the above factors on seat and person impedance were then explored. Finally, a seat-person model was developed to predict seat transmissibility with a variety of vibration environments. The following sections summarise the experimental and analytical studies. The separate studies are presented in full in the cited publications.

2.2 Mathematical model for the apparent mass of the seated human body exposed to vertical vibration (Wei and Griffin 1998a).

2.2.1 Previous experiment results

The vertical whole-body driving-point apparent masses of sixty persons (12 children, 24 men, and 24 women) were obtained with the subjects seated on a rigid force platform (Figure 2.2.1).

Subjects were exposed to 1.0 ms^{-2} r.m.s. random vertical vibration over the range 0.25 to 20 Hz. The subjects sat in a normal upright posture with their feet supported on a footrest that vibrated in phase with the seat.

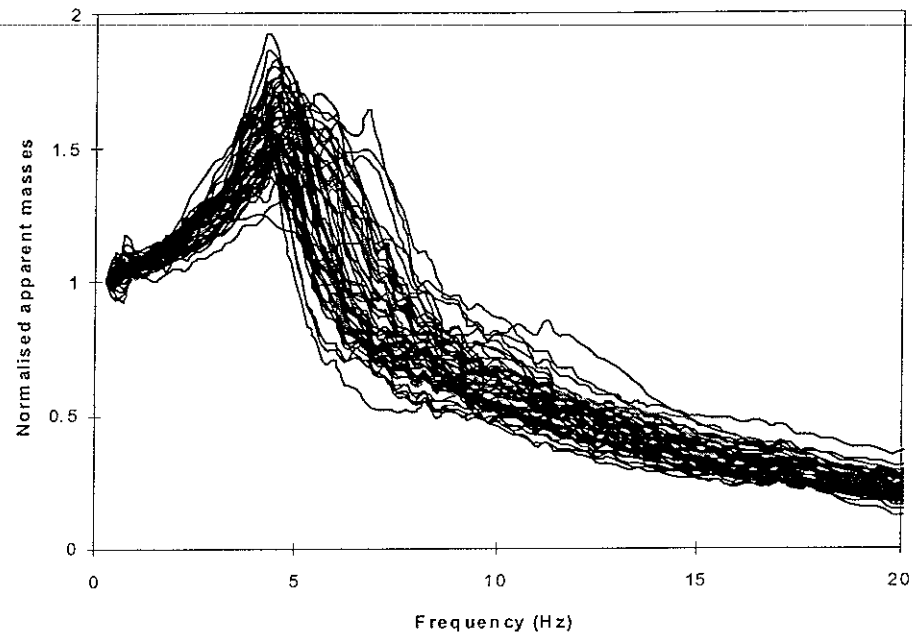

Figure 2.2.1 Normalised apparent masses of 60 seated subjects in the vertical axis (from Fairley and Griffin 1989).

2.2.2 *Seated person mathematical models*

Four models were developed. They were two one-degree-of-freedom models and two two-degree-of-freedom models (Figures 2.2.2, 2.2.3, 2.2.4 and 2.2.5).

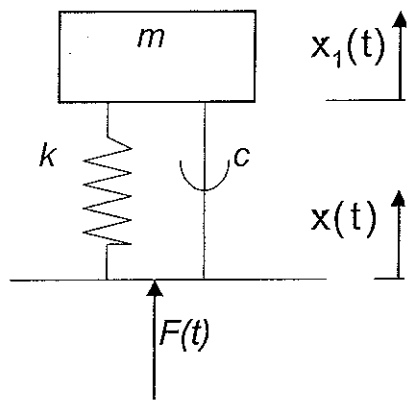

Figure 2.2.2 Single degree-of-freedom model (model 1a)

A curve fitting method was used to obtain model parameters. Two methods were adopted: fitting the modulus and fitting the phase. Through a comparison of the four models and two fitting methods, reasonable model parameters were obtained.

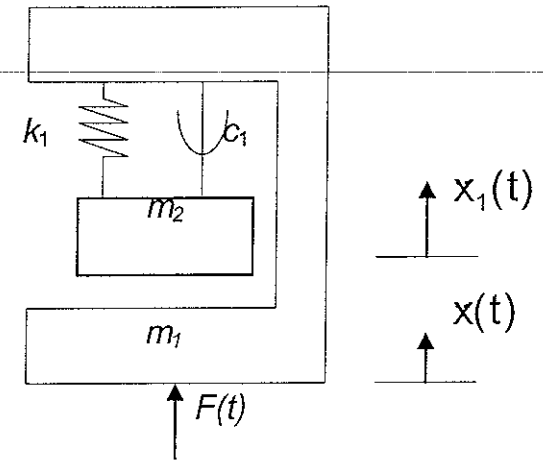

Figure 2.2.3 Single degree-of-freedom model with rigid support (model 1b)

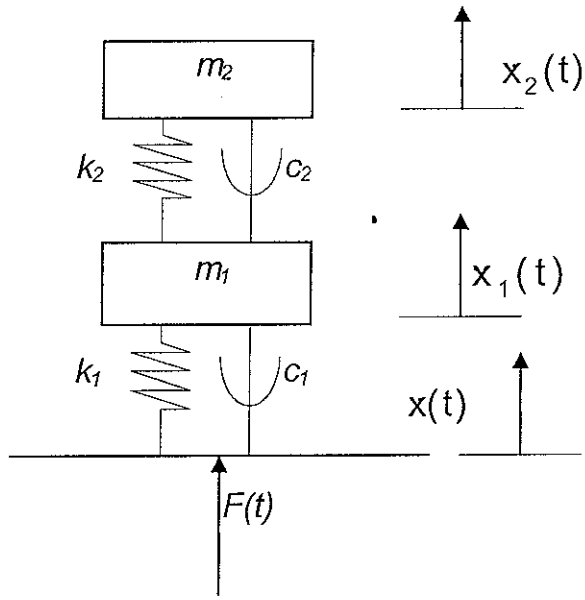

Figure 2.2.4 Two degree-of-freedom model (model 2a)

2.2.3 Discussion

The apparent masses were obtained under strict conditions in this study. Further studies for investigating the effect of seat backrest, vibration magnitude, hard seat and soft seat and vibration spectra, are needed to improve human body models.

2.2.4 Conclusions

By comparing the responses of the four models with the measured responses, model 1b (single degree-of-freedom with a rigid support) and model 2b (two degrees-of-freedom with a rigid support) were selected as the most suitable models for representing the apparent masses of subjects exposed to vertical vibration.

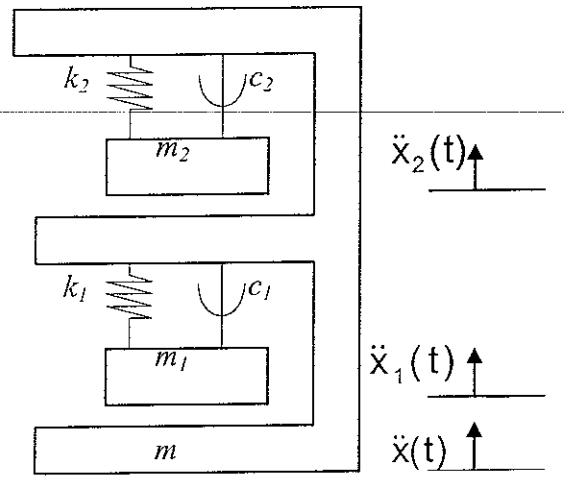

Figure 2.2.5 Two degree-of-freedom model with rigid support (model 2b)

Curve fitting has allowed the development of mathematical models that provide a good fit to measured values of the normalised apparent masses of subjects.

The single degree-of-freedom model and the two-degree-of-freedom model both provided results close to the measured modulus of apparent mass. However, the two-degree-of-freedom model provided a better fit to the phase and also a better fit near the principal resonance at 5 Hz. For best results a two-degree of freedom model is therefore recommended.

When predicting the transmissibility of seats, it is recommended that the two-degree-of-freedom model with a support mechanism is used.

2.3 Predicting laboratory measured seat transmissibility from measures of seat and foam impedance (Wei and Griffin 1998b).

2.3.1 Experiments

The experiments were conducted separately with a car seat and with a rectangular sample of foam. The car seat was the driving seat from a modern small family car. It was constructed from a steel frame with moulded foam supported from beneath by a contoured steel seat pan and fully encased within a cover. The TDI foam in the seat had a density of 50 kg.m^3. The rectangular sample of foam was 500mm wide by 420mm deep and 120mm thick. It is described as a 'soft feeling type' polyurethane foam used for car seating. It had a density of approximately 40 kg.m^3 and a hardness of about 7.0 kPa.

Three types of measurements were undertaken. The mechanical impedance of both the seat and the foam were measured and their transmissibilities determined using both inert objects on the seat and using a group of human subjects.

Three seat test methods were employed: (a) loading with a sand-bag, (b) loading with a rigid mass and (c) loading with an indenter. The latter is different from the former two methods because the indenter was fixed.

2.3.2 *Seat model*

A simple seat model was set up. The model parameters were obtained through curve fitting. The model could be combined with the above one and two degree-of-freedom human body models (Section 2.2) to compose a seat-person system model (Figure 2.3.1 and 2.3.2).

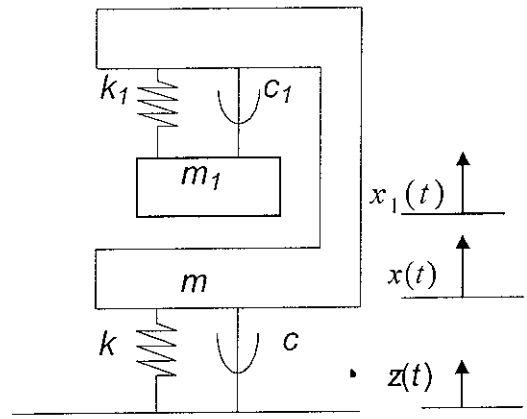

Figure 2.3.1 Two degree-of-freedom seat-person system model.

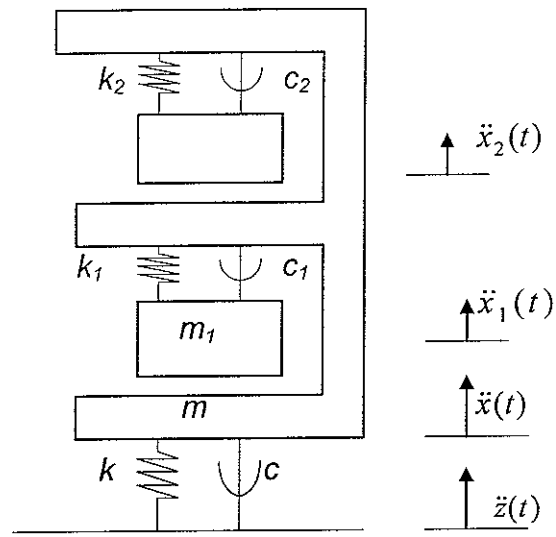

Figure 2.3.2 Three degree-of-freedom sea-person system model.

With one seat and one foam sample, transmissibility predictions were made. The measured and predicted seat transmissibilities were found to be similar.

2.3.3 *Discussion*

Accurate prediction of seat and foam transmissibility were obtained (see Wei and Griffin, 1998b). However, it is not yet shown that the method applies to different conditions on real seats. Further study will be needed to explore the optimisation of the seat-person model so that it can be used under real test conditions. The prediction method is required for all seats and real test conditions.

2.3.4 *Conclusions*

The rigid mass gave similar seat dynamic stiffness to that obtained with the indenter. However the indenter was preferred as it provides a more controlled condition: a mass tends to rotate and move when placed on a seat during exposure to vibration.

A sand-bag of the correct mass had an excessively large contact area with the seat (including the edges of the seat) that can influence the measured dynamic properties.

Two alternative models of the seat-person system were investigated. A single degree-of-freedom model adequately reflected the dynamic characteristics of the human body at low frequencies and could be used to predict seat transmissibility at the seat resonance, usually seen around 3 to 5 Hz. However a two degree-of-freedom model provided better predictions of seat transmissibility: it predicted the second resonance, often seen in measurements of seat transmissibility around 8 Hz, and may give useful predictions of seat transmissibility at frequencies up to 25 Hz.

The encouraging results obtained from the prediction method suggested that it may allow the prediction of SEAT values for seats used in specific vibration environments.

2.4 The influence of contact area, vibration magnitude and static force on the dynamic stiffness of polyurethane seat foam (Wei and Griffin 1997).

2.4.1 *Experimental conditions*

Five different seat foams were used with different parameters but the same shape. The vertical dynamic stiffnesses of the foams were measured using an indenter applied to the foam. A force transducer was attached to the indenter with five different indenter heads designated as buttocks, SIT-BAR, disk 15, disk 20 and disk 25. The buttock shape was moulded from a HYBRID III exterior. The indenter heads, in increasing order of area, were: disk 15, disk 20, SIT-BAR, disk 25 and buttocks (Figure 2.4.1).

Five different pre-loads from 300N to 700N were applied to the upper foam surface using each of the indenter heads while the foam was exposed to vertical vibration from

beneath. The force on the indenter and acceleration beneath the foam were measured during 60 seconds of random vibration.

Six magnitudes of vibration (0.25, 0.5, 1.0, 1.5, 2.0 and 2.5 ms^{-2} r.m.s.) were used in the experiment over the frequency range of 0.5 to 30 Hz.

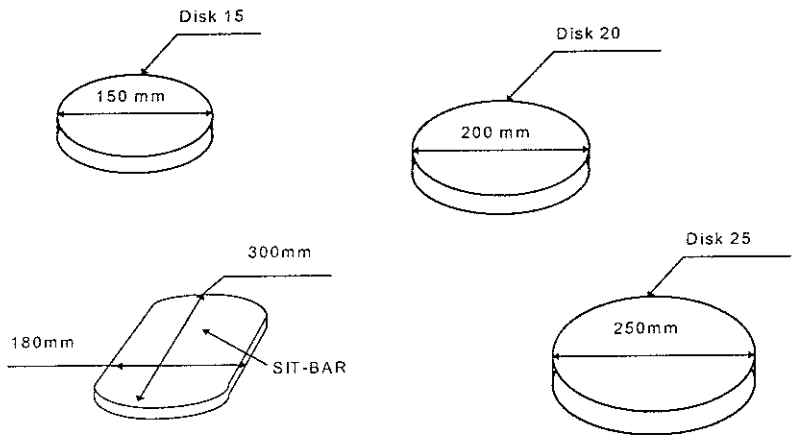

Figure 2.4.1 Different indenter head shapes

2.4.2 Discussion

2.4.2.1 Contact area

The shape of the HYBRID III exterior had the largest contact area, but using a 250mm diameter disk produced a greater foam stiffness and a greater damping. This suggests that the stiffness and damping of the foam were not only affected by the contact area.

The shape of the HYBRID III buttocks is approximately the same as the seated human body, except that it was rigid and the tissues of the body are flexible. If we do not consider other factors, it may seem reasonable to use this for foam testing. However, in this experiment the buttocks appeared to offer different foam dynamic stiffness than that obtained with subjects, so this cannot currently be recommended for obtaining a good prediction of foam transmissibility.

2.4.2.2 Static forces

With the different static forces used in this study, the stiffness and damping increased with some increases in force, but this was not consistent.

2.4.2.3 Vibration magnitudes

It is well known that different input magnitudes affect seat or foam transmissibility when measured with human subjects, but in this study there was not a large or consistent

difference in the foam parameters with changes in vibration magnitude. This indicates that the non-linearity in foam transmissibility may be affected mostly by the human body, whose dynamic properties change with different applied vibration magnitudes.

2.4.2.4 Foam test method

Using five differently shaped heads for the indenter to obtain the foam or seat dynamic properties is only one of several methods of determining foam response to vibration. It is desirable to compare the results using this method with the results obtained when using a rigid mass or a mechanical dummy.

2.4.3 Conclusions

2.4.3.1 Contact area

The contact between the indenter and the foam or seat is important, because with different indenters the foam dynamic response varied. With different contact areas the foam dynamic response changed greatly. In the present tests, disk 25 appeared to provide the most reasonable contact area for a foam test. When using this contact area, the best prediction of foam transmissibility was achieved for one subject.

2.4.3.2 Vibration magnitudes

The foam dynamic properties varied only slightly when the input vibration magnitude increased. For the foams tested it appears that similar results would have been achieved with any reasonable magnitude of vibration.

2.4.3.3 Static forces

The parameters of the foams showed that the stiffness and the damping increased with increasing static load, but when the static force reached about 600N the stiffness and damping decreased. It is recommended that an appropriate static force is needed when determined the foam or seat dynamic stiffness.

2.4.3.4 Foam test method

Using an indenter to obtain foam dynamic properties is useful. It can provide the correct parameters for the foam for setting up a foam mathematical model using a data fitting techniques.

2.5 The influence of seat cushion inclination on subject apparent mass and seat transmissibility (Wei and Griffin 1998c).

2.5.1 Hypotheses

It was hypothesised that seat transmissibility will decrease with increasing seat inclination because the measured 'vertical' acceleration is less than the true vertical acceleration.

It was expected that subject apparent mass would vary with seat inclination because of postural changes (Fairley and Griffin, 1989; Griffin 1990), even if a subject remained upright in the seat.

2.5.2 Experiment conditions

- different inclination angles (0°, 5°, 10°, 15°, 20°)
- 60s, 1.5 m/s^2 Guassian random vibration
- 10 subjects

2.5.3 Results and Discussion

The seat transmissibility changed with seat inclination because either the subject apparent mass changed or the cushion dynamic properties changed. The cushion thickness in the true vertical direction increased as the seat inclination increased, so the cushion stiffness will have slightly decreased and the cushion damping will have varied for similar reasons. The change of subject apparent mass may have affected cushion transmissibility at low frequencies, but it seems insufficient to explain the change in transmissibility at high frequencies. A study of the effect of inclination on cushion dynamic stiffness (i.e. equivalent stiffness and damping) is required to further improve understanding of the influence of seat inclination on seat transmissibility.

Subject postural changes can result in significant changes in apparent mass (e.g. Kitazaki and Griffin, 1998). When subject posture changed from erect to normal and to slouched, the principal resonance frequency of the normalised apparent mass decreased. The effect of subject posture was sufficient to require that subjects keep the same posture in the present experiment as the seat inclination varied. Effects of subject posture on seat transmissibility merit further investigation.

2.5.4 Conclusions

The transmissibility of a cushion changed as the inclination of the cushion increased: as the inclination increased from 0° to 20° the transmissibility decreased at frequencies below about 6 Hz and increased at frequencies above about 6 Hz.

The use of alternative orientations of the accelerometers used to measure the cushion transmissibility in this study gave similar results.

2.6 Seated human-body mathematical model with different vertical vibration magnitudes (Wei and Griffin 2000).

2.6.1 Hypothesis

The two-degree-of-freedom model developed by Wei and Griffin (1998a) is a linear seated body model that was developed at one magnitude of vertical vibration. The null hypothesis for this study was that the model parameters are not affected by vibration magnitude. In other words, there is no correlation between vibration magnitude and model parameters.

2.6.2 Experimental conditions

- 6 vibration magnitudes (0.25, 0.5, 1.0, 1.5, 2.0 and 2.5 ms^{-2} r.m.s.)
- Twelve male subjects seated on a hard seat

Sixty seconds of Gaussian random vibration with equal energy at each frequency was used in the experiment over the frequency range 0.2 to 20 Hz. Signals from the force transducer and the accelerometer were acquired at 100 samples per second using an *HVLab* data acquisition and analysis system.

2.6.3 Discussion and conclusions

The apparent mass differed between subjects, so different model parameters were obtained when fitting the apparent mass for different subjects. Because of large differences in model parameters between subjects, the measurement of the responses of a large number of subjects is needed to obtain a correct model to represent the responses of subjects in the vertical direction (e.g., Wei and Griffin, 1998a).

The fitted results indicate that a two-degree-of-freedom mathematical model can provide a good fit to the measured data. A decrease in both stiffness and damping appeared in the model when the vibration magnitude increased.

Predictions with a two-degree-of freedom model showed that the model is suitable to represent the apparent masses of subjects. However, the model should be considered an equivalent model to the human body only in that it has the same apparent mass, it cannot be used to explain the internal movements of the human body. More degrees-of-freedom model are required to explain the movement of the body, but this is not necessary for the relatively simple purpose of predicting seat transmissibility.

There are clear and consistent differences in the dynamic responses of the body as the vibration magnitude changes. Although the causes of the non-linearity are not clear, it is obvious that the specification of the mechanical impedance, or apparent mass, of the body should be specific to a limited range of vibration conditions. In this study, the effect was expressed as a function of vibration magnitude, but the application of the findings should recognise that the bandwidth of the vibration spectrum may also have an influence. Hence, the response at a given magnitude found in this study may be somewhat different from the response at the same magnitude when a different vibration waveform is used.

The two degree-of-freedom model parameters determined in this study differed from the model parameters developed in the earlier study (i.e., Wei and Griffin 1998a), because different apparent masses were measured in the experiment. In the previous study, the model stiffness and damping for the mean measured data were fixed: k_1=35007 N/m, k_2=33254 N/m, c_1=815 Ns/m and c_2=484 Ns/m. However, in this study, they are expressed by an equation in which the stiffness and damping depend on the input vibration magnitude. Wth an input vibration magnitude of 1.0 ms^{-2} r.m.s., the same as the previous study (i.e., in Wei and Griffin, 1998), the corresponding parameters of stiffness and damping of the model derived are 35095 N/m, 35163 N/m, 750 Ns/m and 637 Ns/m. There is therefore rather little difference in parameters between the two models. The differences are -88 N/m (k_1), -1909 N/m (k_2), 65 Ns/m (c_1) and –153 Ns/m (c_2). Therefore, the parameters of the original model (Wei and Griffin, 1998a) at different vibration magnitudes should be the values calculated from the modification equation, plus the differences shown above.

2.7 Human body dynamic properties on a hard and a soft seat with vertical vibration

It has been shown that the sitting posture, footrest, backrest and vibration magnitude all cause changes in body apparent mass and mechanical impedance. However, there has been little consideration of the effect of a soft seat on the body apparent mass. A systematic investigation of the effect of a soft seat on subject apparent mass is needed to decide whether it is necessary to modify the seat-person model to allow for the compliance of the surface on which the body is sitting.

2.7.1 Hypothesis

The null hypothesis was that there are no differences in human body dynamic response between a hard seat and a soft seat.

Any differences may be caused by:

- The vibration magnitude on the seat surface differing from the magnitude beneath the seat, so giving rise to a different response due to the body non-linearity.
- The use of Guassian random vibration with equal energy at each frequency when determining the driving point apparent of the body with the hard seat, but a vibration energy distribution on a soft seat surface that varied according to the seat transmissibility (see Figure 2.7.1).

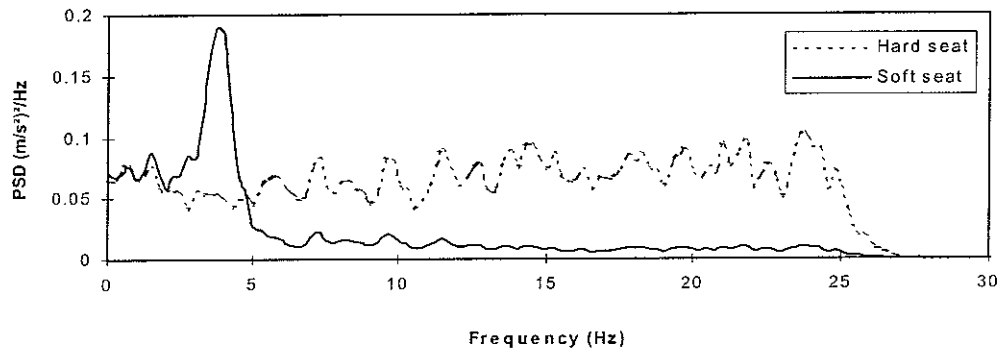

Figure 2.7.1 Power spectral density on the seat surface

2.7.2 Experiment conditions

A hard (i.e. rigid) seat, a shaker and instruments were used to conduct the experiments. The soft seat was the same hard seat on which a square block of foam was placed. The input vibration was a random vibration with a flat constant bandwidth acceleration spectrum between 0.5 and 20 Hz at an unweighted acceleration magnitude of 1.5 ms^{-2} r.m.s. The input signal was 60s duration. Ten male subjects participated in the study.

Due to the differences in the input vibration to the seated subject (Figure 2.7.1), an investigation of the effect of input spectrum is needed to investigate whether the change of subject apparent mass was caused by the different input spectra or the different seats. In other words, the soft seat may not be the cause of the apparent change in body response to the vibration. The influence of the input spectrum on apparent mass is considered in the next section.

2.7.3 Subject model on hard seat and soft seat

Figures 2.7.2 and 2.7.3 show two models. One is for the hard seat and another is for the soft seat. In these models, the stiffness, k, and damping, c, represent the seat dynamic performance that can be obtained with an indenter test and subsequent data curve fitting.

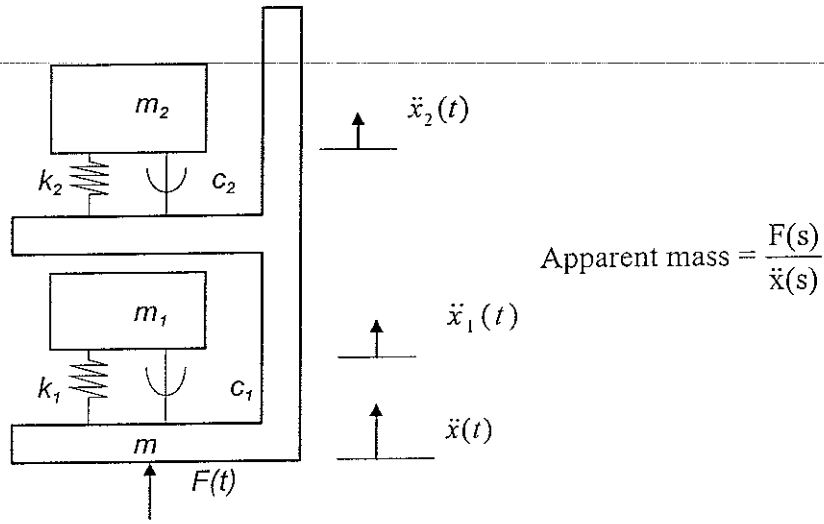

Figure 2.7.2 Model of person on hard seat

The curve fitting method is used to obtain model parameters. With the hard seat, the fitting procedure is the same as in the above study, however it is different with the soft seat. There are two steps to calculating the body apparent mass on the soft seat:

- Measure the dynamic stiffness of foam using an indenter.
- Fit a 3 degree-of-freedom model to the measured apparent mass (k and c from fitting to the measured foam dynamic stiffness).

2.7.4 Model fitting results

Figure 2.7.4 shows the mean apparent masses of ten subjects measured on the hard and soft seat. The mean of the fitted curves for the hard and soft seats are also shown in Figure 2.7.4. The individual measured and fitted curves are similar to the curves showed in Figure 2.7.4, so they are not shown here.

All parameters acquired by curve fitting are shown in Table 2.7.1, where the model frame mass, m, is invariable. It can be seen from this table that there are significant differences of the model parameters between the two test conditions (hard and soft seats). The stiffnesses, k_1 and k_2, the damping, c_1 and c_2, and the mass, m_2, decrease, but the mass, m_1, increases with the soft seat compared to the hard seat. Taking vibration magnitude into account, this means that the stiffness, the damping and the mass, m_2, decreased but the mass, m_1, increased as the vibration magnitude decreased. This result differs from the previous conclusion, in which the stiffness and the damping of the model decreased with an increase in vibration magnitude. The reason for this phenomenon is presumably either: (i) a change of the model mass, (ii)

the apparent mass is influenced by the soft seat, or (iii) the increased number of degrees-of-freedom prevented an accurate determination of the model parameters.

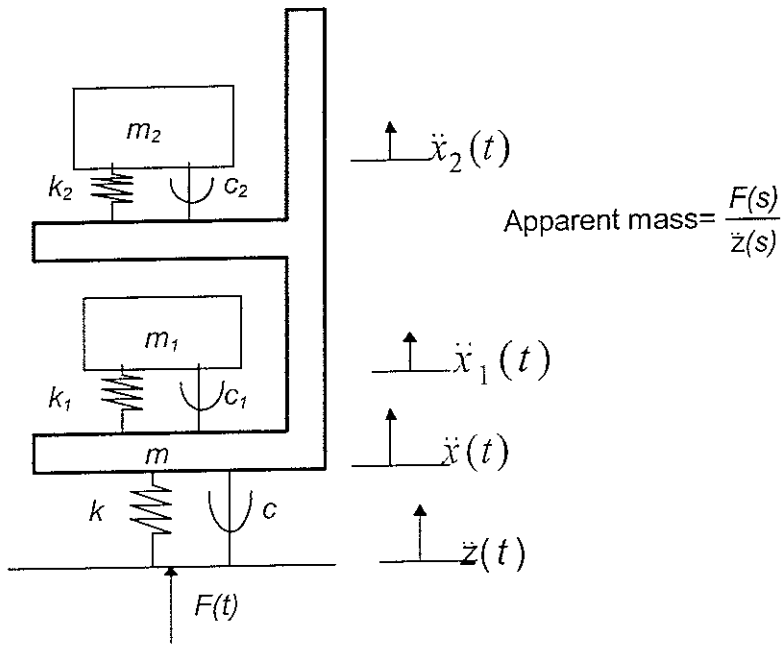

Figure 2.7.3 Model of person on soft seat

2.7.5 *Comparison of prediction results*

Figure 2.7.5 shows the seat dynamic performance as predicted by the two-degree-of-freedom model. The model parameters come separately from fitting the measured apparent mass on the hard seat and on the soft seat. It is clear that the model parameters coming from the hard seat provide a better prediction, especially at frequencies greater than 6 Hz. It can also be observed that the real seat transmissibility is always in between the two prediction curves when the frequency is below 6 Hz.

2.7.6 *Discussion*

There were significant differences in vibration between the surface of the hard seat and the surface of the soft seat. These changes may have resulted in a variation in the human body dynamic response.

It appears reasonable to use a two degree-of-freedom model to represent the human body dynamic response in the vertical direction. Using this model, a good representation of apparent mass on a hard seat can be obtained. The same form of model may also allows a representation of apparent mass on a soft seat.

Table 2.7.1 Two-degree-of-freedom-model parameters

Subjects	Seat	k_1 (N/m)	c_1 (Ns/m)	k_2 (N/m)	c_2 (Ns/m)	m (kg)	m_1 (kg)	m_2 (kg)	Total mass (kg)
1	Hard	30192	204	45183	821	19.6	7.6	36.8	64
	Soft	1757	167	26764	478	19.6	13.6	31.9	
2	Hard	40162	340	49490	632	16.7	7.2	31.3	55.2
	Soft	4896	314	23723	252	16.7	14.1	19.3	
3	Hard	28715	323	34534	2131	15.8	21.4	40.7	78.7
	Soft	16773	117	1654	1663	15.8	15.3	47.0	
4	Hard	25192	304	46453	735	16.6	8.4	38.8	63.8
	Soft	9342	293	35764	598	16.6	16.2	30.2	
5	Hard	2875	33	47497	1635	15.8	4.0	36.9	57.1
	Soft	8716	70	13933	494	15.8	6.8	25.2	
6	Hard	13198	143	24979	1137	9.3	11.9	31.6	52.8
	Soft	3310	308	16805	244	9.3	20.6	22.2	
7	Hard	2545	357	75827	1783	15.8	21.6	24.8	63.3
	Soft	12714	215	2274	603	15.8	16.8	22.1	
8	Hard	43783	368	45157	638	19.7	10.3	30.5	60.5
	Soft	18517	197	7156	474	19.7	14.0	21.1	
9	Hard	17134	208	65195	752	16.5	16.2	19.8	53.5
	Soft	994	65	21208	370	16.5	5.2	23.9	
10	Hard	40162	340	47320	632	16.5	10.2	30.9	57.6
	Soft	5896	294	19723	433	16.5	14.1	25.8	

The parameters of the human body two degree-of-freedom mathematical model of apparent mass were different for the hard seat and the soft seat. This could suggest that predictions of seat dynamic performance using body model parameters derived from a hard seat may not be applicable to a soft seat. However, other interpretations are possible. The study showed that the body model parameters determined using a hard seat gave better predictions of seat transmissibility than those determined using a soft seat.

2.7.7 Conclusions

The parameters of the two-degree-of-freedom model derived from the hard seat and the soft seat were different. The data from the soft seat did not give good predictions of seat transmissibility and may not be suitable for the prediction of seat transmissibilities. However, these data may be of interest in other fields.

When subjects changed from sitting on a hard seat to sitting on a soft seat, the model stiffnesses, k_1 and k_2, model damping, c_1 and c_2, and mass, m_2, decreased, but the model mass, m_1, increased, except for some subjects.

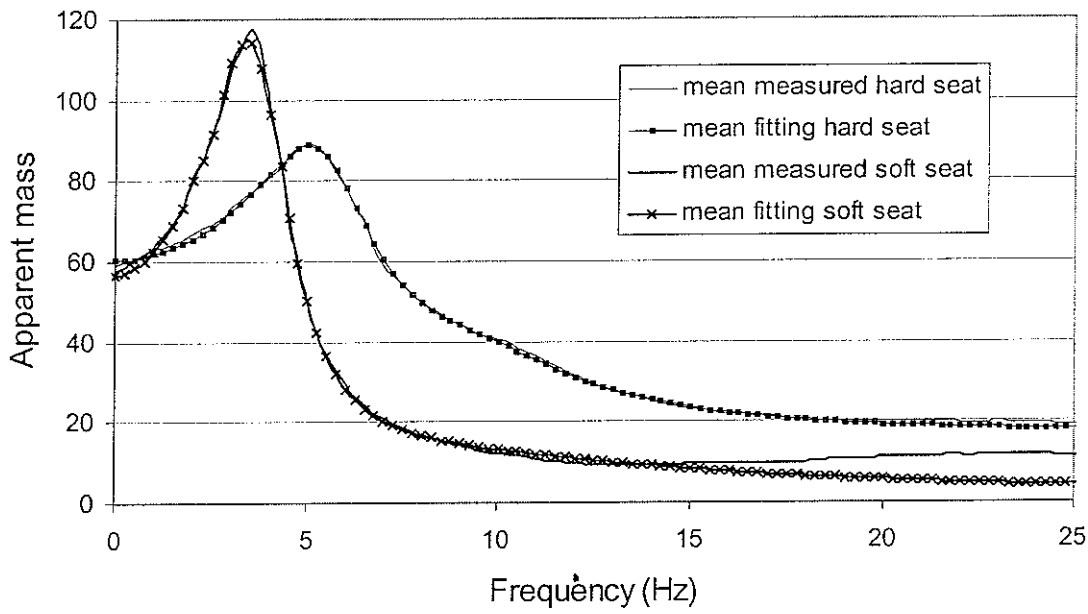

Figure 2.7.4 Mean measured apparent mass on soft and hard seat as well as the curve fitting results.

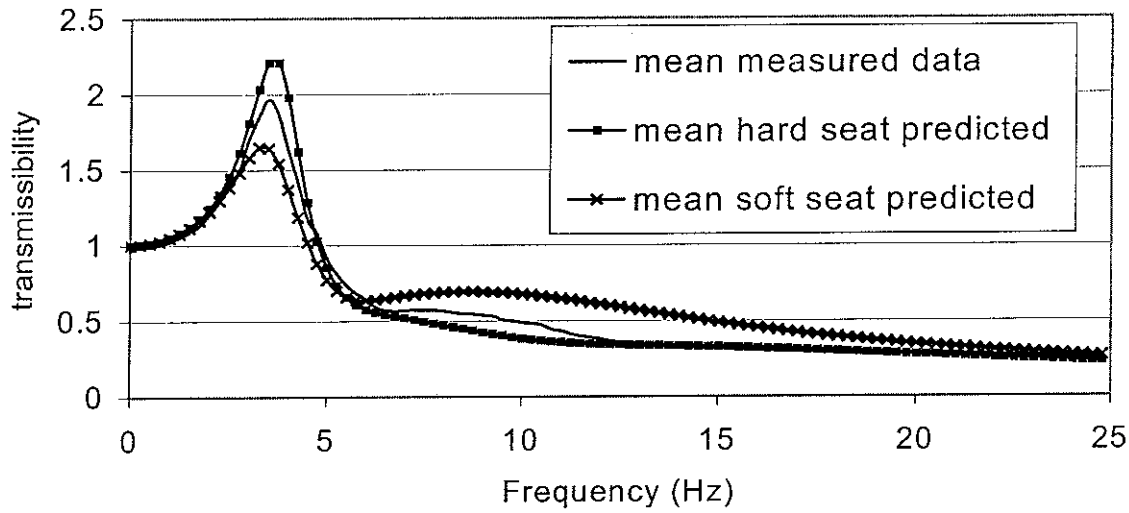

Figure 2.7.5 Seat transmissibility prediction by using hard seat and soft seat acquired model parameters

2.8 Modelling the effect of backrest angle on the vertical apparent masses of seated subjects (Wei and Griffin 1999)

2.8.1 Hypothesis

The null hypothesis was that the apparent mass of seated subjects is not affected by backrest conditions or input vibration spectra, so a linear two degree-of-freedom model (see Section 2.2) is a suitable model to represent a seated subject with different backrest conditions and different vibration spectra.

2.8.2 Experimental conditions

- Six different backrest conditions: (a) no backrest, (b) rigid vertical backrest (i.e. 0^0), (c) soft backrest at 0°, (d) rigid backrest at 10°, (e) rigid backrest at 15°, and (f) rigid backrest at 20°.
- Three different 60 second input vibration spectra: (i) random vibration with a flat constant bandwidth acceleration spectrum between 0.5 and 30 Hz at an unweighted acceleration magnitude of 0.5 ms^{-2} r.m.s., (ii) vertical floor vibration measured in a car and presented at a magnitude of 0.5 ms^{-2} r.m.s. (unweighted), and (iii) vertical seat surface vibration measured in the same car at the same time and presented with the same unweighted vibration magnitude of 0.5 ms^{-2} r.m.s. (see Figure 1).
- 10 subjects.

2.8.3 Discussion and conclusion

The apparent mass of the body differed between subjects and different model parameters were obtained for each subject. However, fitting to the mean subject data provided a model that represented the average response of subjects (see Wei and Griffin, 1998). The fitting result suggests that the two degree-of-freedom mathematical model used here can provide a good fit to the measured mean data with different backrest conditions.

When the aim is to represent subject apparent mass, a two degree-of freedom model is reasonable. However, a simple model of this type does not explain the movement of the human body. More degrees-of-freedom are required to represent the internal movement of the body (e.g. Matsumoto, 1998), but this is not necessary for the prediction of seat transmissibility.

This study showed clear and consistent differences in the dynamic response of the body as the backrest condition changed. Although the causes of the changes are not

clear, it is obvious that the specification of the apparent mass of the body should depend on the backrest conditions.

Using three very different spectra with the same unweighted r.m.s. acceleration, there was a statistically significant effect of the spectra on apparent mass, but the magnitude of the effect was small. This is reasonably consistent with the study conducted by Sandover (1978) who found no difference in apparent mass when using two input vibration spectra of the same vibration magnitude, with one spectrum having more energy at high frequencies and the other having more energy at low frequencies. The differences in apparent mass between the spectra were small compared to differences previously seen with a fixed spectrum of vibration at different magnitudes. It seems that when different input spectra have the same energy (e.g. the same unweighted r.m.s. magnitude) over a range of low frequencies but a different energy distribution, the measured apparent masses may be similar.

It is concluded that a two degree-of-freedom mathematical model can provide a good fit to the apparent mass of the seated human body in the vertical direction. A decrease in the mass m_1, and an increase in both the stiffness k_1 and the damping c_1 might be used to represent changes that occur when there is increased contact with a backrest. However, further investigation of the interaction between the seated body and backrests is required.

2.9 Predicting seat transmissibility measured in vehicles

The seat transmissibility measured in the field could differ from that measured in the laboratory for several reasons. Seat transmissibility is sometimes measured in the laboratory using random vibration with equal energy at each frequency while subjects keep an upright posture. In a vehicle a driver leans against the seat backrest and the input vibration has a spectrum that is characteristic of the car and the road. In addition, any cross-axis coupling in the dynamic response of a seat-person system may have important implications in field measurements where vibration occurs in many axes. Predicting seat transmissibility in the field is therefore far more difficult than predicting seat transmissibility in the laboratory. The overall aim of the research is to make it possible to predict seat transmissibilities in practical situations.

2.9.1 Experimental measurements

2.9.1.1 Seat transmissibility measurements

Measurements were conducted separately in the passenger seats of three cars: Ford Mondeo, Ford Fiesta and a Jaguar-Daimler Sovereign. The transmissibilities of the

seats were measured while they supported 6 subjects driving over 4 different roads at three different speeds: 70, 40 and 30 miles per hour. The four roads were a concrete motorway, a tarmac motorway, a tarmac A class road, and tarmac rural road. The vibration at the subject-seat interface was measured using an Entran piezo-resistive accelerometer (type EGCSY-240*-10) in an SAE pad (see ISO 10326-1, 1992). The vibrations at the seat base were measured using four Entran piezoresistive accelerometers at the four seat supporting corners so that the seat input vibration could be obtained. All subjects maintained a normal posture with their backs touching the seat backrest, which had a 20° inclination, and with their hands resting on their knees.

2.9.1.2 Measurement of seat mechanical impedance with an indenter

The same indenter test rig was utilized to acquire seat dynamic properties (see Section 2.3). Four input spectra were used to represent the four different roads. The four input spectra were not the spectra measured from the car floor, they were spectra that came from the seat deflection (i.e. the displacement of the floor subtracted from the displacement on the seat). Three random flat vibration spectra (0.4, 0.8 and 1.2 ms^{-2} r.m.s.) were also used over a frequency range from 0 to 50 Hz.

The measurements were obtained with a pre-load of 500N applied to the surfaces of the three seats. Signals from the force transducer and the accelerometer were acquired at 400 samples per second into an *HVLab* system.

2.9.2 Prediction results

Table 2.9.1 shows seat model parameters determined from the indenter test. Table 2.9.2 shows the body model parameters at 1.0 m/s^2 r.m.s. input magnitude. The parameters of the model used for different magnitudes should be calculated by equations 2.9.1, derived in Section 2.6. Using the seat-person model (Figure 2.7.2) predictions of seat transmissibility for the A road at 30mph are shown in Figures 2.9.1 to 2.9.3. The input vibration magnitudes for the three seats were separately: 0.54 ms^{-2} r.m.s. (Fiesta), 0.67 ms^{-2} r.m.s. (Mondeo) and 0.53 (Jaguar) ms^{-2} r.m.s.

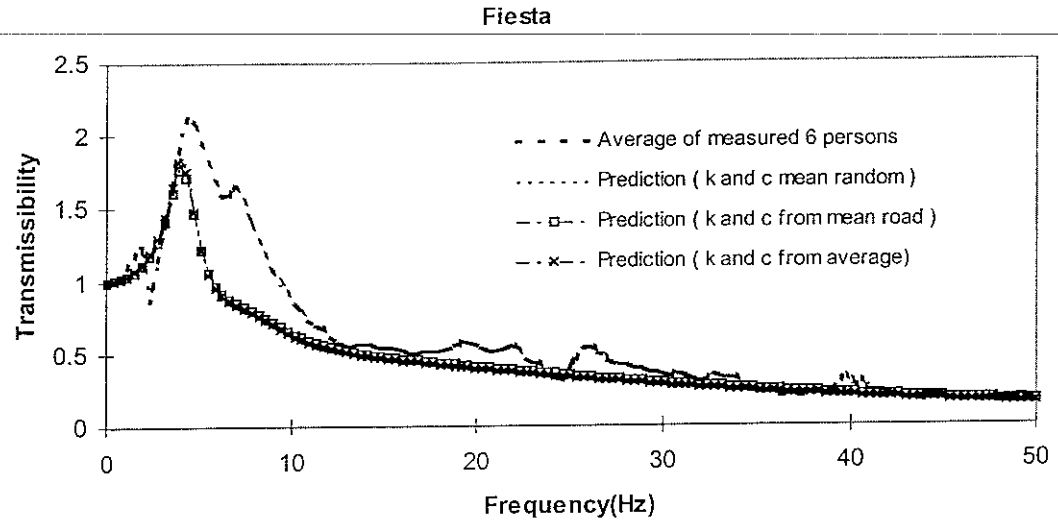

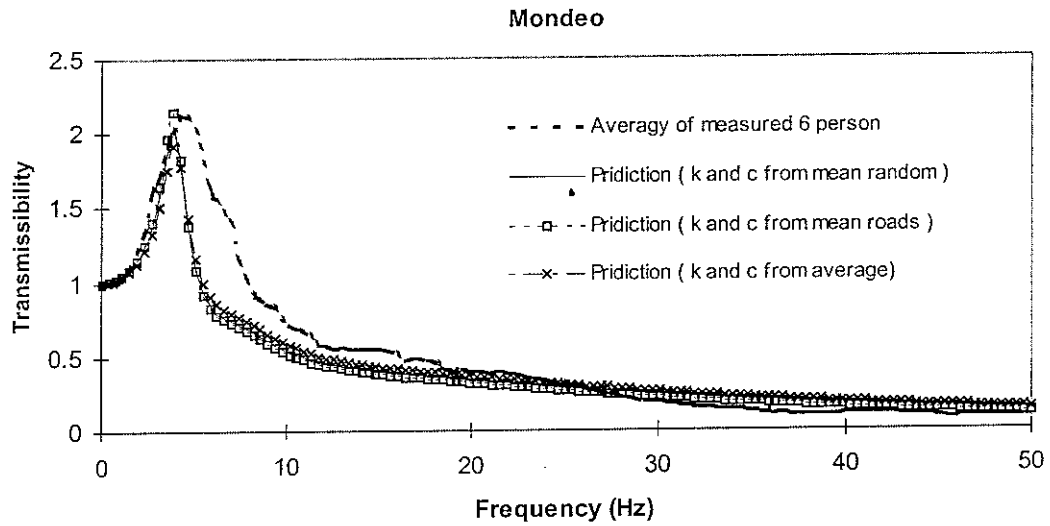

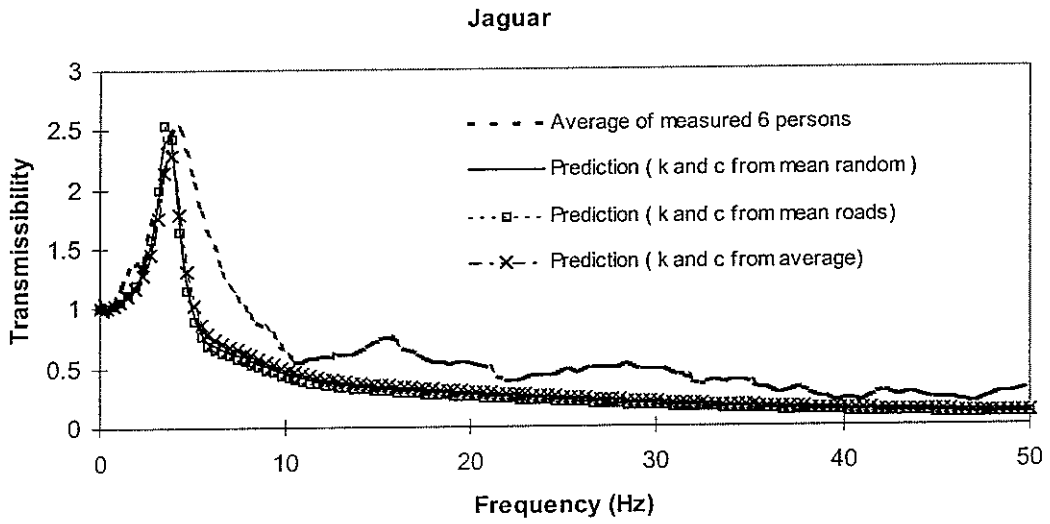

Figure 2.9.1 Predictions of three seat transmissibilities

$$k_1 = -88 + (12442 + 22653 \times \bar{\ddot{x}}^{-0.3537})$$

$$k_2 = -1909 + (4668 + 30495 \times \bar{\ddot{x}}^{-0.3167}) \qquad (2.9.1)$$

$$c_1 = -153 + (696 - 59 \times \bar{\ddot{x}}^{1.0288})$$

$$c_2 = 65 + (1166 - 416 \times \bar{\ddot{x}}^{0.2972})$$

Table 2.9.1 Three seat model parameters

	500 N					
Input vibration	Mondeo		Fiesta		Jaguar	
	k (N/m)	c (Ns/m)	k	c	k	c
Mean roads	71059	192	85229	203	61234	126.375
Mean random	57337	121	78620	181	56392	108.6667
average	67317	172	81924	192	58813	117.5208

Table 2.9.2 Parameters of one degree and two degree of freedom models.

	k_1	c_1	k_2	c_2	m	m_1	m_2
*Model 1	44943	1360			6.0	45.6	
*Model 2	35776	761	38374	458	6.7	33.4	10.7

* Model 1 is a one degree-of-freedom model and model 2 is two degree-of-freedom model

It can be seen that the correspondence between the measured and predicted values (Figure 2.9.1) is not as good as was obtained in Section 2.7 (although still far better than would have been obtained using a rigid mass to measure seat transmissibility). The predicted values and the measured values are similar below 4 Hz. In the frequency range from 4 to 10 Hz, the predicted values are significantly lower than the measured values. The difference might be caused by the seat backrest. The seat backrest can have an effect on body apparent mass (see Section 2.8). Hence, a modified model should be used to provide the correct prediction of the seat transmissibility.

Figure 2.9.2 shows the results of a modified seat-person model for predicting seat transmissibility. Although this model provides an improved prediction, the differences between the measured and predicted values are still greater than expected, especially

in the frequency range from 5 to 20 Hz. This suggests that the effect of the seat backrest on seat transmissibility may not only be caused by the response of the seated person.

The seat-person model developed in Section 2.3 was based on a seat and human body model, derived from measured seat and human body dynamic responses. The role of seat backrest has not been fully considered. Although, a modified model has been developed representing the human body that leans against a seat backrest, a seat-person model derived from this model does not fully reflect the interaction between the seat and the body. This is an area for further research.

A sensitivity analysis for seat-person model parameters is required to guide the study towards a successful model development.

2.9.3 Sensitivity of seat-person model parameters

Figure 2.9.3 shows the sensitivity analysis of the seat-person model parameters. The original model parameters come from measurements with the Mondeo seat (Table 2.9.1) and the proposed body model (Table 2.9.2). A sensitivity analysis has been performed by making a 10% increase and a 20% increase in the original model parameters.

It can be observed that a change to the mass, m, had the smallest effect on seat transmissibility predictions. An increase in mass, m_1 caused the resonance frequency to decrease but no change at frequencies above 7 Hz. The effect of m_2 is very small. An increase in mass, m_2 decreased the first and second resonance peak value but it did not have any influence at other frequencies. It seems that parameter m_1 is a critical parameter for predicting the measured seat transmissibility, if the measured value has a changed resonance. The second mass, m_2, controls the second peak in the seat transmissibility prediction.

The effects of the subsystem stiffness k_1 and the subsystem damping c_1 were significant. As the stiffness k_1 increased, the resonance frequency and the transmissibility at resonance both increased but at frequencies above resonance the transmissibility decreased between 5 and 12 Hz. When c_1 increased, the transmissibility increased over the frequency range from 4 Hz to 7 Hz and then decreased above 7 Hz.

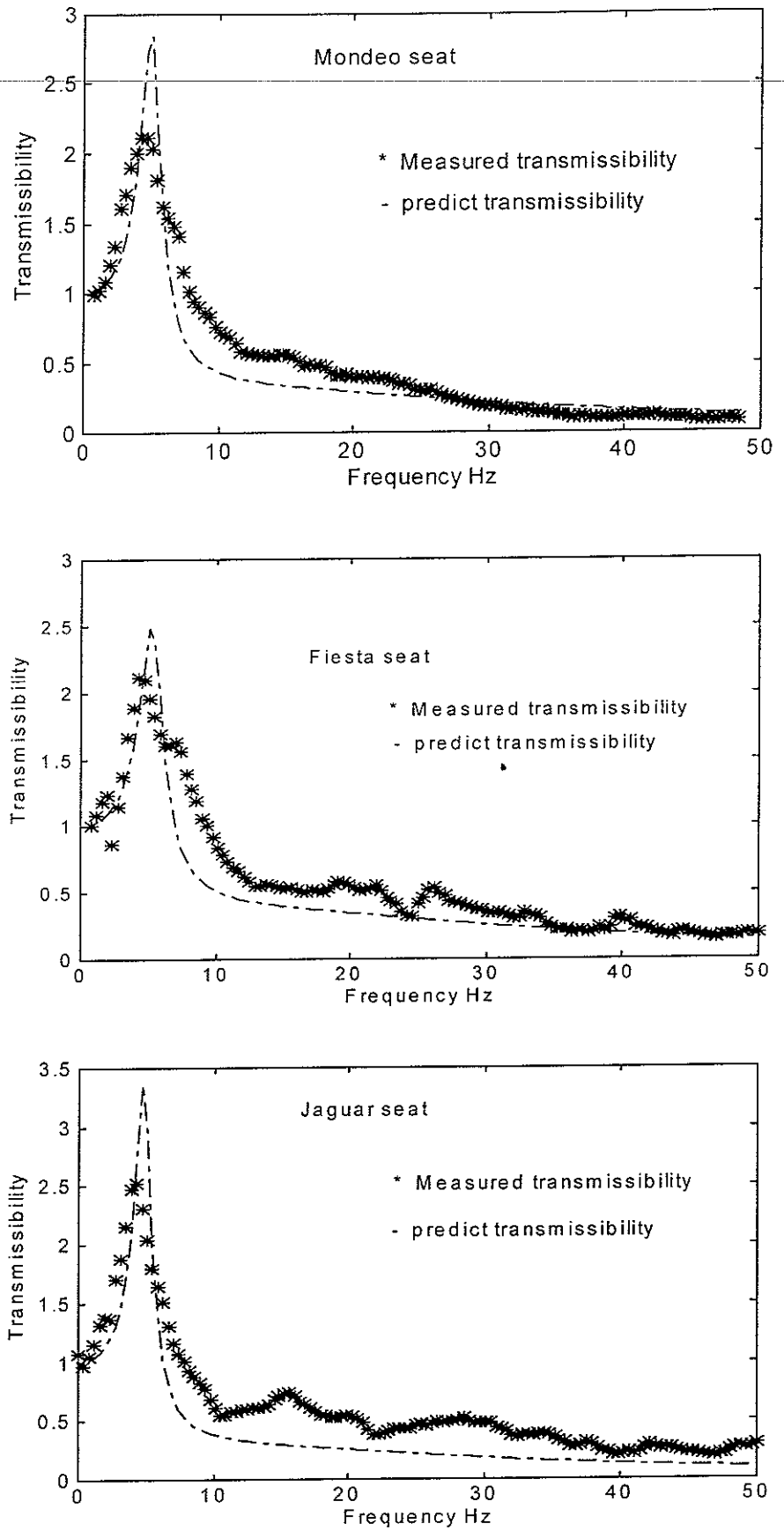

Figure 2.9.2 Comparison between predicted and measured transmissibilities of three seats (using modified model)

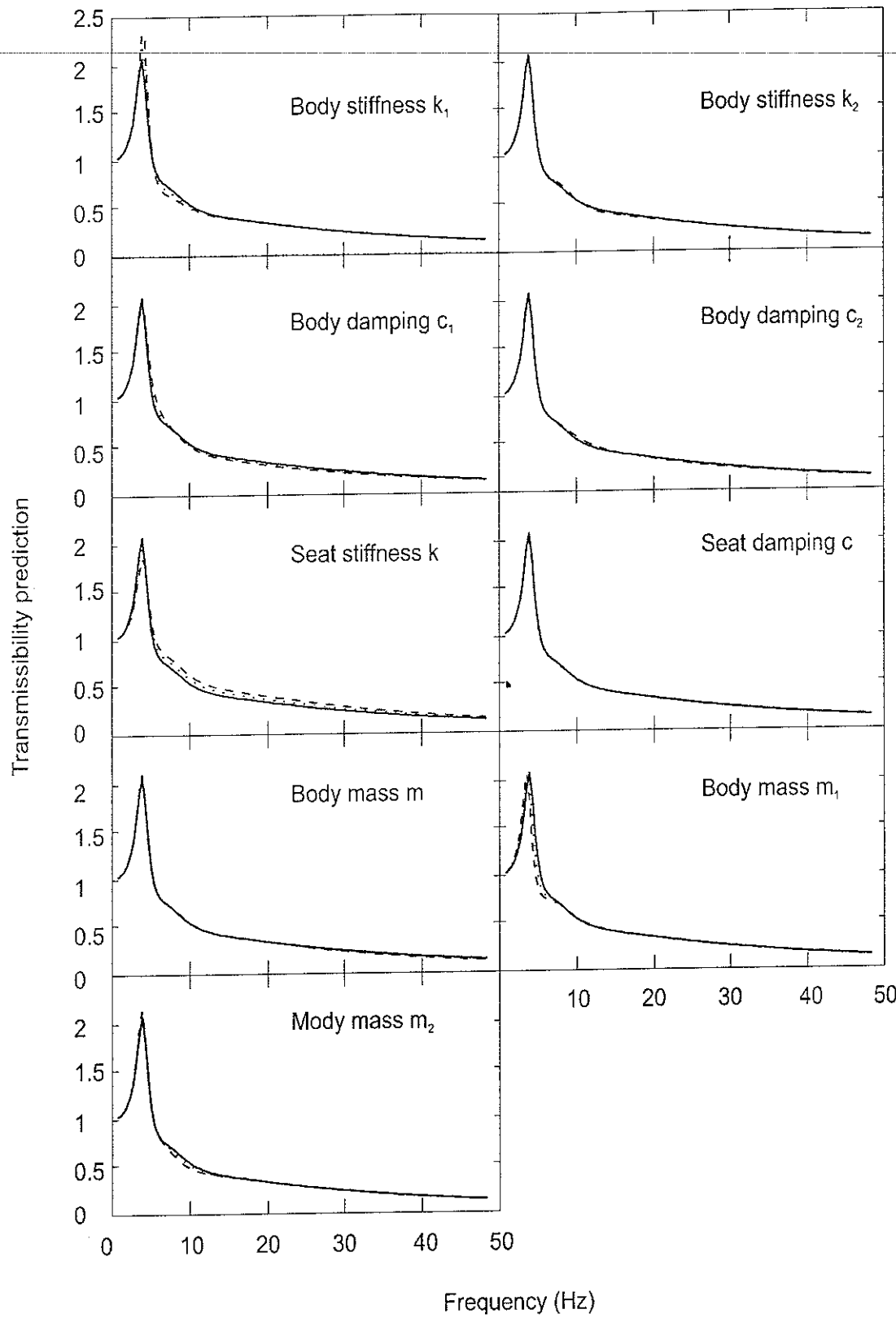

The function of subsystem stiffness k_2 and subsystem damping c_2 are also shown in Figure 2.9.3. These two parameters have only a small effect on seat transmissibility

predictions compared with the same percentage change of stiffness k_1 and damping c_1. The effect of c_2 on seat transmissibility predictions is similar to that of parameter c_1.

The effect of seat parameters k and c on seat transmissibility predictions is different from the corresponding body parameters. As the stiffness k increased, the resonance frequency increased and the seat transmissibility at resonance decreased. Changes in the stiffness k may therefore offset the increase arising from changes in m_1 at the resonance frequency. However, an increase of stiffness k will cause the seat transmissibility to increase at frequencies above the resonance frequency. The influence of the parameter c is very small. Consequently, only a change in parameters m_1, k_1, c_1 and k can make move the predicted seat transmissibility towards the measurements of seat transmissibility shown in Figure 2.9.2.

The seat stiffness is measured from the indenter test and is therefore fixed. Hence, the change of parameters m_1, k_1 and c_1 is only way to obtain an improved prediction of seat transmissibility. The effect of both backrest and input magnitude may produce an increase in both stiffness k_1 and damping c_1 and a decrease of mass m_1. This is consistent with the previous study of the effect of backrest and input magnitude on apparent mass. Although the final results are not yet sufficient, the studies appear to be in the correct direction.

It seems that the differences between the measured and predicted seat transmissibilities may have been primarily caused by interaction with the seat backrest. Although the effect of the backrest has been considered in the body model, the interaction between the seat backrest and the body has not yet been reflected with sufficient accuracy. Therefore, a new model is necessary for this condition.

2.9.4 Revised seat-person model and its function

Figure 2.9.4 shows a seated person with a backrest. There are two forces inputting to the seated person. They are: force, F_v, from the seat cushion and the force, F_b, from the seat backrest. The force from the backrest is composed of a vertical force F_1 and a horizontal force F_2. Because only vertical vibration is considered here, the total forces applied to the subject are the forces F_1 and F_v, and are influenced by the seat cushion and seat backrest stiffness and damping.

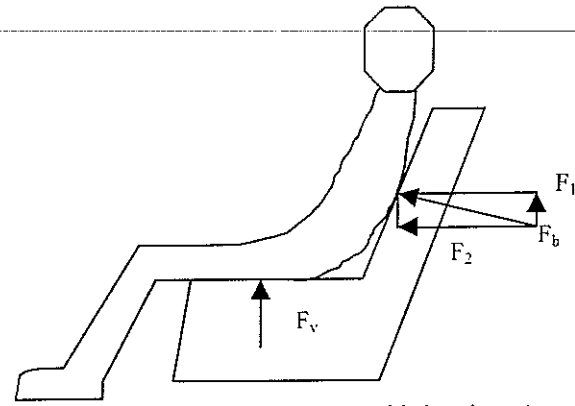

Figure 2.9.4 Seated person with backrest

Based on the above assumption, a new model (Figure 2.9.5) was devised. The model includes additional parameters, the backrest stiffness, k_b, and damping, c_b. Because the mass supported by the seat backrest is only part of the body mass, this is represented by only mass, m_1, connected to the seat base through the backrest stiffness and damping.

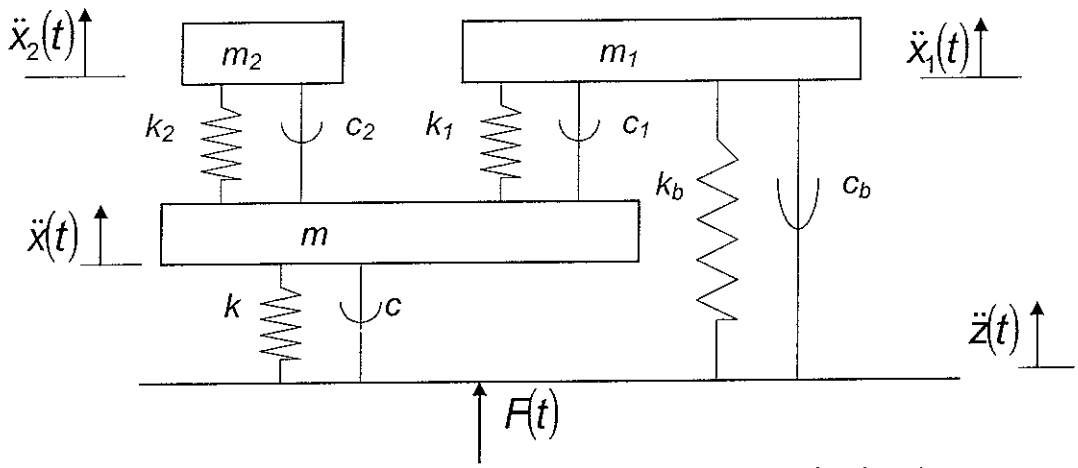

Figure 2.9.5 Model for seat-person system with seat backrest

The equations of motion of the model in Figure 2.9.5 are given by:

$$m_1\ddot{x}_1 + k_1(x_1 - x) + c_1(\dot{x}_1 - \dot{x}) + k_b(x_1 - z) + c_b(\dot{x}_1 - \dot{z}) = 0 \qquad (2.9.2)$$

$$m_2\ddot{x}_2 + k_2(x_2 - x) + c_2(\dot{x}_2 - \dot{x}) = 0 \qquad (2.9.3)$$

$$m\ddot{x} + k(x - z) + c(\dot{x} - \dot{z}) + k_1(x - x_1) + c_1(\dot{x} - \dot{x}_1) + k_2(x - x_2) + c_2(\dot{x} - \dot{x}_2) = 0 \qquad (2.9.4)$$

$$F(t) = m\ddot{x} + m_1\ddot{x}_1 + m_2\ddot{x}_2$$

$$F(t) = k(z - x) + c(\dot{z} - \dot{x}) + k_b(z - x_1) + c_b(\dot{z} - \dot{x})$$

Comparing this model with the previously developed model, it can be seen that the stiffness and damping of the seat backrest will influence the seat transmissibility.

However, the values of these two parameters are unknown. A new test is needed to measure the physical values of these two parameters.

By selecting various values of the model parameters, k_b, and c_b, the influence of the backrest coupling in the new model has been investigated. The other model parameters came from Tables 2.9.1 and 2.9.2. Figure 2.9.6 shows a comparison between predicted and measured transmissibilities of the three seats. It can be seen that the new model can provide improved predictions of the transmissibilities measured in the three cars. The encouraging results obtained from the new model suggest that it may be suitable for predicting seat transmissibilities when there is backrest contact.

Figures 2.9.7 and 2.9.8 show the effect of changes to the assumed backrest stiffness, k_b, and the assumed backrest damping, c_b. When the stiffness, k_b, increases, the resonance frequency and the transmissibility at resonance both increase. An increase in damping, c_b, causes a decrease in the seat transmissibility at resonance. An appropriate value of the stiffness, k_b, and the damping, c_b, can result in the required resonance frequency with the required transmissibility at resonance. This suggests that the effect of a seat backrest on seat transmissibility could be important. It is concluded that a satisfactory model representing a person sitting on a seat with a backrest must include a representation of the backrest interaction.

2.10 Conclusions

Many models have been developed in this study to predict seat transmissibility. Among them, a single degree-of-freedom model and a two degree-of-freedom model (see Section 2.2) both provided good predictions of laboratory measurements of seat transmissibility without a backrest. However, the two degree-of-freedom model appears superior. The two degree-of-freedom model can predict the second resonance, which is often seen in measurements of seat transmissibility around 8 Hz.

The single degree-of-freedom and two degree-of-freedom models can give useful predictions of seat transmissibility in limited conditions, such when the subject is in an upright posture (not touching the backrest).

A modified model, appropriate to different vibration magnitudes and different backrest inclinations, should give improved predictions of seat transmissibility for the practical situation. A new model representing a seat-person system in a car has been developed in this study. The encouraging results suggest that further development and evaluation of the model is appropriate.

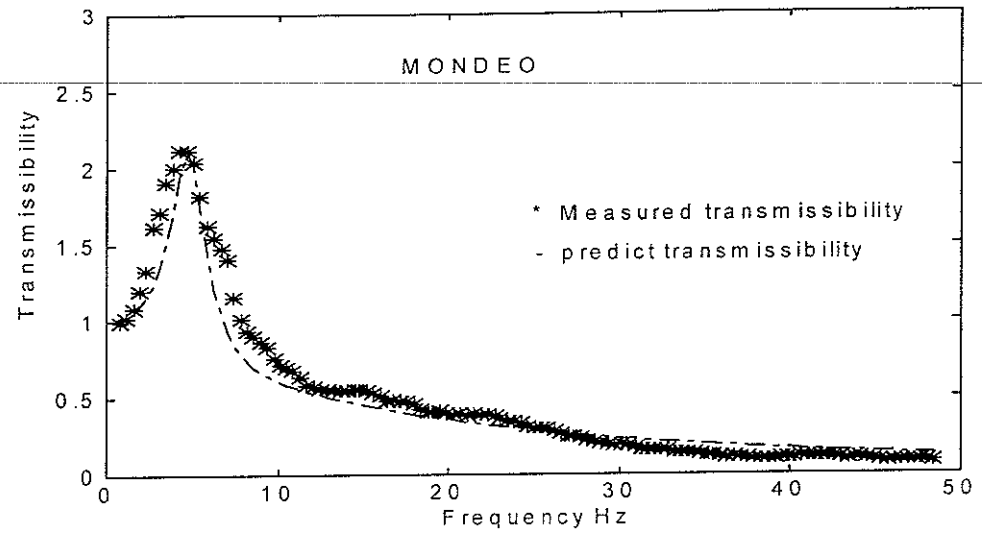

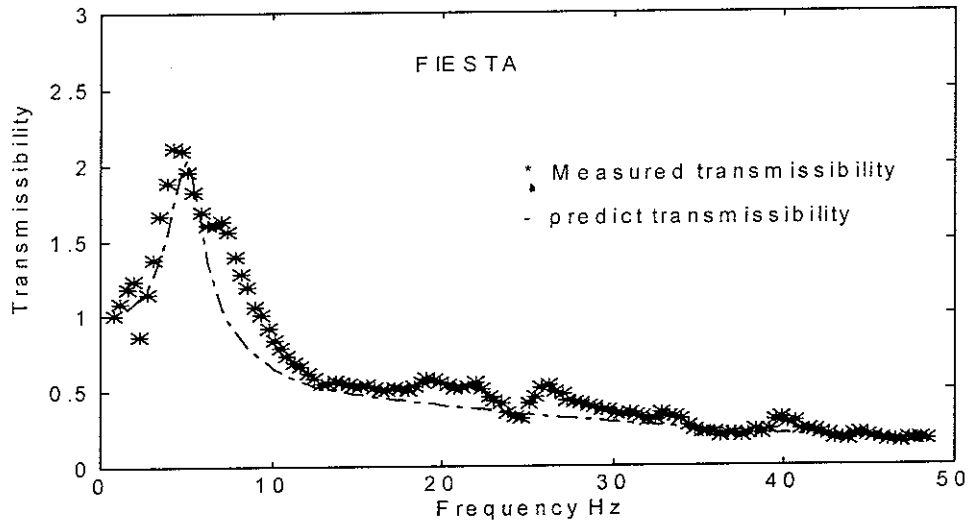

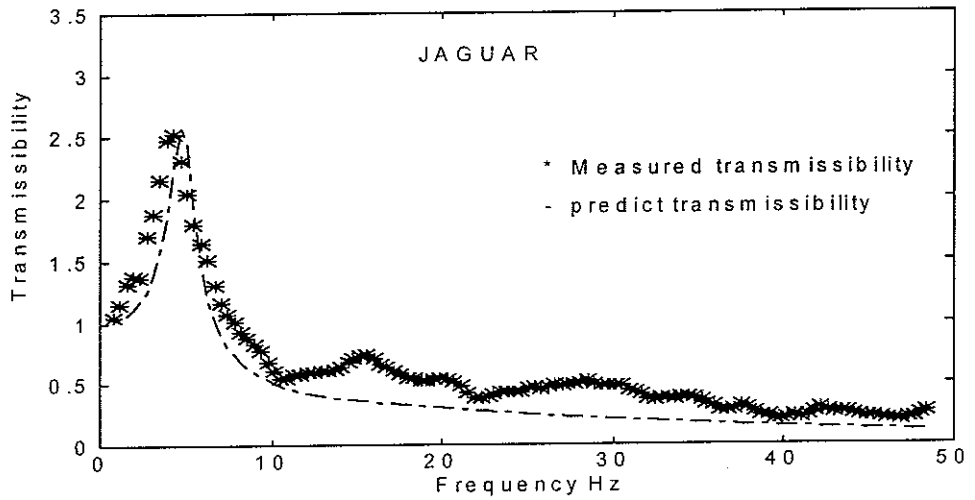

Figure 2.9.6 Comparison between predicted and measured transmissibilities of three seats (using new model with stiffness k_b=13000 N/m and damping c_b=100 Ns/m)

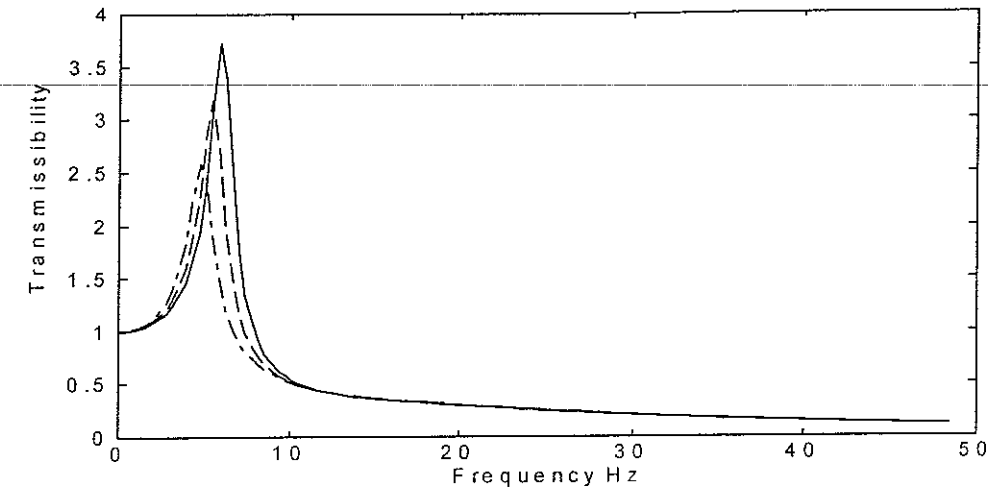

Figure 2.9.7 The effect of backrest stiffness k_b (..... k_b=13000 N/m, ... k_b=23000 N/m, ... k_b=33000 N/m)

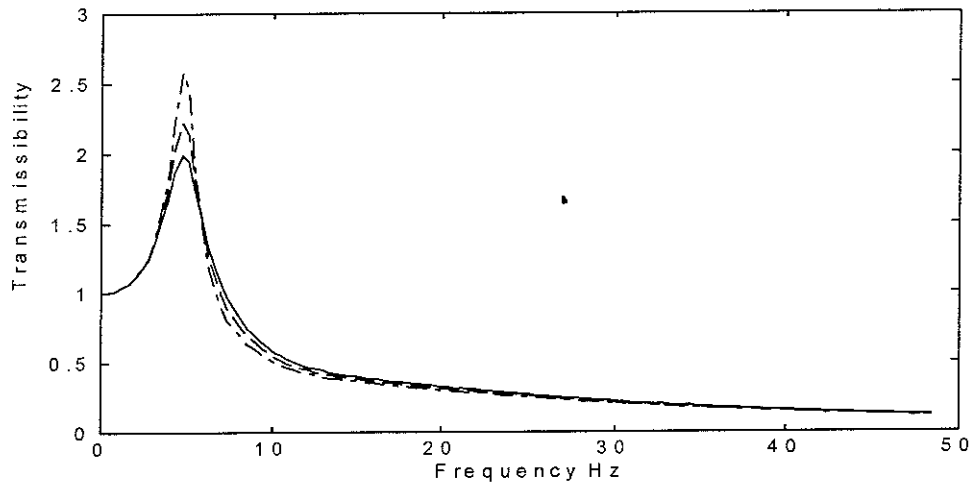

Figure 2.9.8 The effect of backrest damping c_b (..... c_b=100 Ns/m, ... c_b=200 N/m, ... c_b=300 N/m)

3 Measuring seat transmissibility using mechanical analogues of seated humans

3.1 Introduction

The modelling work presented in Section 2 shows that the normalised apparent mass of sixty seated subjects could be adequately represented by ideal mass-spring-damper systems with one or two degrees-of-freedom. This suggests that it should be possible to replace the human subject in a seat test by a simple mechanical dummy.

The use of a mechanical dummy to measure seat transmissibility would circumvent the need for safety precautions with subjects and repeat tests to account for variability between subjects.

Tests with prototype mechanical dummies have shown that they can give similar results to human subjects in measurements of vertical seat isolation carried out on a laboratory simulator (Suggs *et al*, 1969, Huston *et al*, 1998) and in an automobile (Mansfield and Griffin, 1995).

Mechanical suspension components have limitations that restrict their dynamic performance when the excitation magnitude is outside of an optimum operating range. A single degree-of-freedom mechanical dummy was constructed (Mansfield, 1998) so as to investigate the factors that are likely to limit dummy dynamic performance in tests of the vertical vibration isolation of vehicle seats.

A mass of 46 kg was suspended on four compression springs, with a combined stiffness of approximately 45,000 N/m (see Figure 3.1.1). The dummy was initially fitted with a conventional oil-filled damper, which was selected for low friction. The 46 kg mass was constrained to move in the vertical direction, relative to a 6 kg rigid frame by linear ball bushings running on steel shafts. The frame was supported on a SIT-BAR shaped seat indenter (Whitham and Griffin, 1977).

The dummy was supported on a force platform (Kistler model Z 13053), which was mounted on an electrodynamic shaker. The acceleration at the base of the dummy was measured using an Entran EGCSY-240-D-10 piezo-resistive accelerometer. The apparent mass of the dummy, $M(\omega)$, was calculated from:

$$M(\omega) = \frac{G_{af}(\omega)}{G_{aa}(\omega)} \qquad (3.1.1)$$

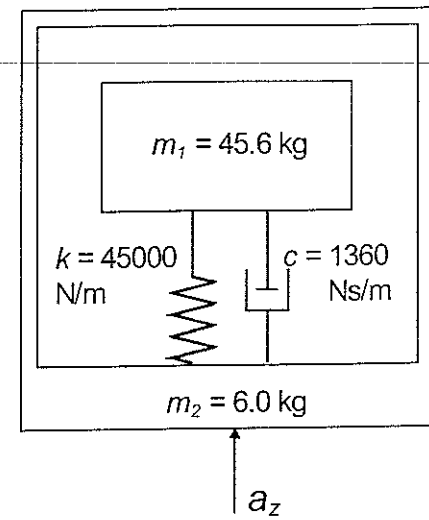

Figure 3.1.1. A single degree-of-freedom mechanical system with an apparent mass similar to the mean of sixty seated subjects (after Fairley and Griffin, 1989).

where $G_{af}(\omega)$ is the cross-spectral density of the force and acceleration and $G_{aa}(\omega)$ is the power spectral density of the acceleration at the base of the dummy at radial frequency ω. Figure 3.1.2 shows the dummy apparent masses measured with vertical broad-band (0 Hz to 20 Hz) random vibration at five magnitudes between 0.35 ms^{-2} and 2.0 ms^{-2} r.m.s.

With a conventional damper, the magnitude of the apparent mass of the dummy was affected markedly by the vibration magnitude at most frequencies between 1 Hz and 20 Hz (see Figure 3.1.2). At lower magnitudes of vibration the response was increasingly influenced by friction, resulting in lower apparent masses in the region of the resonance frequency and higher apparent masses at frequencies above about 6 Hz. Most of the friction in the mechanism could be attributed to the damper, even though the damper used had been specially designed to minimise friction. Valves incorporated in the damper, to achieve a pressure drop proportional to velocity, may also have contributed to the non-linear response.

3.1.1 Performance requirements

A mechanical dummy for making standardised measurements of seat transmissibility, both in laboratory conditions and in a variety of real vehicles, should be capable of representing the apparent mass of a human subject with a wide range of seat vibration characteristics.

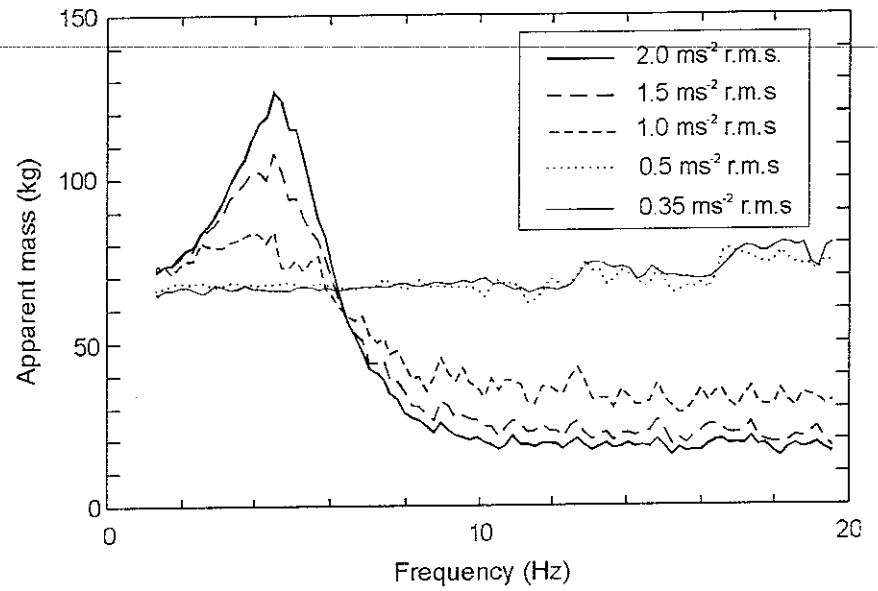

Figure 3.1.2. Apparent mass of prototype dummy with conventional oil-filled damper, measured at five vibration magnitudes.

The apparent mass of a seated subject has been shown to be affected by the magnitude of the seat vibration. Fairley and Griffin (1989) showed that the main resonance frequency in the apparent masses of eight subjects consistently decreased with increasing vibration magnitude. The mean resonance frequency decreased from 6 Hz to 4 Hz when the magnitude of the broad-band seat vibration increased by a factor of eight, from 0.25 ms-2 to 2.0 ms-2 r.m.s.

A dummy that was fully representative of human subjects would have a similar characteristic. However, since the effect of vibration magnitude is similar to inter-subject variability, an apparent mass characteristic that did not change over a wide range of vibration magnitudes can be expected to provide useful results for many seat test applications. A fixed characteristic provides a more easily defined yardstick than a characteristic that varies according to the test input magnitude.

For carrying out standard seat tests, the most important characteristic is to give repeatable results. It should not be possible to introduce a significant variation in results with small variations in test conditions.

3.2 Development of a Passive Anthropodynamic Dummy

3.2.1 Required complexity

Fairley and Griffin (1989) found that the mean normalised apparent mass of sixty seated subjects could be represented by an ideal single degree-of-freedom mass-spring-damper system with a natural frequency of 5 Hz. The apparent mass of the single

degree-of-freedom system was within ± 1 standard deviation of the mean measured normalised apparent mass at most frequencies between 0 Hz and 20 Hz. This suggests that, for the purposes of a standardised test, a single degree-of-freedom system should be sufficient to represent the load presented to a seat by a human subject. Additional degrees of freedom require additional mechanical complexity, which is likely to result in decreased reliability, and decreased maintainability, leading to reduced repeatability.

3.2.2 Contribution of the damper to apparent mass response

3.2.2.1 Dynamic stiffness measurements on alternative dampers

As reported in Section 3.1, most of the friction in the Mansfield and Griffin dummy could be attributed to the damper, even though the damper used had been specially designed to minimise friction.

Alternative damper designs were sought that eliminated the need for sliding oil seals or valves. Two custom made devices have so far been investigated: these are illustrated in Figure 3.2.1. One device comprised a viscous dashpot, in which an open tube moves in and out of an open bath of viscous fluid. The other device is a combined air spring and fluid damper, using a rolling rubber diaphragm to contain the damping fluid. The air spring incorporated in the second device could be configured to replace both the conventional damper and the compression springs in the prototype dummy. Measurements were made of the force-response characteristics of these devices so as to determine their suitability for use in a dummy for seat testing.

The dynamic characteristics of a damper may be characterised by its dynamic stiffness. The dynamic stiffness, $S(\omega)$, is a complex quantity, which is equivalent to:

$$S(\omega) = K(\omega) + j\omega C(\omega) \qquad (3.2.1)$$

where $K(\omega)$ is the equivalent spring stiffness and $C(\omega)$ is the equivalent viscous damping at radial frequency ω, and $j = (-1)^{-2}$.

Hence the equivalent spring stiffness and viscous damping may be derived from:

$$K(\omega) = \text{real}(S(\omega)) \qquad (3.2.2)$$

and

$$C(\omega) = \text{imag}\left(\frac{S(\omega)}{\omega}\right) \qquad (3.2.3)$$

In an ideal damper, the viscous damping would be independent of frequency (i.e. $C(\omega) = c$ (the damping constant), and $K(\omega) = 0$ for all ω).

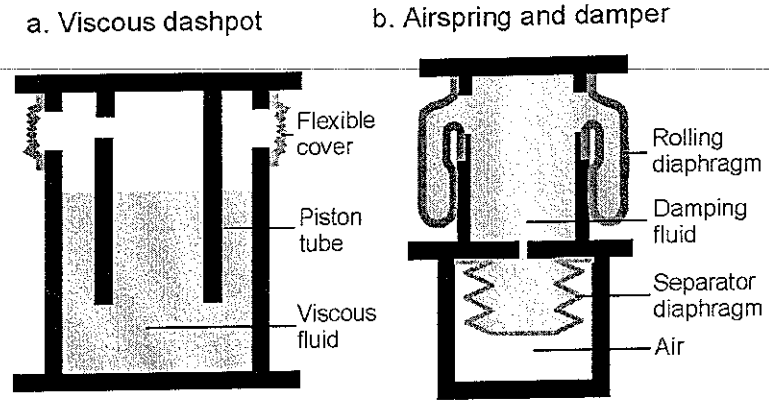

Figure 3.2.1. Sections through (a) the viscous dashpot and (b) the air spring and damper.

The dampers were mounted between an electrodynamic shaker and an immovable frame. The acceleration across the damper was measured by an accelerometer on the shaker mounting, and the applied force was measured by a force cell (Kistler type 9321 A) between the damper and the fixed frame. Each damper was excited by broad-band random vibration at three magnitudes, and the dynamic stiffness, $S(\omega)$, was calculated from:

$$S(\omega) = \omega^2 \frac{G_{af}(\omega)}{G_{aa}(\omega)} \qquad (3.2.4)$$

The power spectral density of the input acceleration signal is shown in Figure 3.2.2a. The acceleration spectrum was shaped so as to represent the accelerations across the damper of the ideal single degree-of-freedom model, when the base of the model was excited by the broad-band random acceleration spectrum shown in Figure 3.2.2b. The acceleration signals had W_b frequency-weighted magnitudes of 0.25, 0.75 and 1.25 ms^{-2} r.m.s (BS 6841, 1987).

An ideal damper would have constant viscous damping at all frequencies, and no spring stiffness. Figure 3.2.3 and Figure 3.2.4 show that, particularly at low excitation magnitudes, the response of a conventional damper as used by Mansfield and Griffin (1996) departed from ideal characteristics. Most of the departure from the ideal response can be explained by the presence of friction, particularly in the sliding seals, even though this damper had been specially selected for low friction.

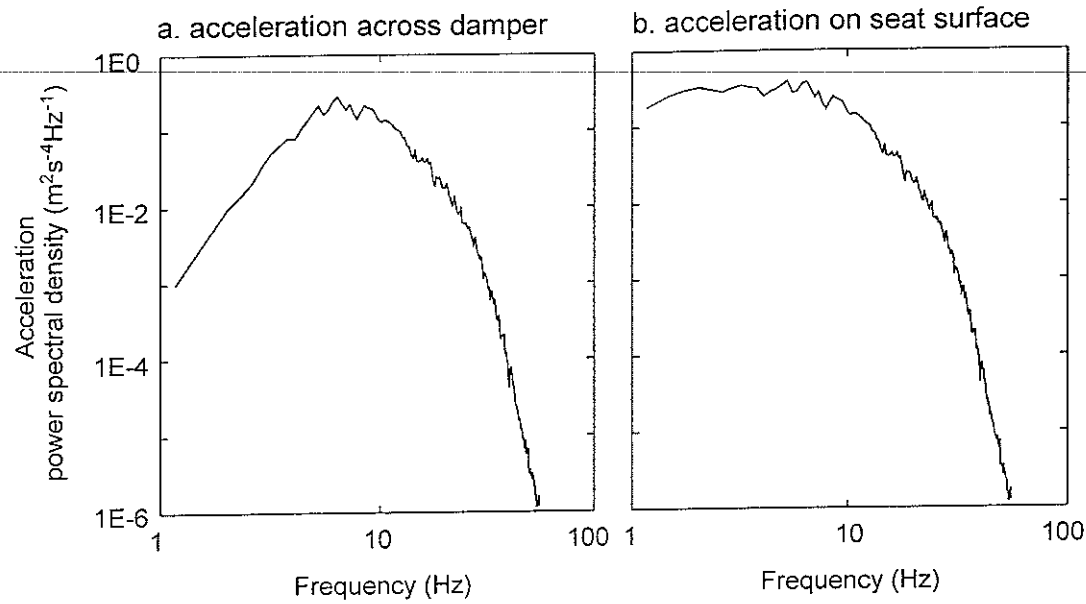

Figure 3.2.2. Power spectral densities of the input accelerations used to measure the dynamic stiffness of the dampers (a) and the apparent mass of the revised prototype dummy (b). The signal in (a) is representative of the acceleration across the spring and damper of an ideal single degree-of-freedom system when excited at the base by the acceleration in (b).

Measurements with the combined air spring and damper indicated a greater dependence of the viscous damping on excitation frequency than with the conventional damper (see Figure 3.2.5). The spring stiffness was constant at higher frequencies, but less at very low frequencies (see Figure 3.2.6). There was little variation in viscous damping with excitation magnitude, but the spring stiffness was higher at lower magnitudes. The equivalent viscous damping and the equivalent spring stiffness of the test unit both departed from ideal values at 5 Hz, so adjustments would be required to both the air volume and orifice sizes to achieve the desired resonance frequency. The reduction in spring stiffness with increasing excitation magnitude in this unit might be capable of reducing the resonance frequency of the apparent mass, as observed in human subjects.

Figure 3.2.7 shows the equivalent viscous damping of the viscous dashpot, as a function of excitation frequency. It can be seen that the damping provided by this device tended to reduce with increasing excitation frequency. Figure 3.2.8 shows that the force response of the viscous dashpot also had a significant spring stiffness component, which increased with increasing frequency. However, there was little variation in either the equivalent viscous damping or in the equivalent spring stiffness over a five-to-one range of excitation magnitudes. The results indicate that the apparent mass of a mechanical dummy in which the damping was provided by a viscous dashpot would be virtually unaffected by vibration magnitude, at least up to the

highest excitation magnitudes employed in the measurements. The high stiffness of the viscous dashpot would require a compensatory reduction in the stiffness of the compression springs so as to achieve the same resonance frequency in the dummy.

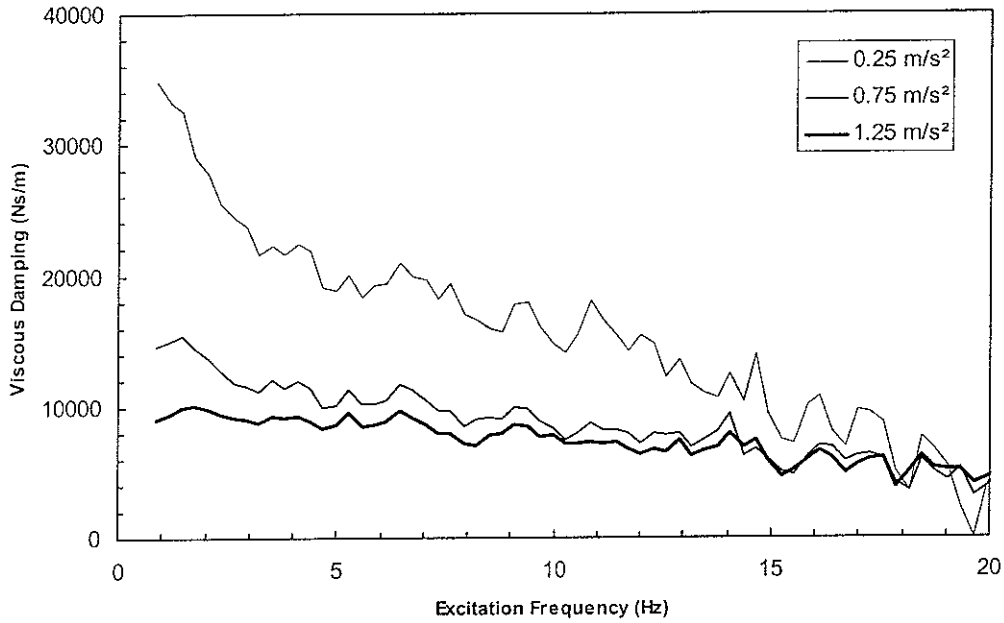

Figure 3.2.3. The measured equivalent viscous damping of the conventional damper, as a function of frequency and excitation magnitude.

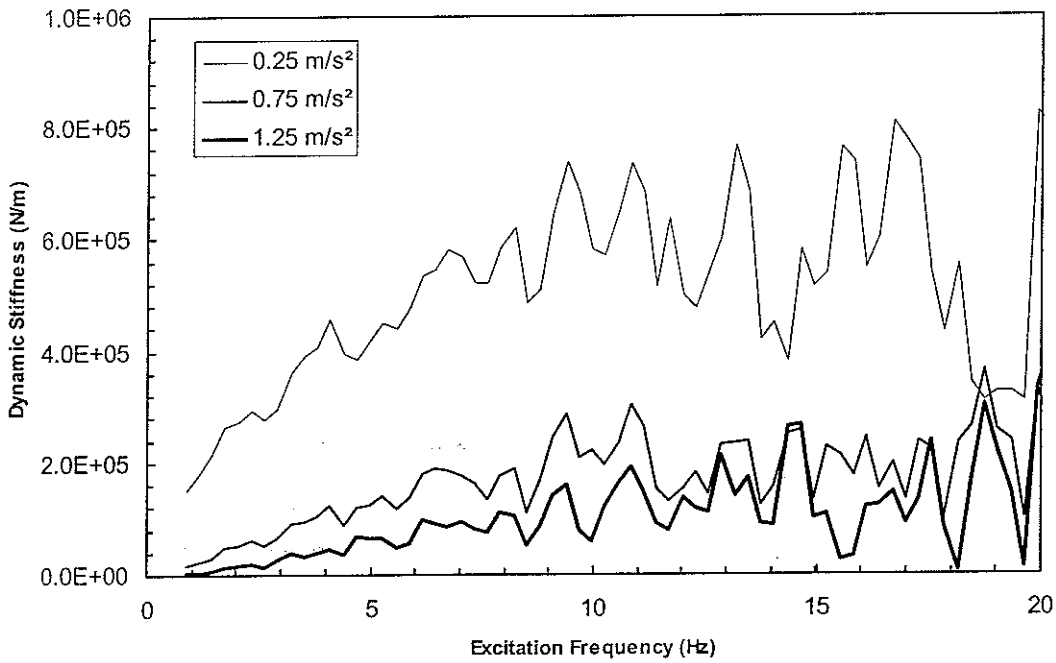

Figure 3.2.4. The measured equivalent spring stiffness of the conventional damper, as a function of frequency and excitation magnitude.

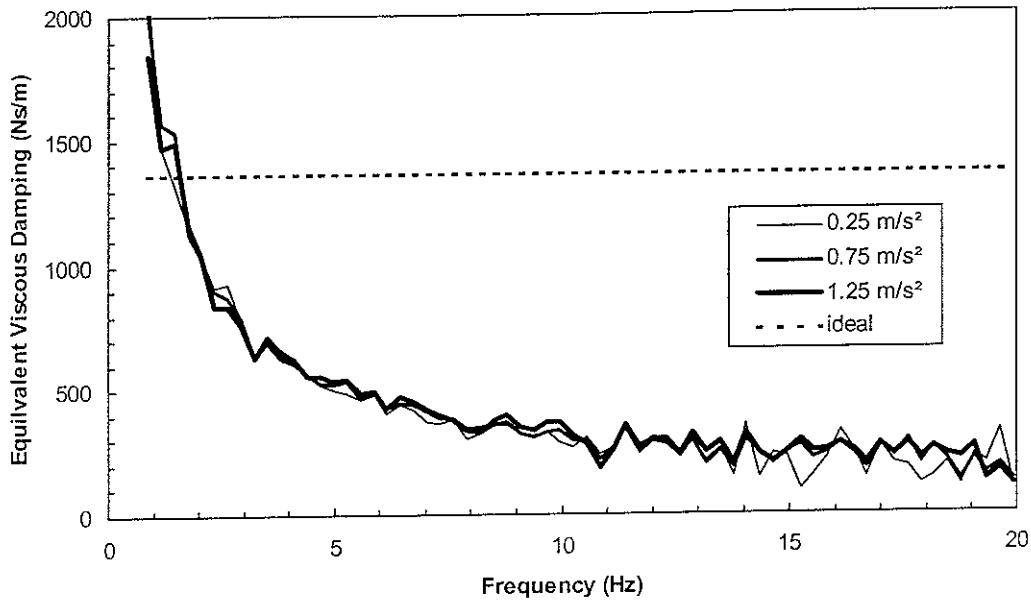

Figure 3.2.5. The equivalent viscous damping of the combined air spring and damper, as a function of frequency and excitation magnitude.

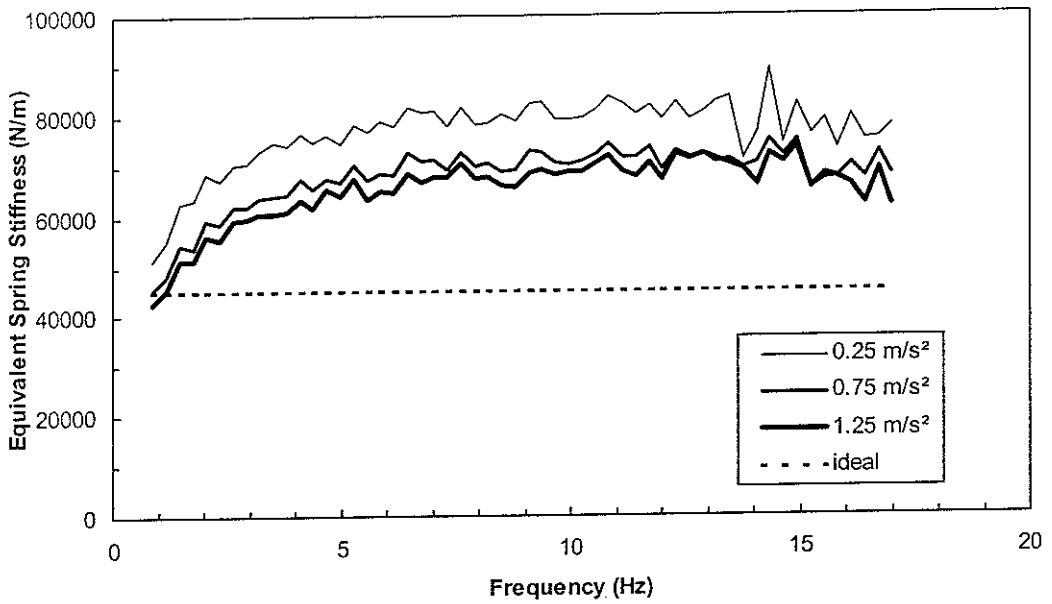

Figure 3.2.6. The equivalent spring stiffness of the combined air spring and damper, as a function of frequency and excitation magnitude.

The apparent mass of a dummy using the viscous dashpot may be expected to deviate from that of the equivalent single degree-of-freedom model at frequencies above and below resonance due to the variation in viscous damping and spring stiffness with excitation frequency.

Figure 3.2.9 shows that the viscous damping provided by the viscous dashpot varies linearly with end-plate separation (i.e. with the depth of the piston-tube in the viscous fluid: see Figure 3.2.1a) over a small range. This gives the possibility of adjusting the damping by up to 25%. Figure 3.2.10 shows that there is only a small variation in apparent spring stiffness with end-plate separation, especially at low frequencies.

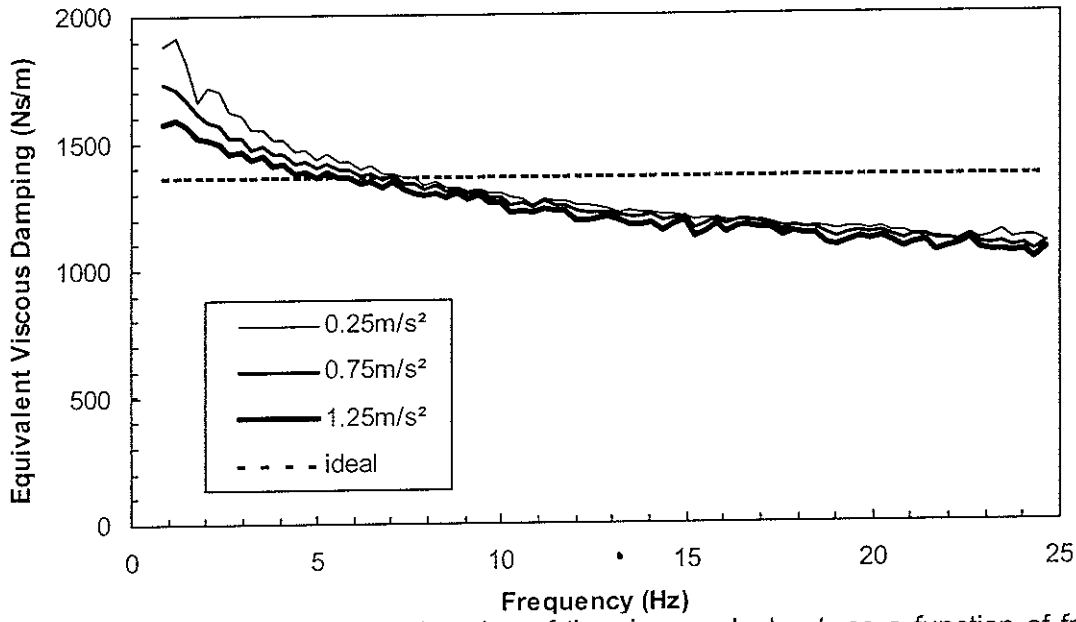

Figure 3.2.7. The equivalent viscous damping of the viscous dashpot, as a function of frequency and excitation magnitude.

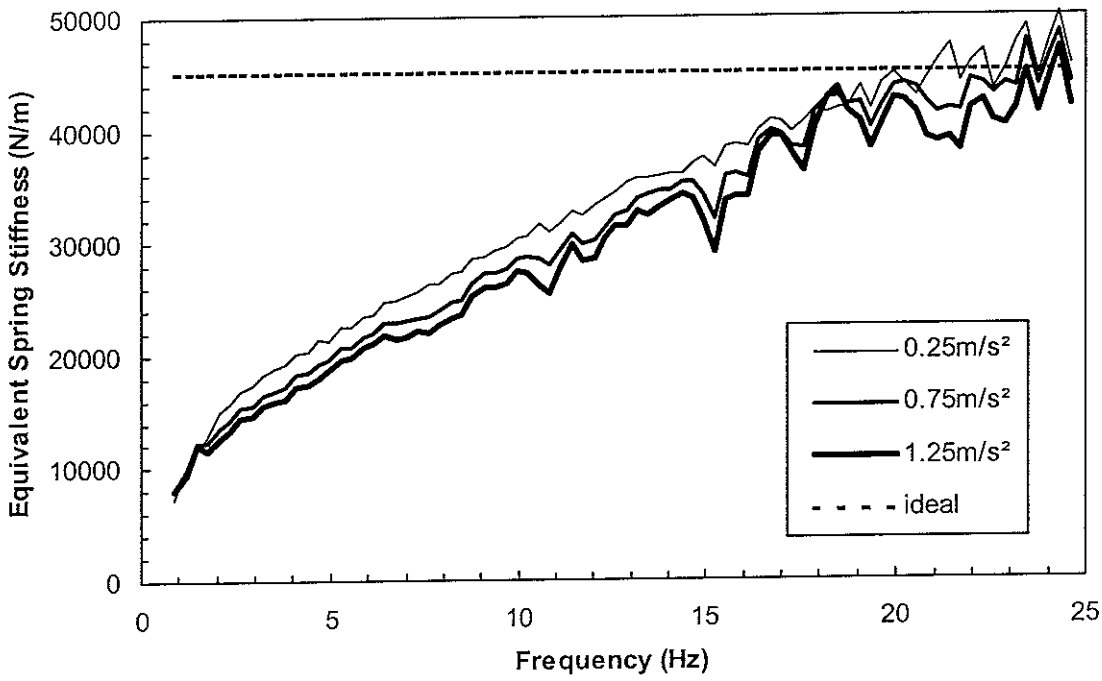

Figure 3.2.8. The equivalent spring stiffness of the viscous dashpot, as a function of frequency and excitation magnitude.

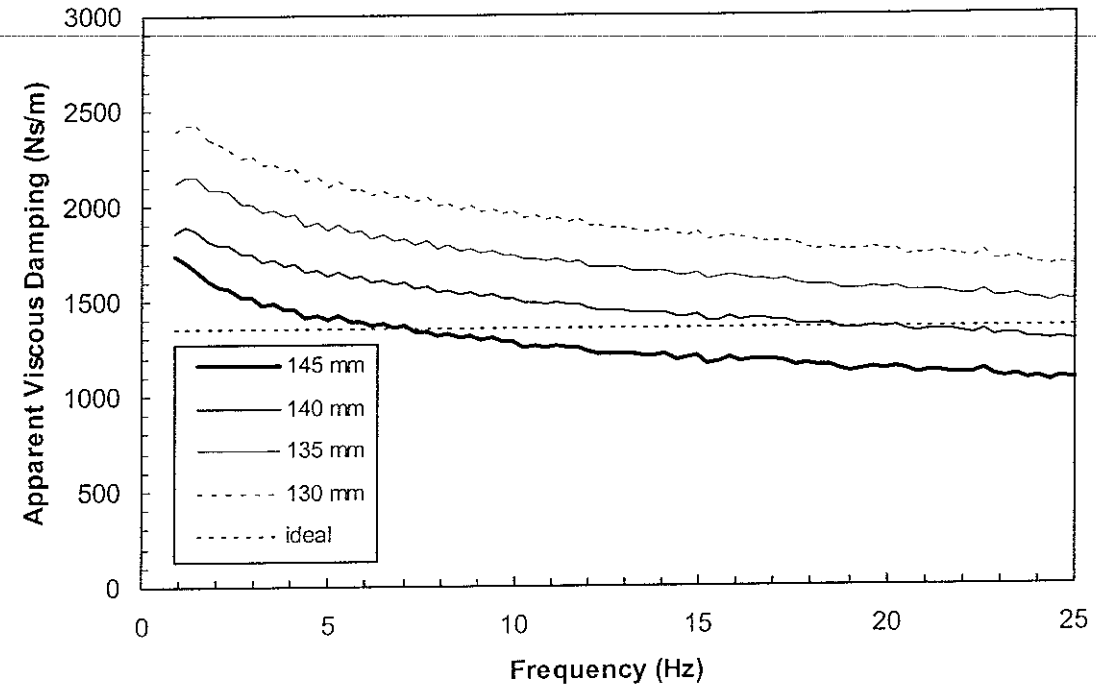

Figure 3.2.9. The effect of end-plate separation on viscous damping of the viscous dashpot.

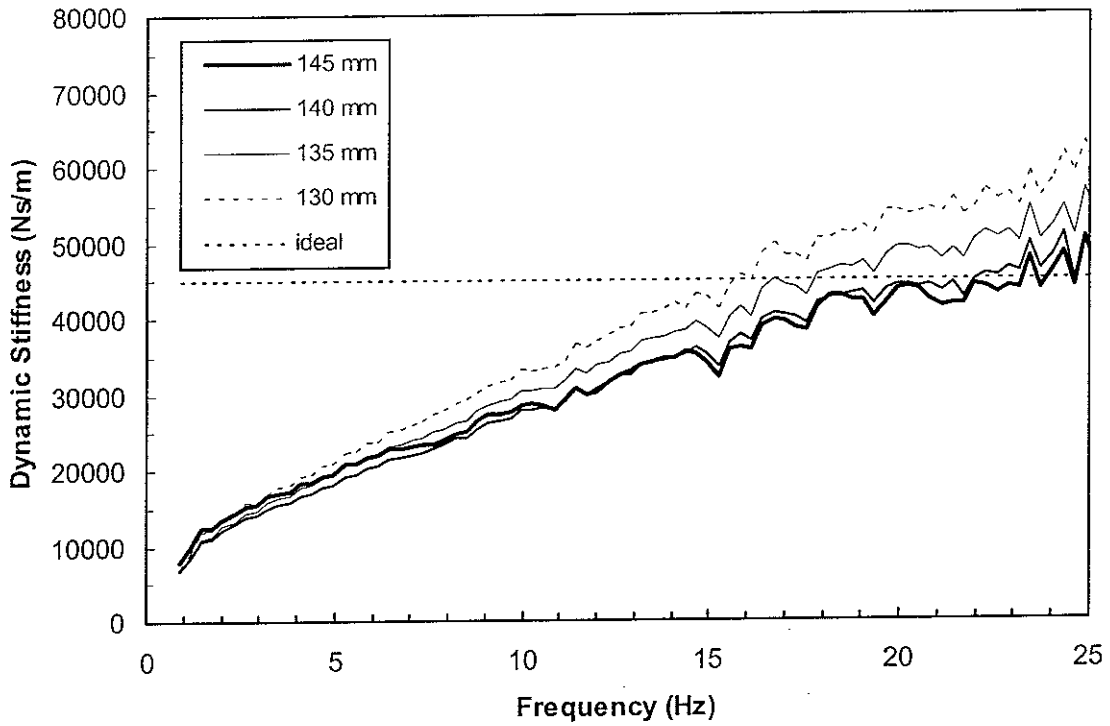

Figure 3.2.10. The effect of end-plate separation on the equivalent spring stiffness of the viscous dashpot.

3.2.3 *Predicting the response of a single degree-of-freedom dummy*

3.2.3.1 *Frequency domain model*

In the frequency domain, the apparent mass of the single degree-of-freedom mechanical dummy may be calculated from:

$$M(\omega) = m_1\left(\frac{S(\omega)+k}{-\omega^2 m_1 + S(\omega)+k}\right) + m_2 \qquad (3.2.5)$$

$$= m_1\left(\frac{j\omega C(\omega)+K(\omega)+k}{-\omega^2 m_1 + j\omega C(\omega)+K(\omega)+k}\right) + m_2$$

where m_1 is the sprung mass, m_2 is the mass of the fixed frame, k is the stiffness of the compression springs and $S(\omega)$ is the dynamic stiffness of the damper.

Figure 3.2.11 shows the predicted apparent mass modulus of a single degree-of-freedom mechanical dummy with the viscous dashpot and optimised compression springs, compared with the apparent mass of the single degree-of-freedom model by Fairley and Griffin (1989). Although the predicted apparent mass modulus of the dummy is close to that of the single degree-of-freedom model at frequencies up to 20 Hz, Figure 3.2.12 shows that the predicted phase lag of the dummy is greater than that of the model at higher frequencies. Figure 3.2.13 shows the predicted apparent mass of a single degree-of-freedom mechanical dummy with the air spring and damper: the apparent mass was predicted from dynamic stiffness measurements with optimised springing and damping (so as to give a similar apparent mass at resonance to that of the ideal model).

3.2.3.2 *Comparison of predicted and measured responses*

The conventional damper in the prototype dummy was replaced by the viscous dashpot, and the stiffness of the compression springs was reduced towards the value used in the predictions shown in Figure 3.2.11 (the actual value was slightly higher, due to the availability of stock spring components).

The apparent mass of the dummy was measured using the procedure described in Section 3.1, but using the input accelerations shown in Figure 3.2.2. The measured apparent masses are compared in Figure 3.2.14 with the apparent mass from an equivalent one degree-of-freedom system. Figure 3.2.14 confirms that the modulus of the measured apparent mass is close to the predicted values with W_b frequency-weighted (BS 6841, 1987) input magnitudes in the range 0.25 ms^{-2} r.m.s. to 1.25 ms^{-2} r.m.s.

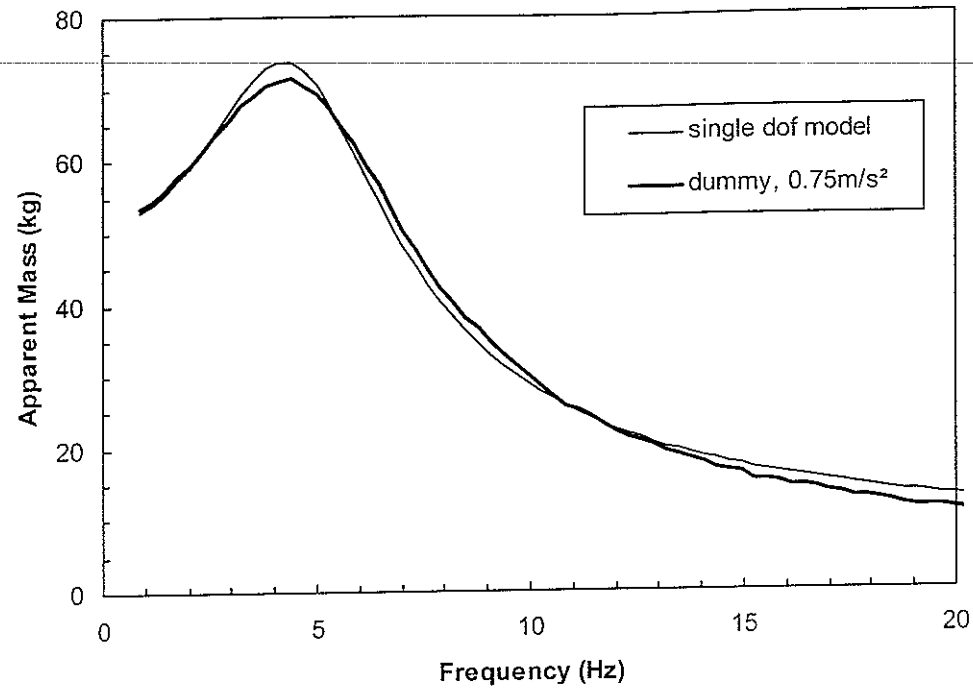

Figure 3.2.11. Comparison of the apparent mass modulus of the Fairley and Griffin (1989) model with the apparent mass of a mechanical dummy with a viscous dashpot, predicted for an excitation magnitude of 0.75 ms^{-2} r.m.s.

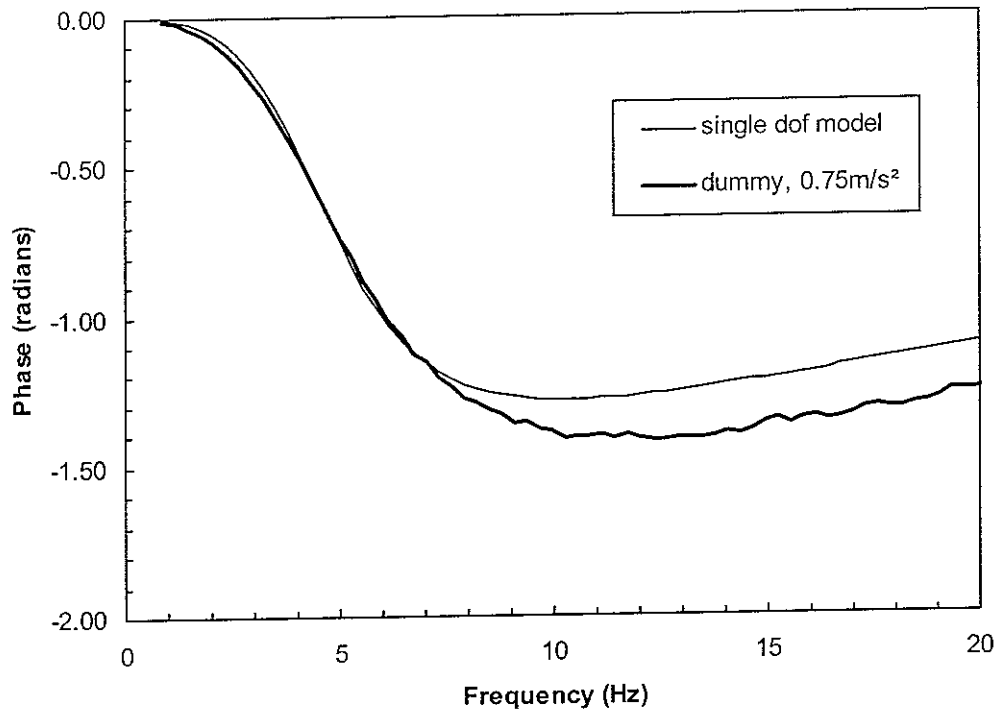

Figure 3.2.12. Comparison of the apparent mass phase of the Fairley and Griffin (1989) model with the apparent phase of a mechanical dummy with a viscous dashpot, predicted for an excitation magnitude of 0.75 ms^{-2} r.m.s.

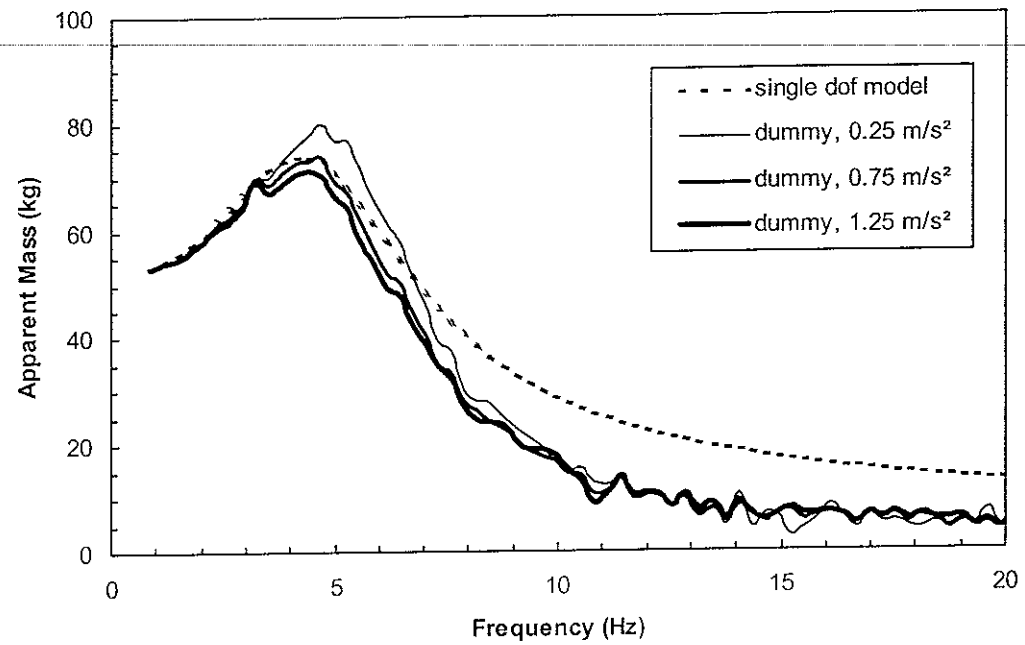

Figure 3.2.13. Comparison of the apparent mass modulus of the Fairley and Griffin (1989) model with the apparent mass of a mechanical dummy with a combined airspring and damper, predicted for three excitation magnitudes.

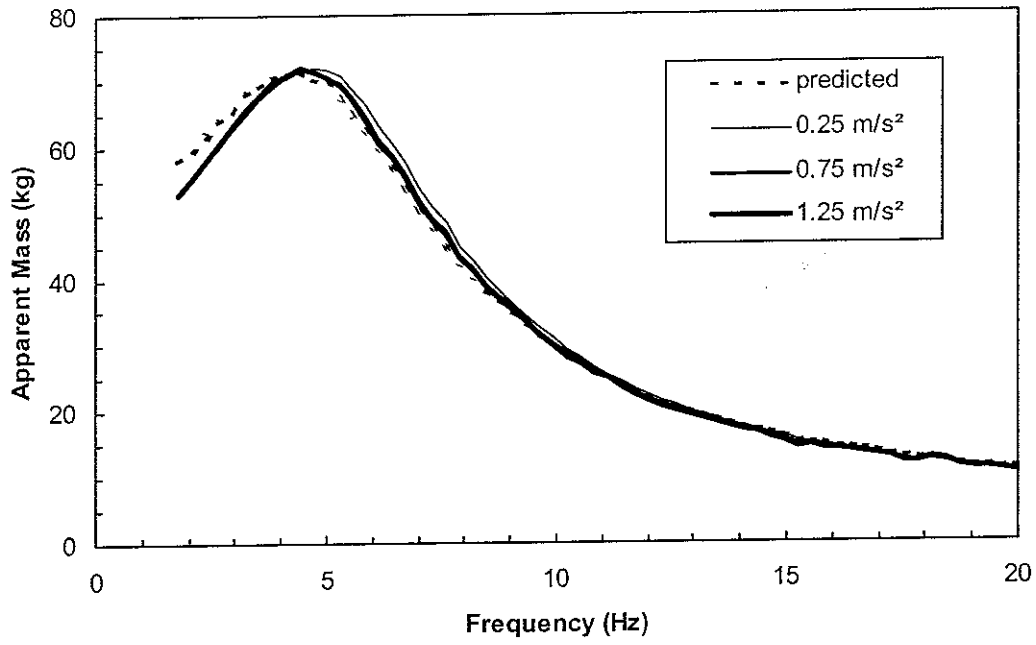

Figure 3.2.14. Effect of excitation magnitude on the measured apparent mass modulus of a single degree-of-freedom mechanical dummy with a viscous dashpot.

3.3 Car seat tests using prototype dummy and subjects

3.3.1 Road tests using prototype dummy and subjects

Measurements have been made in test cars supplied by Ford. The transmissibility of the front passenger seat was measured with four different road and speed conditions, using six human subjects, and six runs with the dummy. The isolation of the seat is indicated by the *SEAT* value, given by:

$$SEAT = \frac{a(seat)_{W_b}}{a(floor)_{W_b}} \qquad (3.3.1)$$

where $a(seat)_{Wb}$ and $a(floor)_{Wb}$ are the r.m.s. magnitudes of acceleration measured on the seat and floor respectively, after frequency weighting with the W_b weighting defined by BS 6841(1987).

3.3.1.1 SEAT values in a Ford Mondeo

In the Ford Mondeo there was good agreement between SEAT values measured with subjects and the dummy in all but one condition (see Figure 3.3.1). The dummy correctly predicted the rank order of the *SEAT* values obtained with subjects on the different roads.

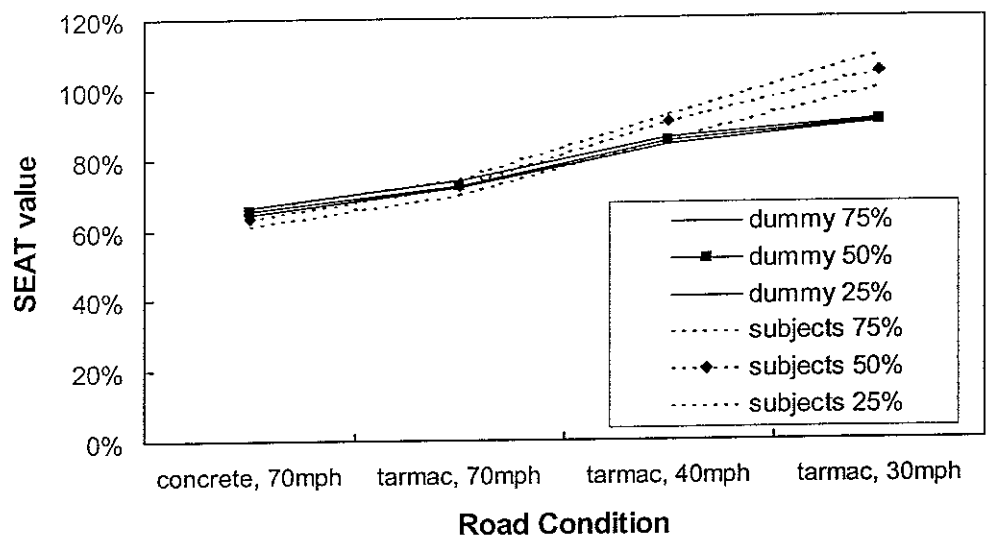

Figure 3.3.1. Seat values measured in Mondeo: medians and interquartile ranges.

3.3.1.2 Seat transmissibilities of a Ford Mondeo seat

Figure 3.3.2 shows that the peak transmissibilities of the Mondeo seat with the dummy were similar to the peak transmissibilities measured with subjects. On the country road (the condition under which the *SEAT* values with dummy and subjects differed most),

the resonance frequency was higher with the dummy. Transmissibilities at higher frequencies were generally greater with the dummy than with subjects.

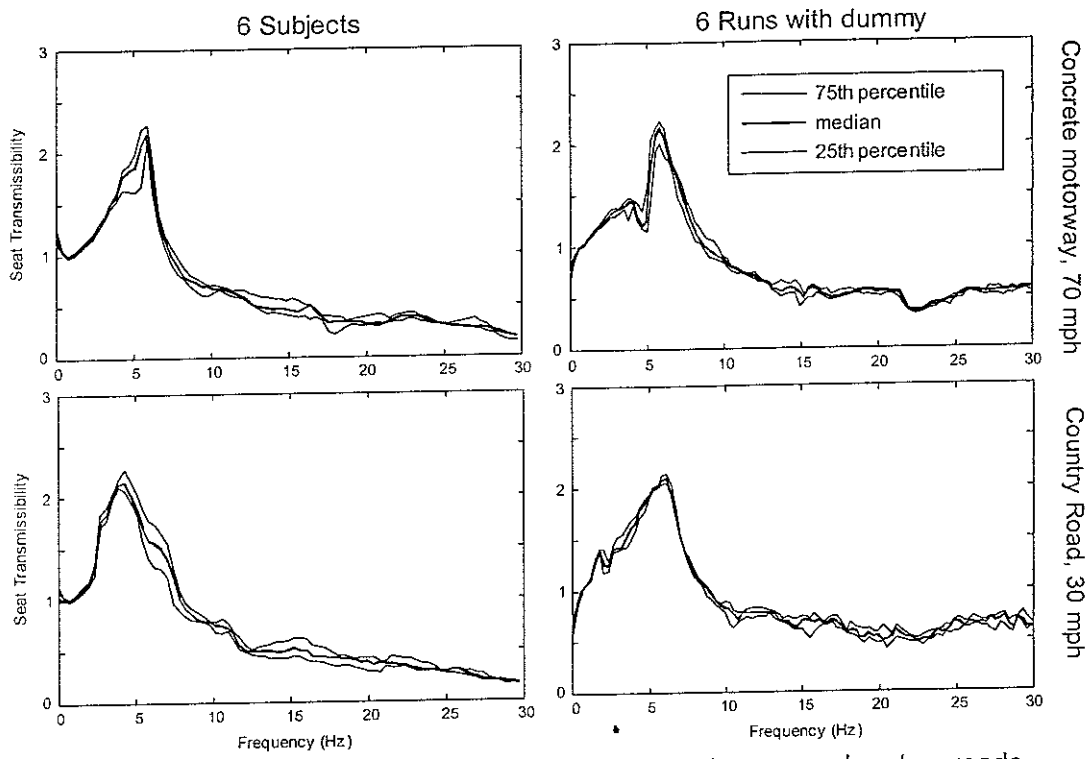

Figure 3.3.2. Transmissibilities of the Mondeo seat measured on two roads

3.3.1.3 *SEAT values in a Jaguar Sovereign*

In the Jaguar (a Jaguar-Daimler Sovereign), the *SEAT* values measured with subjects were overestimated by the dummy in the motorway conditions, but were similar on the slower roads. As with the Mondeo, the rank order of the *SEAT* values with the dummy was the same as for the subjects (see Figure 3.3.3).

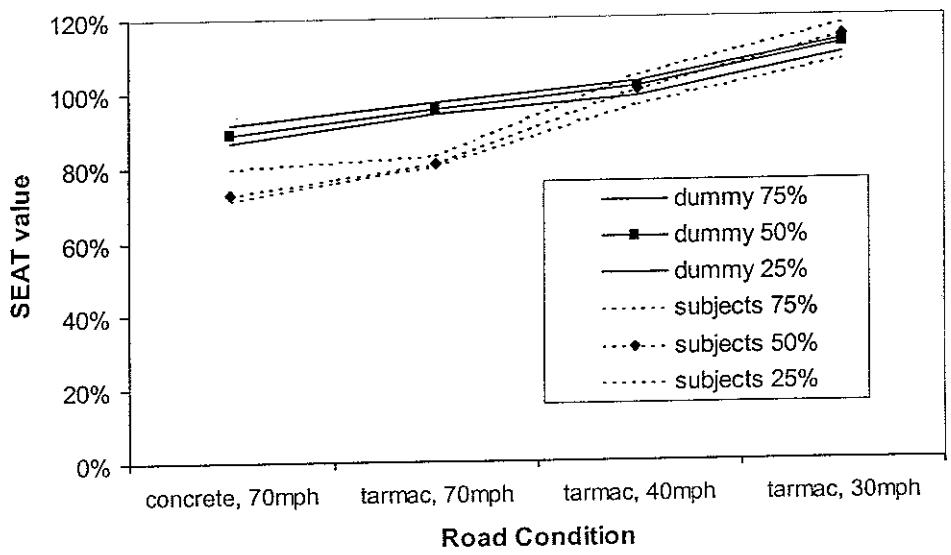

Figure 3.3.3. Seat values measured in Jaguar: medians and interquartile ranges.

3.3.1.4 *Transmissibilities of a Jaguar Sovereign seat*

The transmissibilities measured with subjects in the Jaguar were better predicted with the dummy at frequencies above 5 Hz than at lower frequencies (see Figure 3.3.4). The transmissibility peak with the dummy had the correct magnitude, although the frequency was greater on the country road.

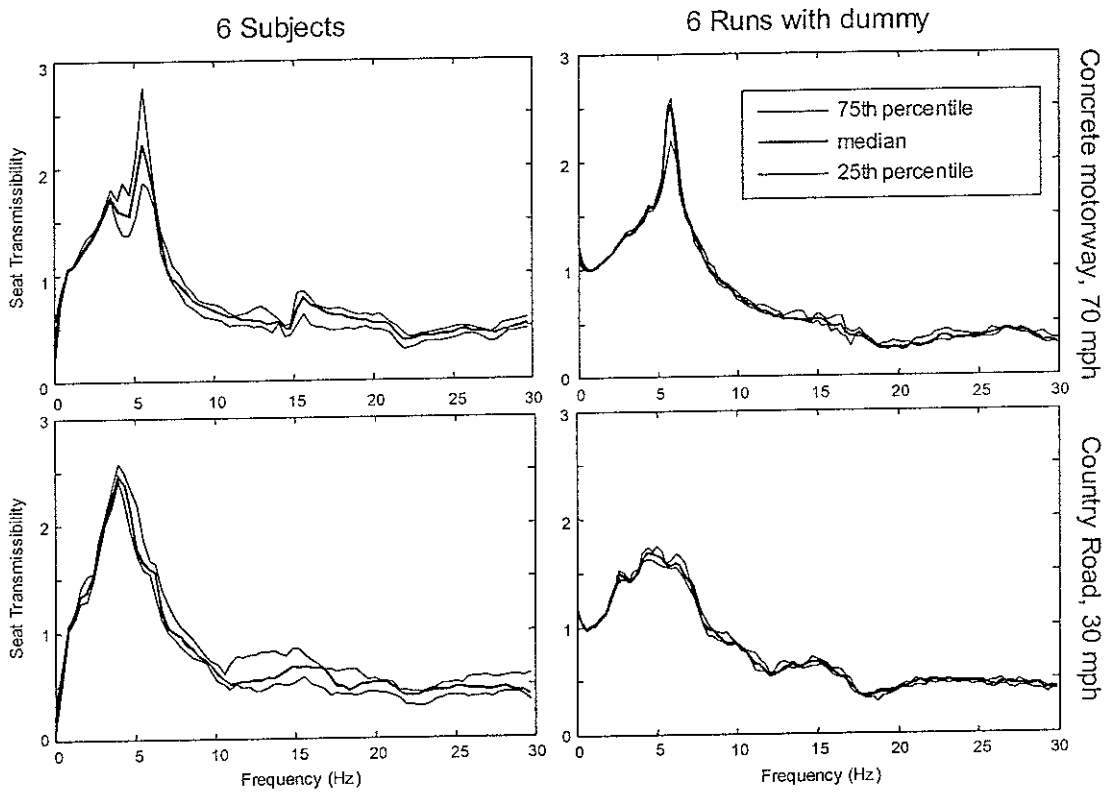

Figure 3.3.4. Transmissibilities of the Jaguar seat measured on two roads

3.3.2 *Laboratory seat tests using prototype dummy and subjects*

The seats from the test cars were mounted on the platform of an electro-hydraulic vibrator and excited by vertical broad-band (0.5 to 40 Hz) vibration. The input motion was presented for 60 seconds at unweighted vibration magnitudes of 0.25, 0.5, 1.0 and 2.0 ms^{-2} r.m.s. Seat transmissibilities were measured using the six human subjects and the anthropodynamic dummy that were used in the road tests.

3.3.2.1 *Comparison between dummy and human subjects*

Figure 3.3.5 compares the transmissibilities of the Mondeo seat measured with the prototype anthropodynamic dummy and a 51 kg rigid mass (i.e. the same as the total mass of the dummy) with the 25th and 75th percentiles of the transmissibilities with the six subjects. The transmissibility measured with the dummy was within the inter-quartile range of the transmissibilities with subjects at frequencies between about 4 Hz and 26 Hz. It can be seen that the transmissibility with the dummy is much closer than that with

the rigid mass to the measurements with subjects at most frequencies above 4 Hz. The resonance peak in the transmissibility with the rigid mass is higher by a factor of more than two, and occurs at a higher frequency than with subjects or with the anthropodynamic dummy.

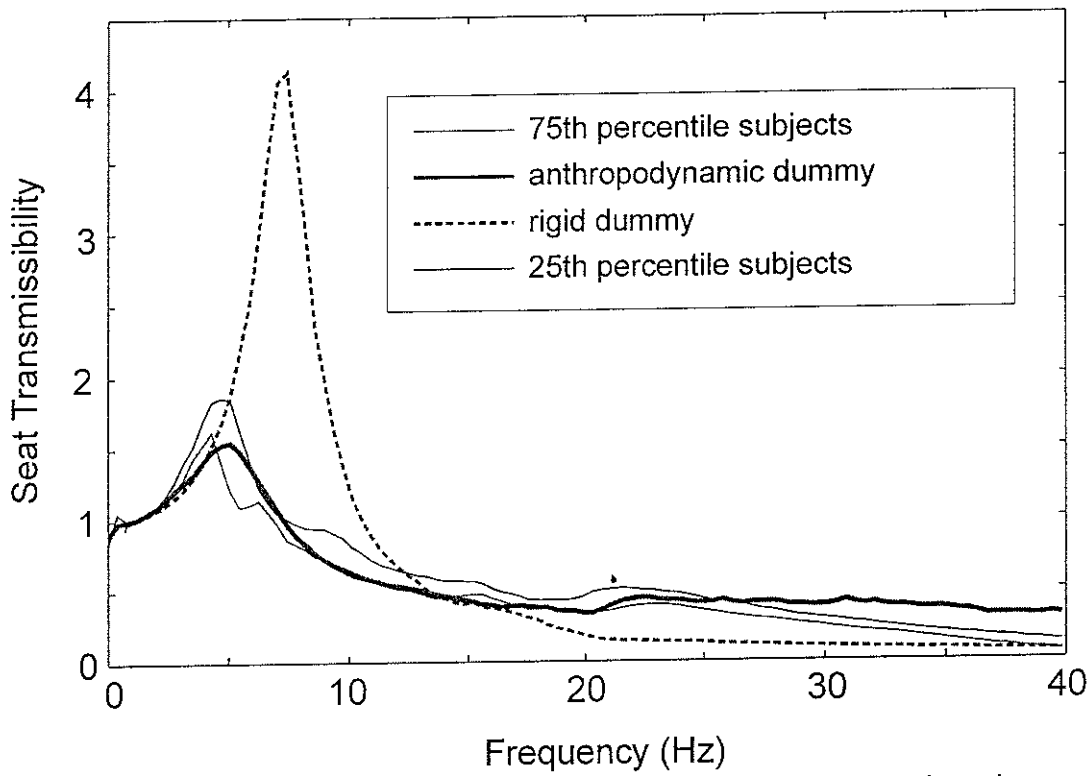

Figure 3.3.5. Mondeo seat transmissibility measured with subjects, dummies and broad-band vibration (1 ms^{-2} r.m.s.)

The transmissibility of the Jaguar seat with the dummy is compared with the inter-quartile range of the transmissibilities with the six subjects in Figure 3.3.6. On the Jaguar seat, the resonance frequency with the subjects was overestimated by the dummy by about 1 Hz. The transmissibility with the dummy is close to the 25th percentile of the measurements with the six subjects at frequencies above 7 Hz, but departs from the inter-quartile range with the subjects over much of the frequency range between 2.5 Hz and 7 Hz.

3.3.2.2 Interaction of dummy with seat back

In the tests reported in Section 3.3.1, the prototype dummy was supported on the seat back by an indenter having the same geometry as that supporting the weight of the dummy on the seat surface. The backrest indenter was rigidly coupled to the fixed frame (see Figure 3.3.7) and was adjusted so that the dummy leant against the backrest with an angle of five degrees from the vertical. Road measurements made by

Mansfield and Griffin (1996) showed that the original prototype anthropodynamic dummy (with a conventional damper), which had a similar backrest support to the dummy described above, gave a good indication of the vertical resonance frequency of the seats in two small cars on six road surfaces.

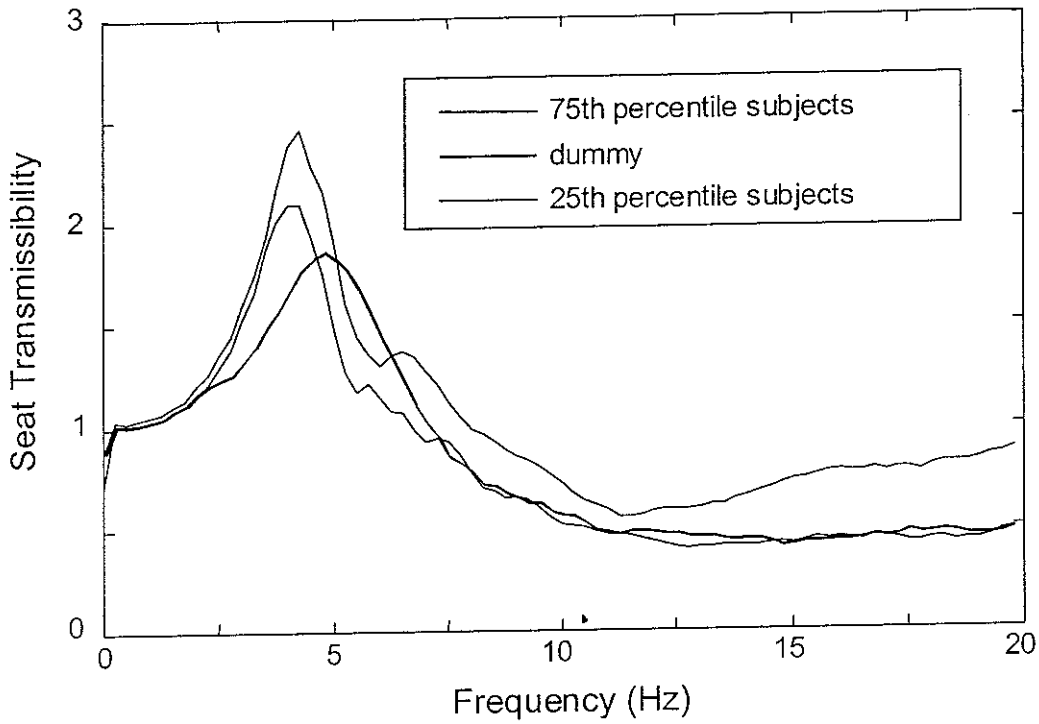

Figure 3.3.6. Jaguar seat transmissibility measured with subjects, dummies and broad-band vibration (1ms^{-2} r.m.s.)

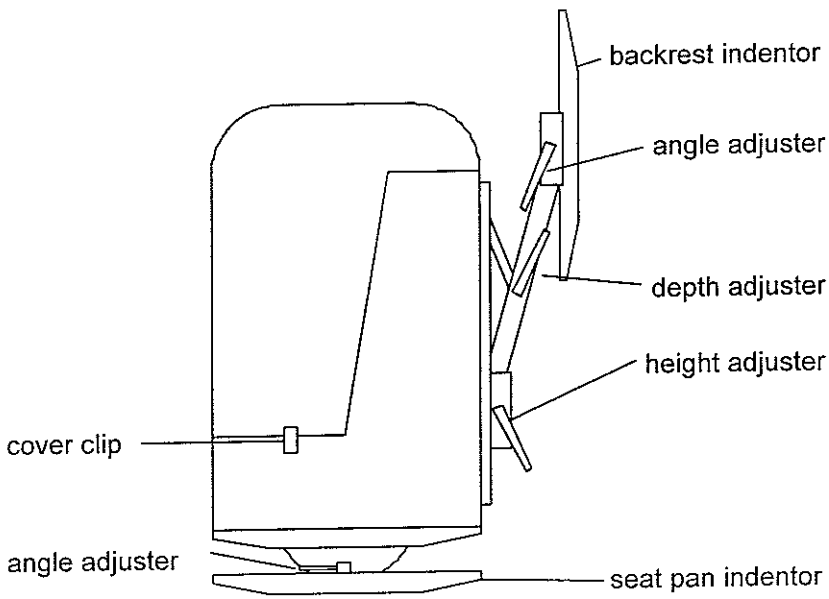

Figure 3.3.7. Seat and seat back supports on the prototype dummy used for the in-vehicle seat tests.

Laboratory measurements of the transmissibility of a car seat with a suspended backrest, showed that the form of backrest contact with a seated subject can have a significant influence on the vertical transmissibility of the seat cushion (Lewis and Griffin, 1996). The backrest on the seat used in that study could be decoupled from the seat frame, allowing it to move freely with the subject in the vertical direction. When the backrest was fixed relative to the seat frame, the resonance in the vertical transmissibility of the seat cushion consistently increased by the order of 0.5 Hz (see Figure 3.3.8).

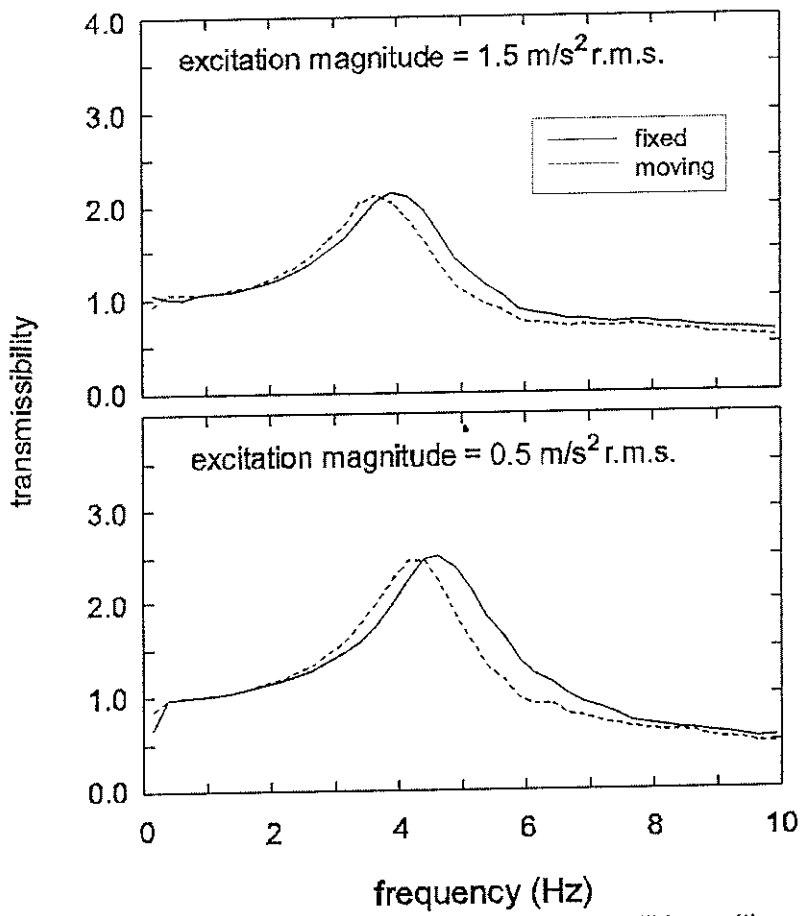

Figure 3.3.8. Comparison of mean vertical seat transmissibilities with a fixed and a moving backrest (after Lewis and Griffin, 1996).

If interaction with the backrest can affect the transmission of vibration through the seat cushion with human subjects, a similar effect may occur with an anthropodynamic dummy. To investigate the effect of backrest interaction with the dummy, a new support was designed for the backrest indenter, incorporating a swinging arm to allow the indenter to move freely in the vertical direction. This had the effect of de-coupling the dummy from the seat backrest.

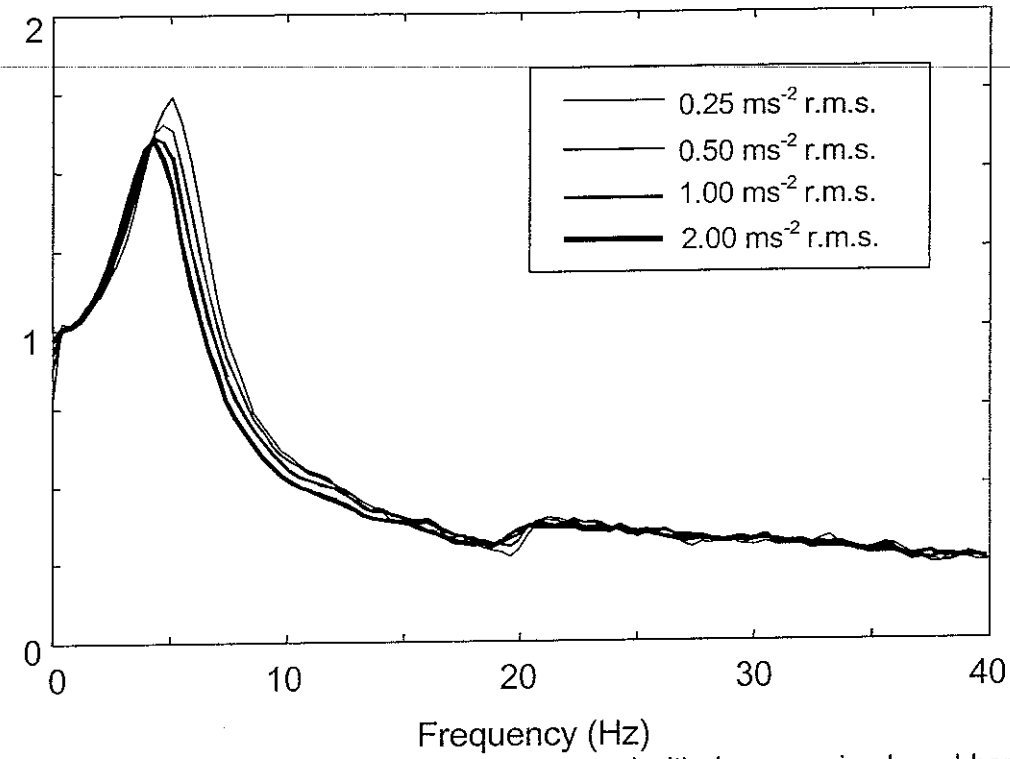

Figure 3.3.9. Transmissibility of Mondeo seat measured with dummy using broad-band vibration: dummy de-coupled from backrest.

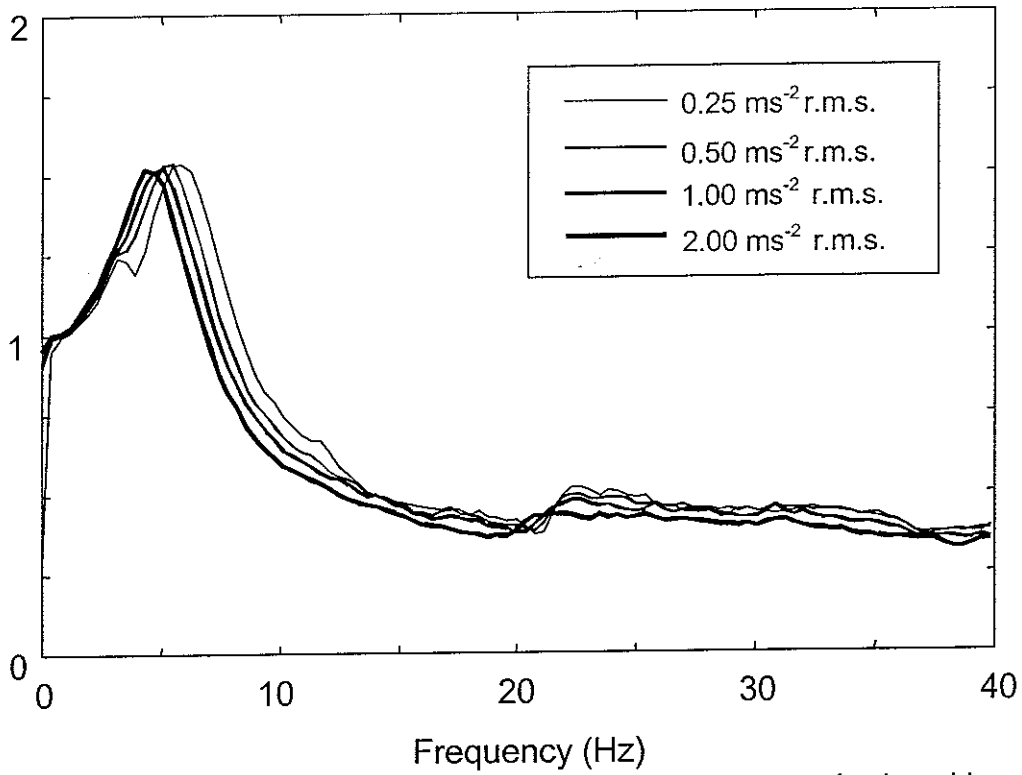

Figure 3.3.10. Transmissibility of Mondeo seat measured with dummy using broad-band vibration: dummy coupled to backrest.

Figure 3.3.9 shows transmissibilities of the Mondeo seat measured with the dummy decoupled from the backrest. By comparison, Figure 3.3.10 shows the transmissibilities measured in similar conditions, but with the fixed backrest support as reported in Section 3.3.1. It can be seen that with a rigidly attached indenter, the transmissibility is more dependant on the vibration magnitude. At the three lower magnitudes of vibration used in the tests, the main resonance in the seat transmissibility occurred at a higher frequency when the backrest indenter was fixed. At the lowest vibration magnitude, a dip in transmissibility was induced at frequencies around 4 Hz when the backrest indenter was fixed. There are large variations in the acceleration spectra in cars between about 2 Hz and 8 Hz, so backrest interaction can be expected to influence results in this frequency range. An important requirement for a standard seat test dummy is a consistent response over a range of excitation magnitudes. The response should also reflect, as realistically as possible, the interaction of human subjects with a seat and seatback. When the dummy is decoupled from the backrest it represents the response of a subject who is also not in contact with the seat back. Further research and testing will be required to develop a dummy that can realistically represent the coupling of a human subject with a seat back.

3.3.3 Development of an improved prototype dummy

It has been shown that it is possible to realise a mechanical dummy with an apparent mass modulus that is close to that of an ideal system up to 20 Hz, and does not vary over a range of excitation magnitudes.

A new prototype dummy is under development, based on the single degree-of-freedom model described above. This prototype incorporates an articulated backrest support and removable masses that can be carried separately, so that it can be easily carried and placed in a seat (see Figure 3.3.11).

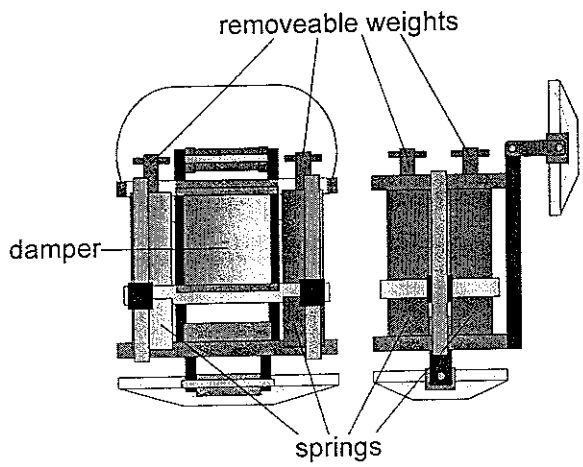

Figure 3.3.11. Schematic of new prototype dummy.

3.4 Development of an active anthropodynamic dummy

3.4.1 *Advantages of active control*

Passive anthropodynamic dummies, based on mass-spring-damper systems, have some limitations. For example, the apparent mass of a passive dummy can only be changed by replacing the components. It would be desirable to be able to easily change the apparent mass of the dummy to match different elements of a population, such as 5th and 95th percentiles, or males and females. The incorporation of an active control system may make it possible to change the response of the dummy by operation of a switch, or by selecting parameters in software.

The response of a passive dummy can be affected by non-linearities and changes in the components with temperature. Active control should be able to reduce the effects of changes in the response of the components. Active control should also make it possible to introduce desired non-linearities in the response, to match the changes in the apparent mass of humans over a range of input accelerations (measurements have shown that the resonance frequency tends to decrease with increases in the magnitude of the seat vibration).

3.4.2 *Description of a prototype active dummy*

The objectives of the preliminary development stage were to show that an electrodynamic vibrator can be used to provide an appropriate damping force to give the same driving-point response as a single degree-of-freedom mass-spring-damper system.

Figure 3.4.1 shows a schematic diagram of the prototype active dummy. Input excitation was provided at the base of the frame by a Derritron VP180LS electrodynamic vibrator. A Kistler force platform was placed between the dummy frame and the shaker so as to measure the excitation force, $f(t)$. The aluminium frame base dimensions were 280mm x 260mm x 20mm. Precision linear guides were situated at the corners of the frame base, each with a diameter of 12mm and rising to a height of 600mm. A movable aluminium platform, on low friction linear bearings, was free to slide vertically along these guides and rested on four springs (70mm in length and 40mm in diameter) that encompassed the linear guides at each corner of the frame base. The total spring stiffness, K, provided by the springs was 46,680 Nm^{-1}. The actuator was fixed to the moving platform. The actuator used in the first prototype was a Derritron VP4 electrodynamic shaker. The mass of the VP4 (38.5 kg) provided a large contribution to the total desired moving mass, m, of 45.0 kg. The moving part of the

actuator was fixed to the aluminium top plate of the dummy frame via a force transducer. The top plate and vibrator armature were immobile with respect to the linear guides and constitute part of the total frame mass, m_B. An LVDT displacement transducer was fixed between the top plate and the body of the actuator so as to measure the relative velocity, *u(t)*, between the moving mass and the frame. Setra 141A capacitive accelerometers were fixed to the moving mass and the frame to measure their respective accelerations $\ddot{y}(t)$ and $\ddot{x}(t)$.

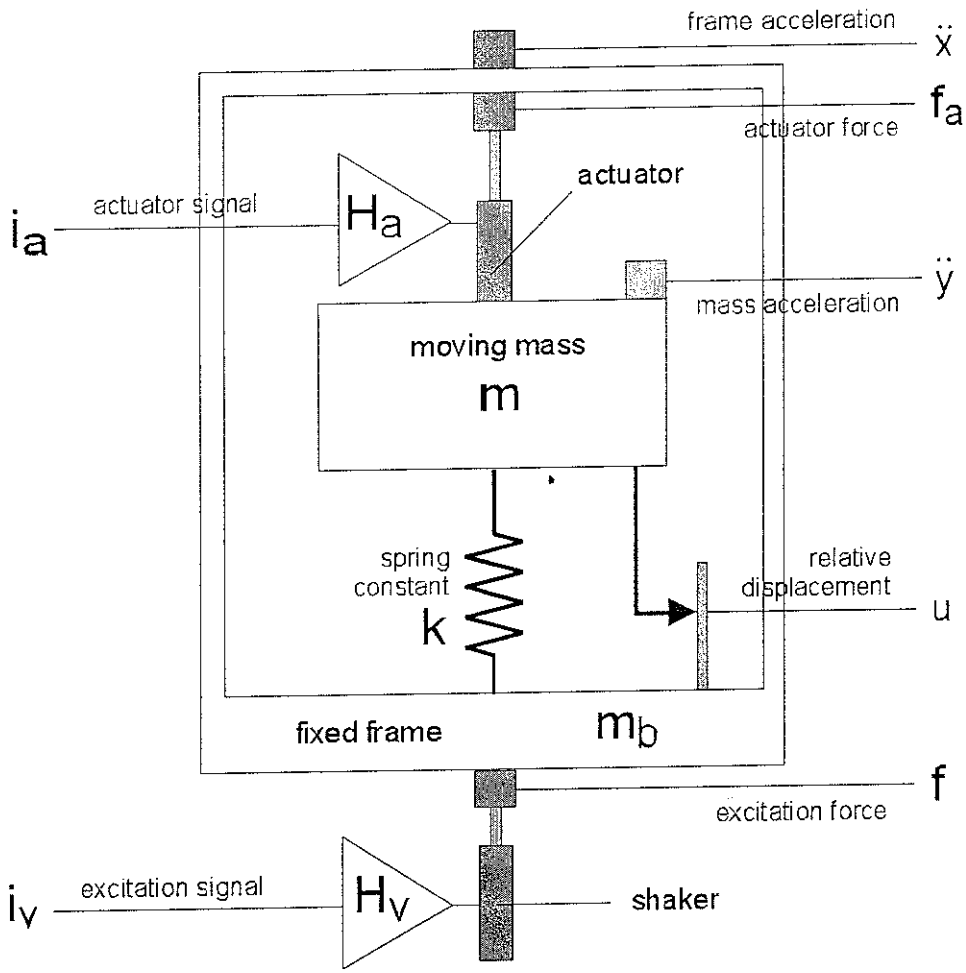

Figure 3.4.1. Schematic diagram of active dummy test rig

3.4.3 Predicting the apparent mass of the active dummy

The equation of motion of the dummy can be expressed as:

$$m\left(\frac{d^2y}{dt^2}\right) = ku(t) + f_a = (k + z(\tau))u(t) \qquad (3.4.1)$$

where

$$u(t) = y(t) - x(t) \qquad (3.4.2)$$

assuming zero initial conditions:

$$(Z(s)+K)X(s)=(ms^2+Z(s)+K)Y(s) \qquad (3.4.3)$$

where $X(s)$ and $Y(s)$ are Laplace Transforms of $x(t)$ and $y(t)$, $s \equiv j\omega$, $j = \sqrt{-1}$ and

$$Z(s)=\frac{Fa(s)}{U(s)} \qquad (3.4.4)$$

The motion transfer function of the dummy is then given by:

$$H_{x,y}(s)=\frac{Y(s)}{X(s)}=\frac{Z(s)+K}{ms^2+Z(s)+K} \qquad (3.4.5)$$

and the apparent mass is given by:

$$M(s)=m_B+m\frac{s^2Y(s)}{s^2X(s)} \qquad (3.4.6)$$

$$=m_B+m\left(\frac{Z(s)+K}{ms^2+Z(s)+K}\right)$$

$$=m_B+m\left(\frac{2\zeta\omega_n s+\omega_n^2}{s^2+2\zeta\omega_n s+\omega_n^2}\right)$$

where ω_n is the natural frequency and ζ is the damping ratio of the equivalent single degree-of-freedom mass-spring-damper system.

3.4.4 Dynamic response of first prototype using VP4 actuator

Preliminary tests were performed by applying a broad-band random acceleration to the dummy frame, having an approximately flat acceleration spectrum between 1 Hz and 20 Hz. The dummy was set up as described in Section 3.4.2.

If the actuator is only required to provide damping force:

$$f_a(t)=c\frac{dU(t)}{dt} \qquad (3.4.7)$$

and:

$$Z(s)=cs \qquad (3.4.8)$$

The system should then behave as a single degree-of-freedom system with natural frequency, ω, and damping ratio, ζ, given by:

$$\omega = \sqrt{\frac{K}{m}} \qquad (3.4.9)$$

$$\zeta = \frac{c}{2\sqrt{Km}} \qquad (3.4.10)$$

The signal from the LVDT displacement transducer was digitised (12 bit resolution), differentiated and filtered using a recursive digital filter, and converted back to analogue form to provide an actuator drive signal (i_a in Figure 3.4.1) proportional to relative velocity. The digital differentiation was performed in real time at a sampling rate of 400 samples per second. The output (velocity) signal was delayed relative to the input (displacement) signal by two sampling increments.

Figure 3.4.2 shows the modulus and phase of the apparent mass of the prototype active dummy, measured with two different values of feedback gain (i.e. the relative magnitude of the actuator drive signal compared to the displacement signal). The measured apparent masses are compared with: (a) the Fairley-Griffin (1989) model (with ω_n = 5 Hz, ζ= 0.475) is, and (b) theoretical response of a single degree-of-freedom model with the same mass and spring stiffness as the prototype dummy (with ω_n = 5.125 Hz, ζ = 0.475).

It can be seen from Figure 3.4.2 that an increase in feedback gain, c, from 0.4 to 1.0 results in a more damped response. However, the resonance frequency appears to be slightly higher than the theoretical response and the variation in apparent mass with frequency can be seen to depart from that of an ideal single degree-of-freedom system. The departure may be partly due to imperfections in the digital differentiator that was used to provide velocity feedback, but it is likely that the main contribution came from the non-ideal force/voltage response of the VP4 vibrator (shown by H_a in Figure 3.4.1). In addition, the armature of the VP4 was suspended on a diaphragm suspension, which made an additional contribution to the total spring stiffness and damping in the system.

3.4.5 Requirements for actuator performance

The output force and displacement required from the actuator were determined assuming an ideal single degree-of-freedom response over the frequency range 1 to 30Hz, with seat acceleration magnitudes up to 2 ms^{-2} r.m.s., and crest factors in the range from 3 to 6.

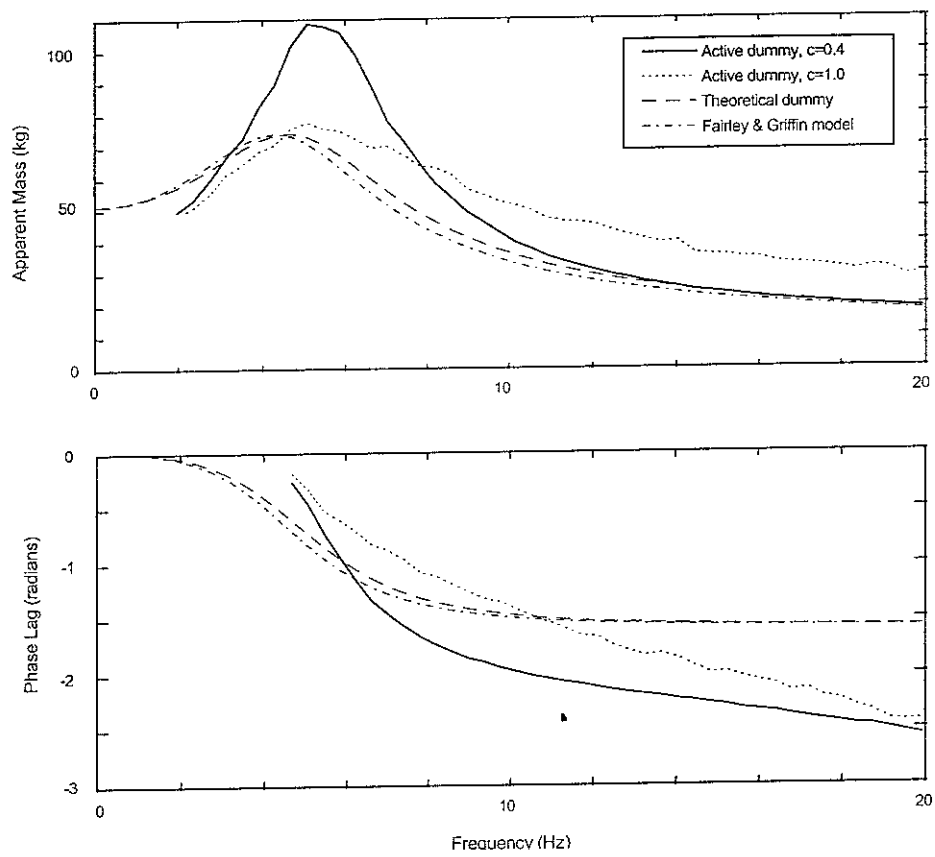

Figure 3.4.2. Apparent mass of dummy with VP4 actuator in comparison with ideal single degree-of-freedom models.

The theoretical relative displacement and damping forces in the Fairley and Griffin (1989) model were determined with two trial input acceleration signals. The first signal comprised band-limited random vibration with an approximately flat spectrum over the frequency range from 1 Hz to 30 Hz. The second signal was measured in the vertical axis on the seat of a car travelling over a rough, unmade road. The characteristics of the two signals are summarised in Table 1, and their acceleration power spectral densities are shown in Figure 3.4.3.

From equations (3.4.1) to (3.4.3), the relative mass/frame motion transfer function between the input acceleration and relative displacement is given by:

$$H_{x.u}(s) = \frac{U(s)}{X(s)} = \frac{-ms^2}{ms^2 + Z(s) + K} \qquad (3.4.11)$$

If the actuator is only required to provide damping force (i.e. $Z(s) = cs$), the transfer function between the frame acceleration and the damping force is given by:

$$H_{\ddot{x}.F_C}(s) = \frac{CsU(s)}{s^2X(s)} \qquad (3.4.12)$$

$$= \frac{-Cs}{s^2 + 2\zeta\omega_n s + \omega_n^2}$$

$$= -m\left(\frac{2\zeta\omega_n s}{s^2 + 2\zeta\omega_n s + \omega_n^2}\right)$$

Using the relationship in equation (3.4.12) the peak damping forces in a single degree-of-freedom dummy excited by the two input signals were estimated to be 260N and 390N (see Table 3.4.1). The corresponding peak relative displacements were 8 mm and 11 mm. Table 3.4.2 shows the displacements and peak forces available from various standard commercially available electro-dynamic actuators.

Table 1. Test signals, with estimated damping forces and displacements for the single degree-of-freedom model.

Acceleration signal	Magnitude (ms^{-2} r.m.s.)	Peak acceleration (ms^{-2})	Peak damping force (N)	Peak displacement (mm)
Broad-band random	2.0	7.19	260	8
Car on un-made road	2.1	13.5	390	11

Although several of the actuators in Table 2 fit the specified performance criteria, their input-to-force characteristics are not all ideal. To illustrate this, Figure 3.4.4 shows the modulus and phase of the input-to-force transfer functions for the Derritron VP4 and the Gearing and Watson M50, when mounted in the dummy frame.

Table 2. Actuator performance comparison

Actuator	Peak Force (N)	Peak displacement (mm)
Ling 408	196	17.6
EE 1501	350	12.5
G&W V55/ SS300	310	12.7
G&W V55/ SS600	444	12.7
G&W M50/ SS300	310	12.7
G&W M50/ SS600	444	12.7
Derritron VP4	222	10.0

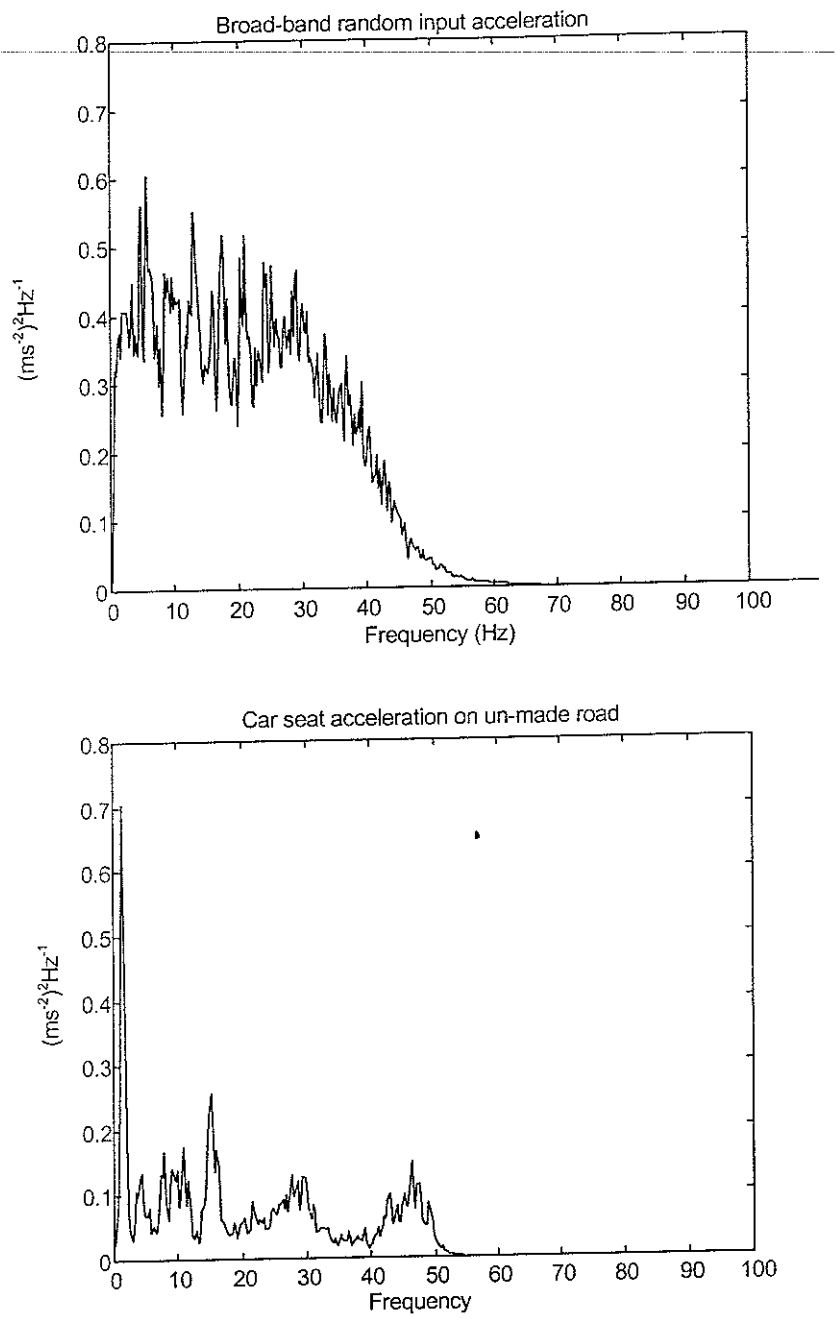

Figure 3.4.3. Acceleration power spectral densities of the two test signals described in Table 3.4.1.

The M50 is an electrodynamic shaker designed specifically for modal testing applications. Unlike the VP4, the armature and drive shaft are not supported by a suspension mechanism but are free to move in linear guides. The power amplifier used with this device was also capable of direct current drive, eliminating back-emf and other artefacts. It can be seen from the figure that the M50 provides a more constant force for a specified input velocity than the VP4 over the frequency range of interest.

The phase response of the M50 is also more consistent than that of the VP4. Variations in gain and phase response may be compensated for, to a certain extent, by compensation filters in the feedback circuitry (e.g filtering the actuator drive signal in Figure 3.4.1 with a response equivalent to the inverse of H_a). However, complex filters can introduce stability problems and it is clearly desirable to minimise phase lag before considering the inclusion of a compensator. Eliminating the need for complex compensation will also make it easier to implement filters in the feedback so as to change the apparent mass as a function of excitation frequency (see Section 3.4.7).

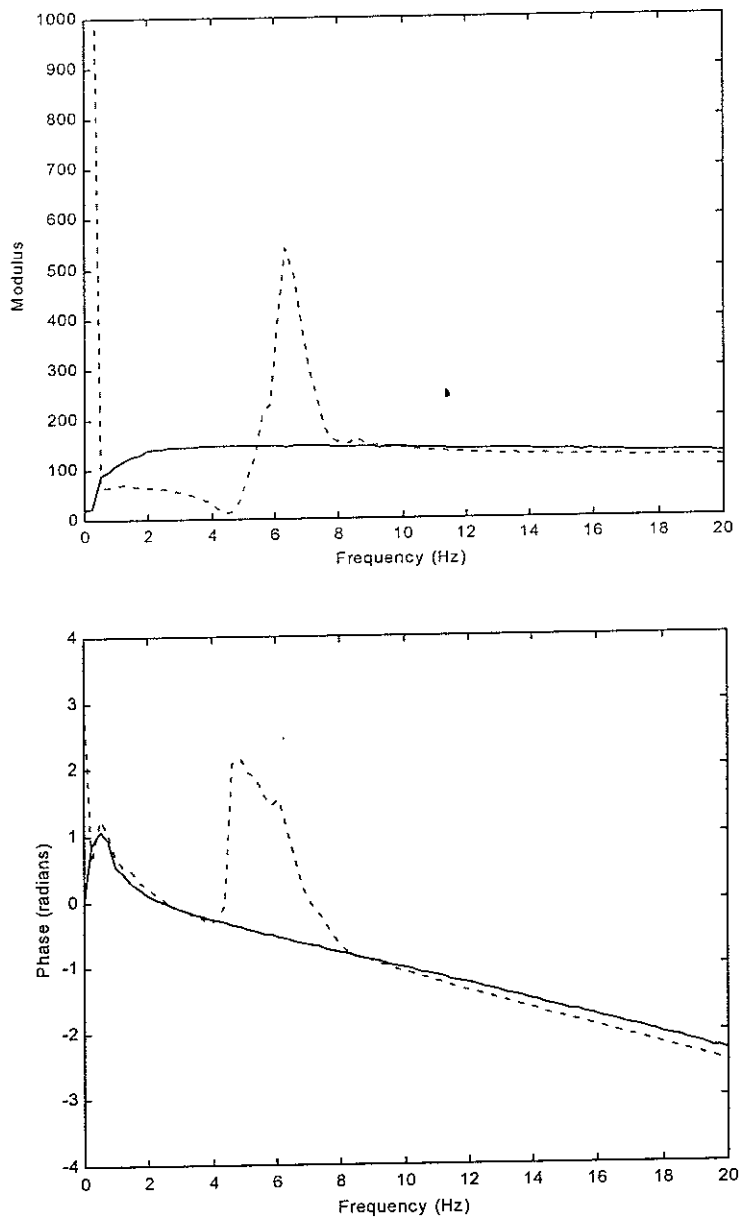

Figure 3.4.4. Actuator transfer functions, $H_a=F_a/l_a$, measured with VP4 (dashed) and M50 (solid) actuators.

3.4.6 *Apparent mass measurements using M50 actuator*

3.4.6.1 Active control of damping force

A revised prototype active dummy was built, with a Gearing and Watson M50 shaker as the actuator. The LVDT displacement transducer was replaced by an inductive velocity transducer, eliminating the need to derive the velocity feedback signal by differentiation. The actuator input, i_a, was connected to the output of the velocity transducer via an amplifier with gain c. Hence the response of the system should be in accordance with equations (3.4.8) to (3.4.10). It can be seen from equation (3.4.6) that the apparent mass of the dummy is determined by the product of the moving mass and the mass/frame transfer function. Hence the dynamic response of the dummy can be determined by measuring this transfer function rather than the driving point transfer function defined by equation (3.1.1).

Figure 3.4.5 shows the mass/frame transfer function of the revised prototype dummy in comparison with a single degree-of-freedom model with f_n=5 Hz and ζ=0.475. The results show that it is possible to achieve an apparent mass that is close to that of the Fairley and Griffin (1989) model with the M50 actuator with minimal compensation for the actuator response. The measured resonance frequency and damping appear to be slightly lower than predicted: this difference may reflect an error in the estimation of the relative masses of the fixed and moving parts of the M50 shaker.

3.4.6.2 Active control of resonance frequency and damping

A particular advantage of active control is that it can allow the resonance frequency and damping to be altered by changing feedback parameters. This should enable the dummy to represent a range of mathematical models, fitted to the characteristics of different populations. To change the resonance frequency, the actuator must be able to supplement the spring forces. Since the spring force is proportional to the relative displacement, $u(t)$, the prototype was fitted with parallel displacement and velocity transducers. The actuator drive signal was then derived from:

$$i_a(t) = c\dot{u}(t) + ku(t) \tag{3.4.13}$$

where c is the veliocity feedback gain and k is the displacement feedback gain. The mass/frame transfer function should then be predicted by:

$$H_{x.y}(s) = \frac{Y(s)}{X(s)} = \frac{cs + k + K}{ms^2 + cs + k + K} \tag{3.4.14}$$

where K is the stiffness of the springs supporting the moving mass, m.

The resonance frequency and damping are given by:

$$\omega = \sqrt{\frac{k+K}{m}} \tag{3.4.15}$$

$$\zeta = \frac{c}{2\sqrt{(k+K)m}} \tag{3.4.16}$$

A positive value of displacement feedback, k, will increase the effective overall spring stiffness, and a negative value of k will decrease the overall spring stiffness.

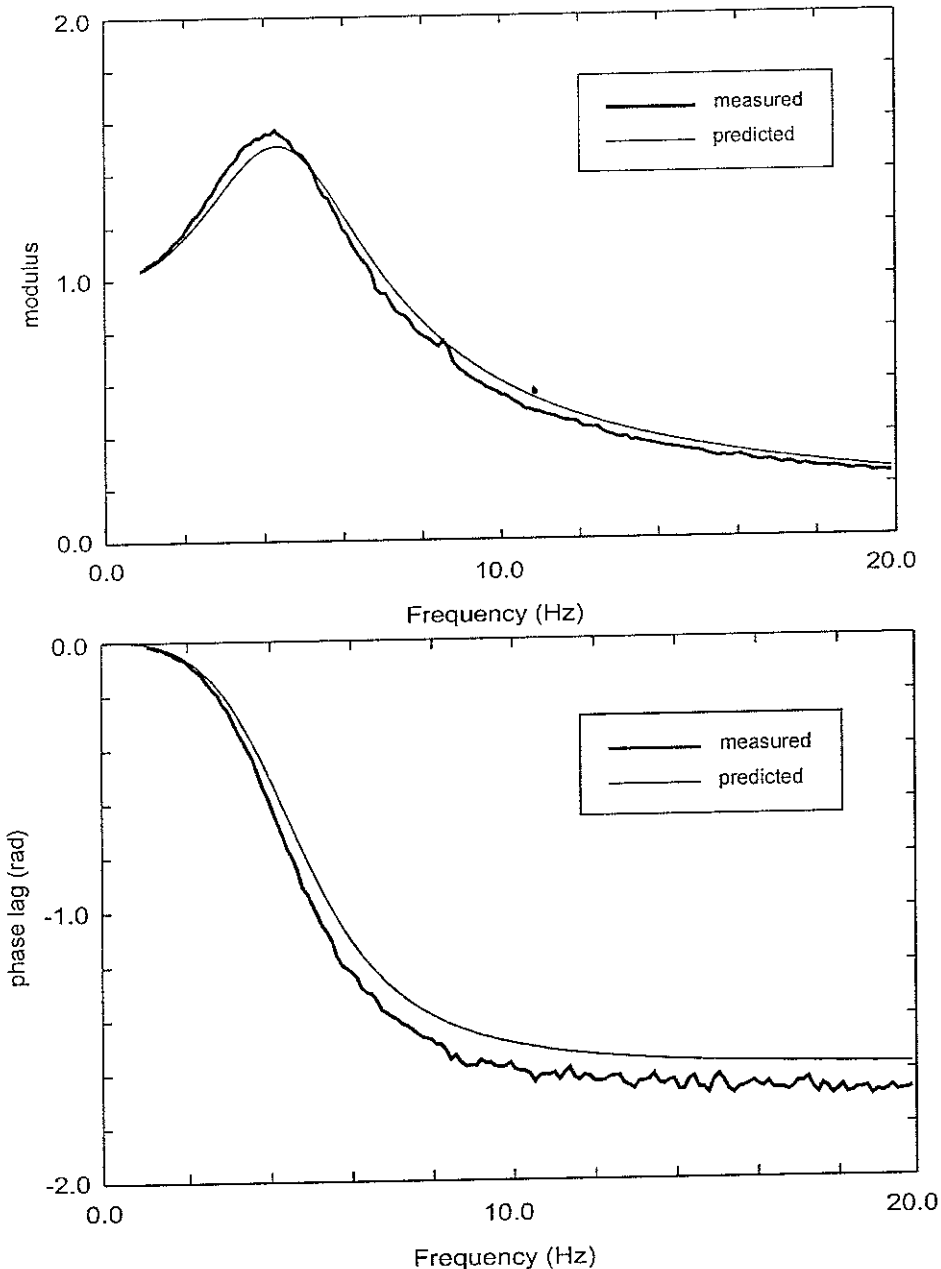

Figure 3.4.5. Frame-to-mass transfer function of dummy with M50 actuator in comparison with single degree-of-freedom model.

Figure 3.4.6 compares predicted and measured mass/frame transfer functions with displacement and velocity feedback set up to give natural frequencies between 4.1 and 6.5 Hz at a constant damping ratio of 0.475.

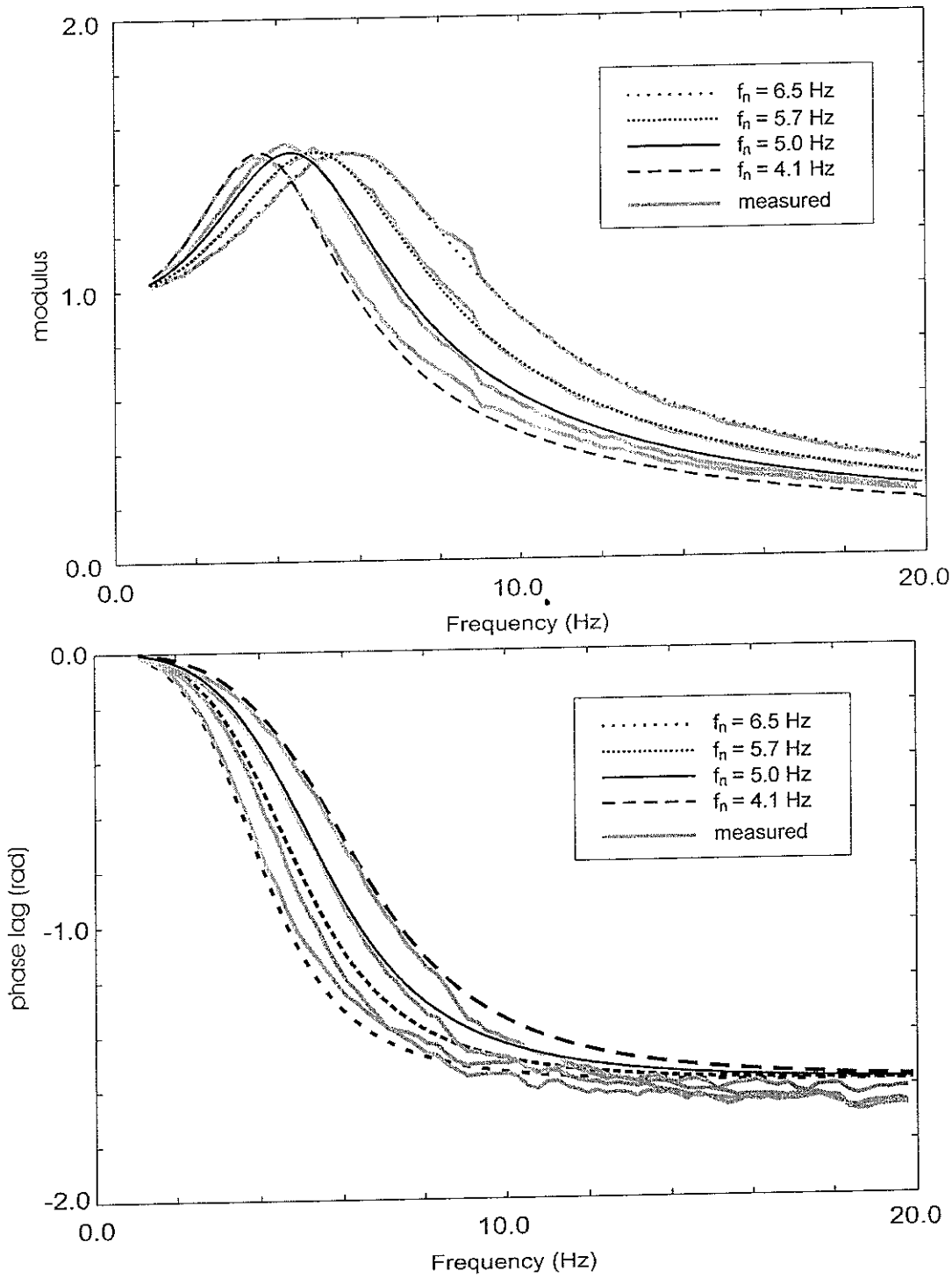

Figure 3.4.6. Predicted mass/frame transfer functions (in black) for combinations of displacement and velocity feedback, giving natural frequencies between 4.1 and 6.5 Hz at a constant damping ratio of 0.475, compared with equivalent transfer functions measured on prototype dummy (in grey).

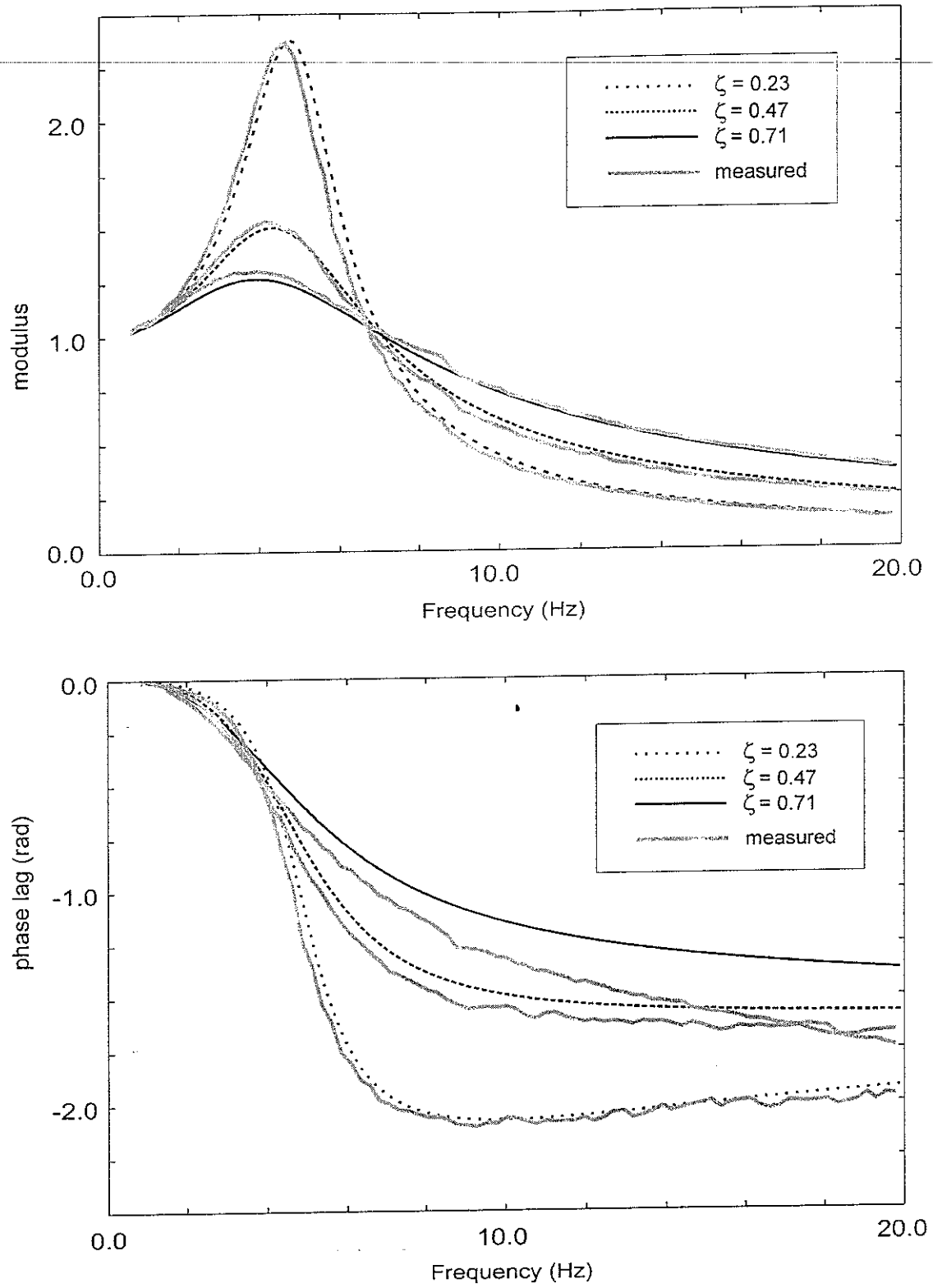

Figure 3.4.7. Predicted mass/frame transfer functions (in black) for combinations of displacement and velocity feedback, giving damping ratios between 0.23 and 0.71 at a constant natural frequency of 5.0 Hz, compared with equivalent transfer functions measured on prototype dummy (in grey).

Figure 3.4.7 compares predicted and measured transfer functions with displacement and velocity feedback set up to give damping ratios between 0.23 and 0.71 with a constant natural frequency of 5.0 Hz. The figures show that both the modulus and phase of the measured transfer functions are close to the predicted values over the frequency range from 0.5 Hz to 20 Hz, with the possible exception of the phase response above about 10 Hz when the damping was high.

3.4.7 Alternative apparent mass characteristics

Results presented in Section 3.4.6 show that the prototype active dummy can be controlled by variable gain displacement and velocity feedback to achieve a response that simulates single degree-of-freedom mathematical models with a range of natural frequencies and damping ratios in the region of those of the Fairley and Griffin (1989) model. A control system for such a system could be achieved using simple analogue circuitry.

A practical dummy would also need to incorporate an accelerometer to measure the frame acceleration, and some means of analysing or recording its output. The addition of a second accelerometer, on the moving mass, would enable the dummy to be calibrated in situ by measuring the mass/frame transfer function. A laptop computer, equipped with an analogue interface, would provide a flexible means of recording and analysing seat acceleration data in a vehicle. If a laptop computer is to be used with the system, it could also provide the means of controlling the dummy. The availability of digital control would make it feasible to incorporate custom filters in the velocity and displacement feedback to vary the apparent mass from that of a simple one degree-of-freedom system, to simulate either a multi-degree-of-freedom model or a measured characteristic.

The degree of control that is possible using compensation filters is still under investigation. One consideration is the necessary data throughput (i.e. sampling rate and associated delays) to be able to achieve an accurate result. The effect of delays in feedback control can be seen in Figure 3.4.8, which shows the effect on mass/frame transfer functions of the phase lags introduced by a low-pass filter (8 pole Butterworth) in the actuator drive circuit. In this example the velocity and displacement feedback were set to give f_n=5 Hz and ζ=0.475. Even the comparatively small lags introduced at around 5 Hz by an 8 pole low-pass filter at 100 Hz (a time delay of about 0.005 s) can be seen to result in a 10% increase in transmissibility (this would result in a similar increase in apparent mass).

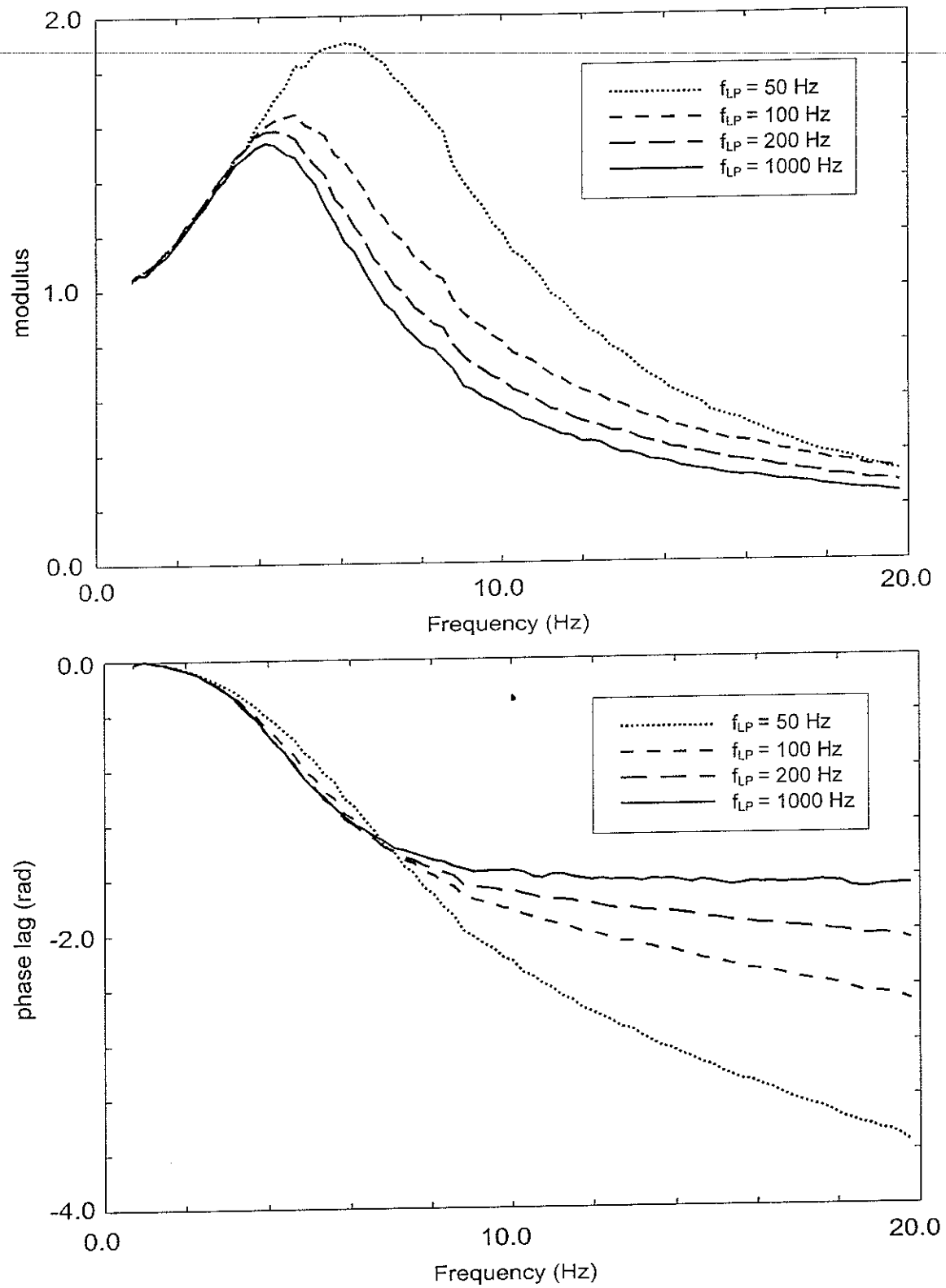

Figure 3.4.8. The effect of low-pass filtering (8 pole Butterworth) the actuator drive signal on mass/frame transfer functions. Velocity and displacement feedback were set to give f_n=5 Hz and ζ=0.475.

3.4.8 Development of a practical active dummy

3.4.8.1 Mechanical considerations

Consideration has been given to the problem of mounting the dummy on a car seat for testing in a vehicle. The prototype frame has a base area with dimensions 280mm x 260mm. If a SIT-BAR shaped seat indenter (Whitham and Griffin, 1977) is attached directly underneath the centre of mass, and the indenter is placed in a similar position to the ischial tuberosities of a normally seated subject, the current frame is likely to contact the seat back. However, measurements of the G&W M50 show that the frame depth could be reduced sufficiently to achieve an acceptable position on the seat when fitted with a backrest support similar to that of the passive dummy shown in Figure 3.3.7.

3.4.8.2 Electrical power requirements

When the dummy was set up to respond as the Fairley and Griffin (1989) model and excited by 0.5 to 30 Hz random vibration at 2 ms^{-2} r.m.s., the average power consumption of the M50 actuator was approximately 16 VA. Assuming typical losses in a D.C. powered amplifier, it may be necessary to supply up to 100 VA to drive the dummy and its associated control system, and an additional 50 VA to drive a laptop computer and analogue interface. This would be within the capabilities of the 12v supply in most vehicles. Alternatively, a sealed lead acid battery pack smaller than a standard car battery would be able to power such a system for more than one hour.

3.5 Conclusions

Passive anthropodynamic dummies, based on mass-spring-damper systems, have been previously described but their performance for testing seats has been limited at low excitation magnitudes by non-linear phenomena such as friction in the mechanical components that provide damping. Alternative dampers, which provide linear force response characteristics down to very low excitation magnitudes, have characteristics which depart from those of an ideal damper and vary with frequency.

Ways of overcoming these mechanical limitations have been demonstrated. A passive mechanical dummy has been realised with an apparent mass that is close to that of an ideal system up to 20 Hz, and with a response that does not vary over a range of excitation magnitudes.

The passive dummy has been tested in cars and in the laboratory, and found to give SEAT values that are in the correct rank order over a range of road conditions, compared with those measured with human subjects. However, the seat transmissibility measured with the dummy departs from that measured with subjects at

some frequencies, partly due to the way that the dummy interacts with the seat backrest. Research is ongoing to develop the backrest support so the dummy can interact with the seatback in a manner that is more consistent with the interaction between a seatback and human subjects.

An active version of the anthropodynamic dummy, in which damping and spring forces are supplied by an electrodynamic actuator in addition to conventional springs, is under development. It has been shown that the apparent mass of a single degree-of-freedom system can be reproduced at the driving point at frequencies up to 20 Hz, and that the resonance frequency and damping can be varied over a wide range by changing feedback control parameters. This makes it possible to change the apparent mass by simply changing switch settings or parameters in software. The resonance frequency and damping of a passive dummy can only be altered by substituting components. The active dummy is currently being engineered into a system that can be used on a car seat and controlled by a laptop computer. The limits of control are being explored to determine the feasibility of changing the apparent mass characteristic to match multi-degree-of-freedom models by the use of feedback compensation filters.

4 Acknowledgements

Parts of the research presented in this report were supported by the Ford Motor Company. The authors would particularly like to thank Mr Alan Brunning and Dr Bill Pielemeier for their suggestions and kind assistance

5 References

British Standards Institution (1987) British Standard guide to measurement and evaluation of human exposure to whole-body mechanical vibration and repeated shock. BS 6841:1987.

British Standards Institution (1989) British Standard Guide to Safety aspects of experiments in which people are exposed to mechanical vibration and shock. BS 7085:1989.

Corbridge,C., Griffin,M.J., Harborough,P. (1989) Seat dynamics and passenger comfort, *Proceedings of the Institution of Mechanical Engineers*, 203, 57-64.

Cramer,H.J., Liu,Y.K., Rosenberg,D.U.von (1976) A distributed parameter model of the inertially loaded human spine, *Journal of Biomechanics*, 9, 15-130.

Dierckx,C. (1995), Curve and surface fitting with splines. *Oxford Science Publications.*

Fairley,T.E., Griffin,M.J. (1986) A test method for the prediction of seat transmissibility, *Society of Automotive Engineers International Congress and Exposition*, Detroit, February 24-28, SAE Paper 860046.

Fairley,T.E., Griffin,M.J. (1989) The apparent mass of the seated human body: vertical vibration, *Journal of Biomechanics,* 22, (2), 81-94.

General Motors (1978) HYBRID III Exterior Body, Proving Ground General Motors Corporation. May 1978.

Griffin,M.J., Lewis,C.H., Parsons,K.C., Whitham,E.M. (1979) The biodynamic response of the human body and its application to standards, AGARD Conference Proceedings CP-253. Models and analogues for the evaluation of human biodynamic response, performance and protection. Paris, 6-10 November, 1978. Editor H.E. von Gierke, Paper A28.

Griffin,M.J. (1990) Handbook of human vibration, Published: Academic Press, London, ISBN: 0-12-303040-4.

Hinz, B. and Seidel, H. (1987) The nonlinearity of the human body's dynamic response during sinusoidal whole body vibration, Industrial Health 25: 169-181.

Huston, D.R., Johnson, C.C. and Zhao, X.D. (1998) A human analog for testing vibration attenuating seating. *Journal of Sound and Vibration*, 214(1), 195-200.

International Organization for Standardization, (1981) Vibration and shock-Mechanical driving point impedance of the human body, ISO 5982:1981.

International Organization for Standardization (1992) Mechanical Vibration - laboratory method for evaluating seat vibration - part 1: basic requirements, ISO 10326-1:1992(E).

International Organization for Standardization (1998) Mechanical vibration and repeated shock, Mechanical vibration and shock - Guide to the safety of tests and experiments in which people are exposed to vibration and shock, Part 1: EN ISO 13090-1:1998.

Kaleps,I., Gierke,H.E.von., Weis,E.B. (1971) A five-degree-of-freedom mathematical model of the body, *Aerospace Medical Research Laboratories-TR-71-29. Symposium on Biodynamic Models and their Applications* held at Dayton, Ohio, 26-28 October. Paper 8, 211-231.

Kitazaki,S. and Griffin,M.J. (1996) Modelling biomechanical responses to human whole-body vertical vibration, *Journal of Sound and Vibration* (awaiting publication).

Kitazaki, S., Griffin,M.J., (1998) Resonance behaviour of the seated human body and effect of posture, *Journal of Biomechanics,* Vol. 31, pp. 143-149

Lee, H.G. and Dobson, B.J. (1991) The direct measurement of structural mass, stiffness and damping properties, *Journal of Sound and Vibration* 145 (1), 61-81

Lewis, C.H. (1988) The implementation of an improved anthropodynamic dummy for testing the vibration isolation of vehicle seats. Presented at the *UK Group meeting on Human Response to Vibration* held at the Health and Safety Executive, Buxton, Derbyshire, England, 16-18, September 1998.

Lewis, C.H. and Griffin, M.J. (1996) The transmission of vibration to the occupants of a car seat with a suspended back-rest. *Proceedings of the Institution of Mechanical Engineers*, 210, 199-207.

Liu,Y.K., Cramer,H.J., Rosenberg,D.U. von (1973) A distributed parameter model of the inertially loaded human spine: a finite difference solution, *AD-773 859, Aerospace Medical Research Laboratory*, Wright-Patterson Air Force Base, Ohio, AMRL-TR-73-65.

Mansfield, N.J. and Griffin, M.J. (1996) Vehicle seat dynamics measured with an anthropodynamic dummy and human subjects. *Inter-noise '96*, Proceedings of 25th Aniversary Congress, Liverpool, Book 4, 1725-1730. Institute of Acoustics.

Matsumoto, Y. (1998) An investigation of linear lumped parameter models with rotational degrees of freedom to represent the dynamic response of the human body.

Proceedings of the United Kingdom Group on Human Response to Vibration, organized by the Health and Safety Executive, Buxton, 16-18 September.

Matthews,J. (1967) Progress in the application of ergonomics to agricultural engineering, *Engineering Symposium of the Institution of Agricultural Engineers*, 12 September, National College of Agricultural Engineering, Silsoe, Bedford.

Mansfield,N.J. (1994) The apparent mass of the human body in the vertical direction - the effect of vibration magnitude, *Paper presented at the United Kingdom Information Group Meeting on Human Response to Vibration held at the Institute of Naval Medicine,* Alverstoke, Gosport, Hants., 19 -21 September 1994.

Mansfield,N.J., Griffin,M.J. (1996), Vehicle seat dynamics measured with an anthropodynamic dummy and human subjects, *Inter-noise '96*, Proceedings of 25th Anniversary Congress, Liverpool, Book 4, Published: Institute of Acoustics, ISBN: 1-873082 91 6, 1725-1730.

Nigam, S. P. and Malik, M., (1987) A study on a vibration model of a human body, *Journal of Biomechanical Engineering*, 109, 148-153.

Sandover, J. (1978) Modelling Human Responses to Vibration, Aviation Space and *Environmental Medicine* 49(1): 335-339.

Smith, S.D. (1994), Nonlinear resonance behaviour in the human exposed to whole-body vibration, *Shock and Vibration* 1(5): 439-450.

Suggs,C.W., Abrams,C.F., Stikeleather,L.F. (1969) Application of a damped spring-mass human vibration simulator in vibration testing of vehicle seats, *Ergonomics*, 12,(1), 79-90.

Vogt,L.H., Coerman,R.R., Fust,H.D. (1968) Mechanical impedance of the sitting human under sustained acceleration, *Aerospace Medicine*, 39,(7), 675-679.

Wei,L., Griffin,M.J. (1995) A method of predicting seat transmissibility, United Kingdom Informal Group Meeting on Human Response to Vibration held at the Silsoe Research Institute, September 1995.

Wei,L., Griffin,M.J., (1997) The influence of contact area, vibration magnitude and static force on the dynamic stiffness of polyurethane seat foam, Presented at the United Kingdom Group Meeting on Human Response to Vibration held at the ISVR, University of Southampton, Southampton, SO17 1BJ, England, 17-19 September.

Wei,L., Griffin,M.J. (1998a) Mathematical model for the mechanical impedance of the seated human body exposed to vertical vibration, *Journal of Sound and Vibration* 212(5), 855-874

Wei,L., Griffin,M.J. (1998b) The prediction of seat transmissibility from measures of seat impedance, *Journal of Sound and Vibration,* 214 (1), 121-137.

Wei,L., Griffin,M.J. (1999) Modelling the effect of backrest angle on the vertical apparent mass of seated subjects, Presented at the United Kingdom Group Meeting on Human Response to Vibration held at the Ford Motor Company, Dunton, Essex, England, 22-24 September.

Wei,L., Griffin,M.J. (2000) Mathematical model of the dynamic response of the seated human body exposed to various magnitudes of vertical vibration (awaiting publication).

Whitham, E.M., Griffin, M.J. (1977), Measuring vibration on soft seats, Society of Automotive Engineers, *SAE Paper 770253*, International Automotive Engineering Congress and Exposition, Detroit, 28 February - 4 March..

Appendix A. Laboratory method for predicting seat transmissibility

1 INTRODUCTION

The transmission of vibration to the body can cause discomfort, impaired performance and health problems. Seats influence the transmission of vibration to the body, either increasing the overall severity of vibration or reducing the overall severity of vibration. The dynamic response of a seat can therefore have a large influence on human responses to vibration.

The transmissibility of a seat depends on many factors, including the seat characteristics and the mechanical impedance of the load on the seat (e.g. the human body). It is not, in general, possible to measure or predict the transmission of vibration without considering the effect of the seat loading. Seats do not normally have the same transmissibility when measured with a subject and a rigid mass.

The transmissibility of a seat can be measured in vehicles or in the laboratory with suitable subjects sitting on the seat. However, this is time-consuming and may impose some risks to the subject. The measurements will also depend on the subject chosen for the studies. Transmissibility may alternatively be measured with a suitable anthropodynamic dummy replacing the human subject.

Seat transmissibility can be estimated without either a human subject or a dummy. From a knowledge of the mechanical impedance of the human body and suitable measurements of the mechanical impedance of the seat, the seat transmissibility can be predicted. This has the advantage that human subjects are not required, and the likely effect of physical changes to the seat (e.g. damping, stiffness, geometry) may be more easily determined.

2 SCOPE

This document specifies the instrumentation requirements, the measurement method and the calculation procedure required to predict seat transmissibility. A standardised means of reporting results is also presented.

The use of the recommended method for measurement and analysis should make it possible to compare test results from different laboratories.

3 NORMATIVE REFERENCES

The following normative documents contain provisions of this test method.

ISO 2631:1997

> Mechanical vibration and shock - evaluation of human exposure to whole-body vibration. Part 1: General requirements. International Standard, ISO 2631-1.

ISO 5347-0:1987

> Methods for the calibration of vibration and shock pick-ups - Part 0: Basic concepts.

Vibration and shock - Vocabulary.

4 SYMBOLS AND INDICES

For the purposes of this test procedure, the following symbols and indices apply.

4.1 SYMBOLS

c	Viscous damping of seat, Ns/m
c_1	Viscous damping of body first subsystem, Ns/m
c_2	Viscous damping of body second subsystem, Ns/m
c_b	Viscous damping for seat-person model with backrest, Ns/m
F	Force, Newton
f	Frequency, in hertz (Hz).
i	Assumed unit ($i^2 = .1$).
k	Stiffness of seat, N/m
k_1	Stiffness of body first subsystem, N/m
k_2	Stiffness of body second subsystem, N/m
k_b	Stiffness for seat-person model with backrest, N/m
m	Model frame mass, kg
m_1	Mass of body first subsystem, kg
m_2	Mass of body second subsystem, kg
PSD	power spectral density expressed as mean square acceleration per unit bandwidth $(m/s^2)^2/Hz$
PDF	probability density function of acceleration amplitudes
r.m.s.	root mean square
$s(\omega)$	Dynamic stiffness
$\|T\|$	Modulus of seat transmissibility
θ	Phase of seat transmissibility
x	Displacement, in metres *(m)*
$\dot{x}$	Instantaneous velocity, in metres per second (ms^{-1}).
$\ddot{x}$	Instantaneous acceleration, in metres per second squared (ms^{-2}).

5 INSTRUMENTATION

5.1 ACCELERATION, DISPLACEMENT AND FORCE TRANSDUCERS

Vibration at the seat base and vibration transmitted to the subject shall be sensed by accelerometers and displacement transducers.

The accelerometers, together with their amplifiers, shall be capable of measuring r.m.s. acceleration levels ranging from 0.05 to 20 m/s^2 with a crest factor of up to 6. The accelerometers and amplifiers shall be capable of an accuracy of .2.5% of the actual r.m.s. vibration level in the frequency range 0.5 to 100 Hz. The resonance frequency of the accelerometers shall be greater than 300 Hz.

One accelerometer or displacement transducer and one force transducer are used on a seat indenter test rig (see Figure 1).

Motion of the vibrator platform is measured using an accelerometer.

> *Note:* A suitable accelerometer is an Entran EGCSY-240D*-10 having a sensitivity of approximately 13 mV/g with an operating range of .10 g.

Displacement of the vibrator platform may be measured using a displacement transducer.

> *Note:* A suitable displacement transducer is a DC-LVDV D2/200A having a sensitivity of approximately 0.16 v/mm with an operating range of ±10 mm.

The driving force whilst testing the seat is measured using a force transducer.

> *Note:* A suitable force transducer is a Kistler 9321A force cell with a sensitivity of approximately .3.97 pC/N.

The characteristics of the vibration measuring system, signal conditioning and data acquisition equipment, including recording devices shall be specified for the relevant tests, especially the dynamic range, sensitivity, accuracy, linearity and overload capacity.

> *Note:* Suitable signal conditioning for the force cell is a Kistler KIAG5001 or a B&K 2635 charge amplifier.

5.2 INDENTER

An indenter is used to apply a pre-load to the seat surface. Figures 1 and 3 show a suitable indenter arrangement. The indenter head consists of a SIT-BAR (Figure 2), attached to a rigid steel frame.

The indenter is moved up and down on to the top surface of the test seat so as to vary the applied static force between indenter and the seat. The indenter is mounted on a bearing which allows it to rotate as the indenter is moved up and down.

5.3 SEAT MOUNTING

The test seat shall be mounted on the platform with the same method of attachment and at the same angle as it is mounted on the floor for the test vehicle. The platform shall be mounted on a vibrator that is capable of generating vibration along the vertical (z-axis).

The seat shall be adjusted to enable the indenter to apply force to the centre of the seat surface.

When the inclination of the seat surface is adjustable, the angle during testing shall be specified.

> *Note:* The seat backrest may influence the seat impedance measured by an indenter. In order to minimise the effect of the seat backrest, it should be adjusted to the upright position. If the seat backrest cannot be adjusted to the upright position, an additional device is needed to fix the seat backrest to prevent horizontal movement during vertical motion of the seat base.

5.4 TRANSDUCER MOUNTING

An accelerometer shall be located on the platform at the support for the seat. If using a displacement transducer, one end of the displacement transducer shall be located at the same location as the accelerometer and the other end shall be located at a still base.

A force transducer shall be located above the indenter over the seat surface (Figures 1 and 3). One side of the force transducer shall be connected to the indenter and the other side connected to the bearing (Figure 3).

5.5 DATA ACQUISITION AND SIGNAL GENERATION

An input signal can be either a sinusoidal or a random signal produced by computer or a signal obtained from the floor of a vehicle. A digital-to-analogy (D/A) conversion card and a filter are needed to produce the required vibration.

Data recording can be achieved using digital recording techniques. In all cases the data recording shall have sufficient dynamic range to ensure that vibration signals over the full frequency range can be reliably recorded.

> *Note:* A suitable data acquisition and signal generation system is *HVLab* developed by the Human Factors Research Unit, Institute of Sound and Vibration Research, University of Southampton. It can acquire and analyse up 16 channels of time varying analogue signals whilst simultaneously outputting 2 channels. The number of channels, sampling rate and duration are controlled by *HVLab* software. An analogue-to-digital and a digital-to analogue computer interface card and a *Techfilter* TF-16 anti-aliasing card are included in the system.

5.6 CALIBRATE

The instrumentation shall be calibrated in accordance with ISO 5347 and, depending on the type of measuring system used, to the relevant part of ISO 5347. The force

transducer should be calibrated in two conditions: static and dynamic. In particular, the calibration procedures should ensure that the acceleration sensitivity varies less than .0.5% of a mean value over the interesting frequency range and less than .6% of the mean value over the full measured frequency range from 0 to 30 Hz.

The effect of ambient temperature on the performance of all instruments shall be known. Instruments shall be operated within the temperature limits to which the required accuracy can be expected.

Calibration shall be made before and after each test series.

6 VIBRATION EQUIPMENT

6.1 VIBRATOR

The minimum required is a vibrator capable of driving a platform in the vertical direction. The dynamic response of the exciter shall be capable of exciting the seat with the indenter and additional equipment, in accordance with the specified test input vibration.

> *Note:* A suitable vibrator is a Derritron VP85 powered by a 1000W Derritron amplifier. A maximum displacement of 25.4 mm is possible and the vibrator is capable of producing a force of 3.3 kN. Mechanical and electrical stops are fitted to the vibrator. Emergency stop buttons are also accessible to the experimenter.

6.2 INDENTER RIG

The indenter rig is shown in Figure 1 and 3. It should be rigid and strong enough to resist motion in the horizontal direction caused by seat surface inclination.

6.3 CONTROL SYSTEM

The frequency response characteristics of the vibration system shall be compensated to ensure that the power spectral density (PSD) and the probability density function (PDF) of the acceleration amplitudes of the vibration at the seat mounting base comply with the requirements of the specified test input. This means that all input signals must be equalised for the response of the system before they are used in a seat test.

7 VIBRATION TESTING OF A SEAT

7.1 TEST AMBIENT CONDITIONS

The tests are to be performed in controlled climatic conditions:

Temperature: 23 ^{0}C . 2 ^{0}C (or as specified in the test schedule)

Relative humidity: the maximum acceptable variation is .15% RH

The seat should be allowed to acclimate to these conditions for a minimum of 12 hours period.

7.2 STATIC TEST

Three repeated compression cycles are performed for each test condition at a compression speed not greater than 100mm/min. The force and displacement measurements during the three cycles shall be recorded.

(1) Pre-conditioning

Three initial compression cycles between 50N (pre-load) and 750N.

(2) Test conditions

400 to 600 N three cycles

300 to 700 N three cycles

200 to 800 N three cycles

7.2.1 Accuracy

The compression axial force shall be measured to an accuracy of .2.5% of the true value.

The compression displacement shall be measured to an accuracy of .2.5% of the true value.

7.3 DYNAMIC TEST

7.3.1 Random excitation with given spectrum

7.3.1.1 Excitation signal

Three different magnitudes of random excitation, each having a nominally flat constant bandwidth acceleration spectrum, or three excitation signals from a vehicle are applied with the vibrator. The duration of each of the three random signals shall be 2 minutes (or as specified).

In some applications, a test may be conducted with additional inputs so as to test for non-linearities in the seat response. The additional inputs may be the standard spectrum presented at different magnitudes or a defined spectrum for a specific vehicle.

When using spectra from a vehicle, care is required to ensure that coherent data are obtained at all frequencies.

> *Note:* The spectrum of the test input from a vehicle shall be determined from the expected seat deflection, not the expected spectrum on the vehicle floor.

The root-mean-square value of the test acceleration shall be within ±10% of the required value. Tests shall be conducted at three magnitudes: 0.5, 1.0 and 1.5 ms^{-2} (or as specified).

7.3.1.2 Preload

The indenter head shall be applied to the seat surface with a specified required pre-load.

> *Note:* When testing seats for normal adults, a pre-load of 550N applied to seat surface is normally appropriate.

After applying the pre-load, there should be a pause of 5 minutes to allow the seat to settle. The pre-load should then be checked and corrected, if necessary, before commencing the tests.

7.3.1.3 Accuracy

The compression axial force time history shall be measured with an accuracy of .2.5% of the true value.

The displacement time history shall be measured with an accuracy of .2.5% of the true value.

7.3.2 Sinusoidal excitation

If required, a sinusoidal displacement signal is to be applied with three different preload forces. Unless otherwise specified, the forces shall be 500N, 600N and 700N.

7.3.2.1 Excitation signal

The displacement excitation must be within the frequency range 1 Hz to 30 Hz. The sinusoidal displacement can be either swept sine, with a sweep rate less than 0.5 Hz/s, or stepped sine with a step 1 Hz.

The test should be repeated for a series of displacement amplitudes: 1, 2 and 5mm. The swept sine (or stepped sine) may be truncated at the upper frequency when the acceleration reaches 10 ms^{-2} r.m.s.

7.3.2.2 Accuracy

The sinusoidal compression force time history shall be measured with an accuracy of .2.5% of the true value at each frequency.

The sinusoidal displacement time history shall be measured with an accuracy of .2.5% of the true value at each frequency.

8 ANALYSIS

8.1 SPECTRAL ANALYSIS

Spectra of the force and displacement shall be calculated with a frequency resolution not greater than 0.25 Hz (corresponding to not less than 96 degrees of freedom).

8.2 COHERENCY

The coherency between the force and acceleration signals shall be determined over the frequency range 0.5 to 30 Hz. The prediction of seat transmissibility in Section 9 shall be assumed to be inaccurate at any frequency where the coherency falls below 0.8.

9. CALCULATION OF EQUIVALENT SEAT STIFFNESS AND DAMPING

If using an accelerometer to measure the motion of the seat base, the acceleration at the seat base shall be integrated twice to obtain the displacement at the seat base.

9.1 SEAT DYNAMIC STIFFNESS

The seat dynamic stiffness, $s(\omega)$, is the complex ratio of force to displacement and is assumed to have the form:

$$s(\omega) = \frac{F(\omega)}{x(\omega)} = k + c\omega i$$

In $s(\omega)$, the real part, k, is the equivalent seat stiffness, and the imaginary part, c, is the equivalent viscous damping.

Note: A curve fitting method can be used to obtain seat parameters k and c (i.e. the effective stiffness and damping) from the real and imaginary components of $s(\omega)$. The least square error method with an optimisation algorithm may be utilised. The parameters in the above equation were refined to minimise the function:

$$error = \frac{1}{N}\sum_{i=1}^{N}\left(k_f(i) - k(i)\right)^2$$

$$error = \frac{1}{N}\sum_{i=1}^{N}\left(c_f\omega(i) - c\omega(i)\right)^2$$

where $k_f(i)$ is the corresponding dynamic stiffness from the curve fit at the ith frequency point and $k(i)$ is the dynamic stiffness in the measured data and c_f . (i) is the corresponding damping from the curve fit at the ith frequency point and c. (i) is the damping in the measured data. Using values for the parameters chosen at random as starting values, the parameters may be varied systematically using the optimisation algorithm.

Note: The measured data may be first converted from *HVLab* data files to ASCII data, and then imported to MATLAB for curve fitting (see Appendix A).

10. CALCULATION OF PREDICTED SEAT TRANSMISSIBILITY

10.1 HUMAN BODY MATHEMATICAL MODEL

The apparent mass of the human body shall be assumed to be represented by the model in Figure 4 and 5 with values of stiffness, viscous damping and mass as defined in Table 1.

Note: The human body has a non-linear response to vibration. Although the parameters given in Table 1 will often be sufficient, some deviation may be necessary with stimuli having high or low magnitudes.

Note: The model shown in Table 1 adequately represents the input impedance of the seated human body. However, it should not be assumed to represent how vibration is transmitted through the body or give any indication of the discomfort or risk of injury produced by vibration. The discomfort and injury potential of vibration should be estimated from the vibration on the seat surface using the appropriate standard.

Table 1 Parameters of single degree-of-freedom model, model A, and two degree-of-freedom model, model B.

	k_1	c_1	k_2	c_2	m	m_1	m_2
Model A	44943	1360			6.0	45.6	
Model B	35776	761	38374	458	6.7	33.4	10.7

10.2 PREDICTION OF SEAT TRANSMISSIBILITY

10.2.1 Model of seat-person system without backrest

Figures 6 and 7 shows the assumed model that combines the seat stiffness and damping with the model of the apparent mass of the human body. The models can be used to predict the transmissibility of a seat without seat backrest.

Note: The MATLAB program for calculating seat transmissibility is given in Appendix B.

Prediction of seat transmissibility using two degree-of-freedom model (Figure 6)

The transmissibility and phase of the seat response are given by:

$$|T| = \sqrt{\frac{A^2 + B^2}{D^2 + E^2}}$$

$$\theta = a\tan\frac{B}{A} - a\tan\frac{E}{D}$$

where:

$$A = KK_1 - (m_1K + CC_1)\ \omega^2$$

$$B = (C_1K + CK_1)\ \omega - m_1C\omega^3$$

$$D = \left(K - (m + m_1)\ \omega^2\right)K_1 + \left(mm_1\omega^2 - Km_1 - CC_1\right)\ \omega^2$$

$$E = \left(KC_1 + K_1C - (m_1C + mC_1 + m_1C_1)\ \omega^2\right)\ \omega$$

Prediction of seat transmissibility using three degree-of-freedom model (Figure 7)

The seat transmissibility and phase are given by:

$$|T| = \sqrt{\frac{F^2 + G^2}{(H + L)^2 + (M + N)^2}} \qquad (1)$$

$$\theta = \text{a tan}\frac{G}{F} - \text{a tan}\frac{M + N}{H + L} \qquad (2)$$

where:

$$F = KP_1 - CP_2\omega$$

$$G = KP_2 - CP_1\omega$$

$$H = P_1P_5 - P_2C\omega - m_1K_1P_3\omega^2$$

$$L = m_1C_1C_2\omega^4 + \left(m_2K_2P_4\omega^2 - m_2C_1C_2\omega^4\right)$$

$$M = P_2P_5 - CP_1\omega - (m_1C_1P_3 - m_1C_2k_1)\ \omega^3$$

$$N = m_2C_2P_4\omega^3 + m_2K_2C_1\omega^3$$

$$P_1 = m_1m_2\omega^4 + K_1K_2 - (m_1K_2 + m_2K_1 + C_1C_2)\ \omega^2$$

$$P_2 = (C_1K_2 + C_2K_1)\ \omega - (m_1C_2 + m_2C_1)\ \omega^3$$

$$P_3 = K_2 - m_2\omega^2$$

$$P_4 = K_1 - m_1\omega^2$$

$$P_5 = K - m\omega^2$$

Substituting seat parameters (*k and c*) and seated human body model parameters (k_1, c_1 , k_2 , c_2 , *m*, m_1 *and* m_2) into equation 1 and 2 gives seat transmissibility predictions.

11. REPORTING OF RESULTS

The following information shall be given:

a) Name and address of the seat manufacturer;

b) Model of seat, product and serial number;

c) Date of test;

d) Duration of run-in period;

e) Characteristics of the simulated input vibration test;

f) The name of the person responsible for the test;

g) Identification of test laboratory.

h) Calculation of seat stiffness and damping (e.g. using a MATLAB program in Annex A).

i) Prediction of seat transmissibility (e.g. using a MATLAB program in Annex B).

12. REFERENCES

Whitham,E.M., Griffin,M.J. (1977) Measuring vibration on soft seats. Society of Automotive Engineers, SAE Paper 770253, International Automotive Engineering Congress and Exposition, Detroit, 28 February - 4 March.

L. Wei, M.J. Griffin (1998), Mathematical model for the apparent mass of the seated human body exposed to vertical vibration, Journal of Sound and Vibration, 212(5), 855-874.

L. Wei, M.J. Griffin (1998), The prediction of seat transmissibility from measures of seat impedance, Journal of Sound and Vibration, 214(1), 121-137.

Dierckx,C. (1995) *Oxford Science Publications.* Curve and surface fitting with splines.

13 FIGURES

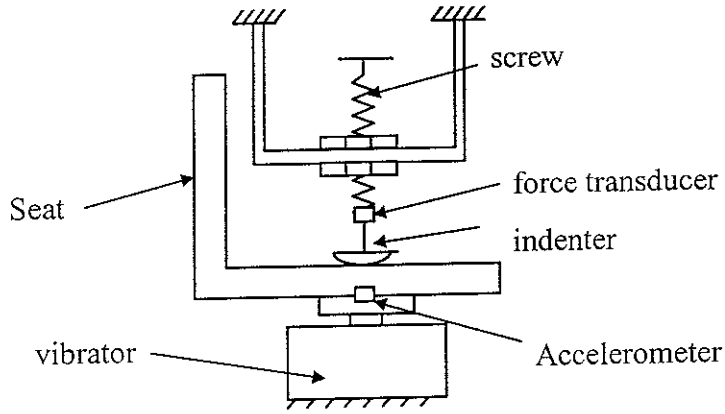

Figure 1 Seat test using indenter rig

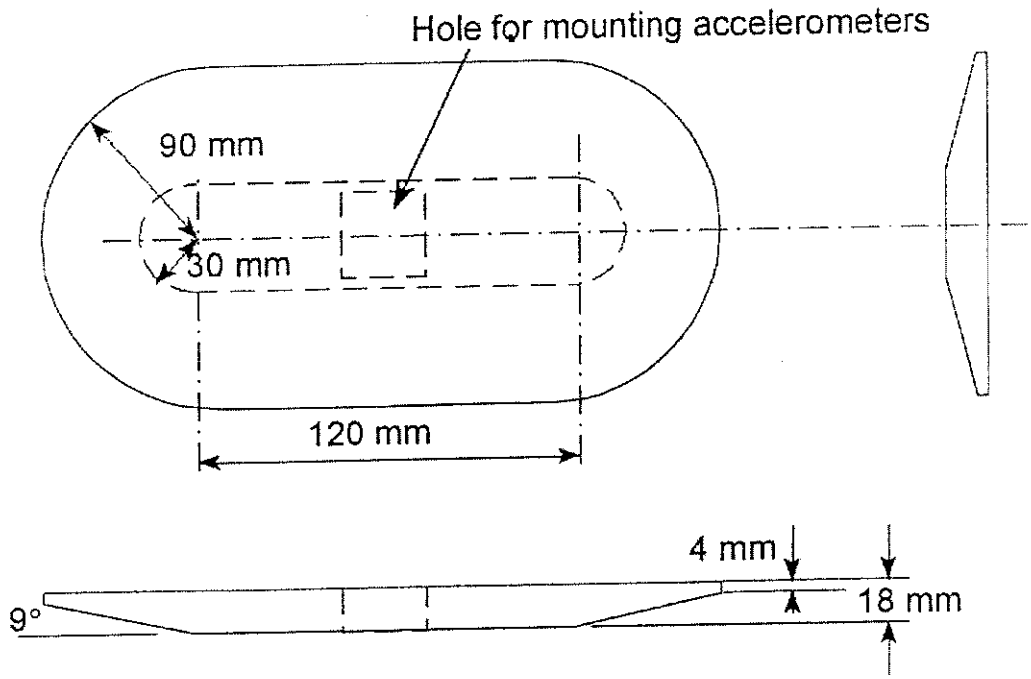

Figure 2 Design of the SIT-BAR (Whitham and Griffin 1977).

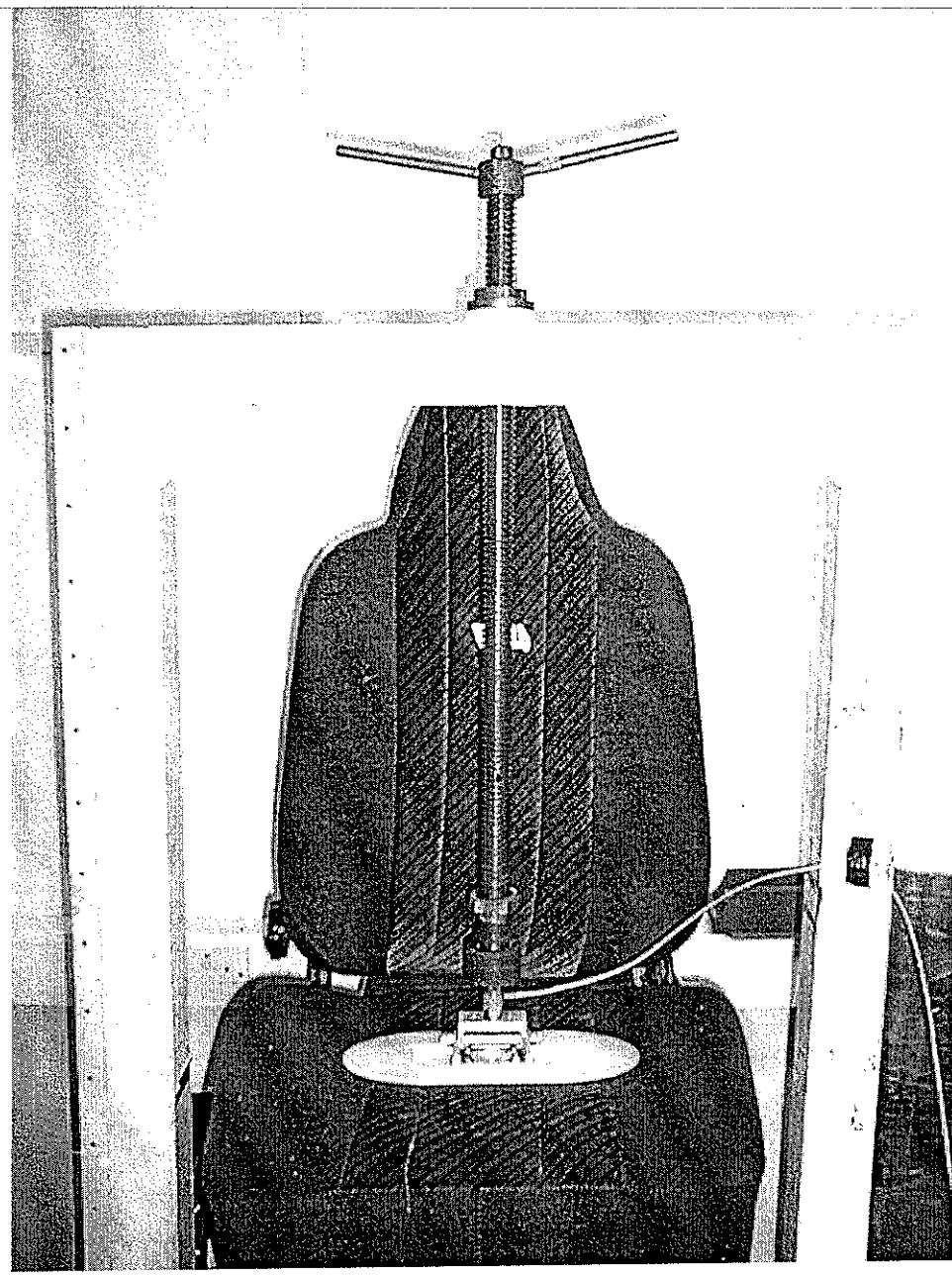

Figure 3 Use of load cell to measure force applied by the indenter (using SIT-BAR as indenter head).

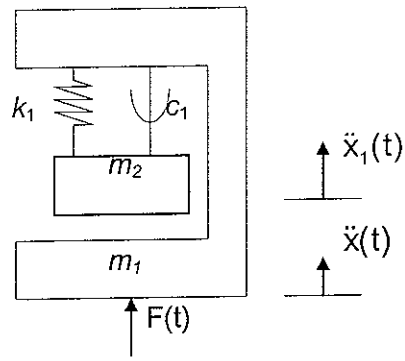

Figure 4 A single degree-of-freedom model with rigid support (model 1b)

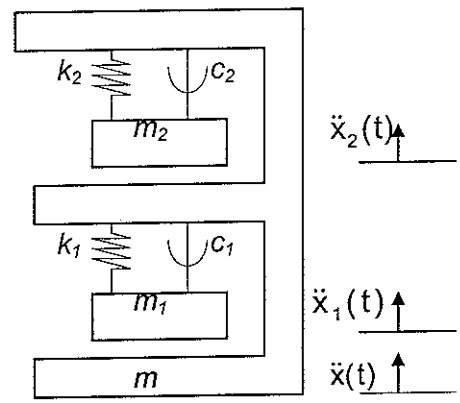

Figure 5 A two degree-of-freedom model with rigid support

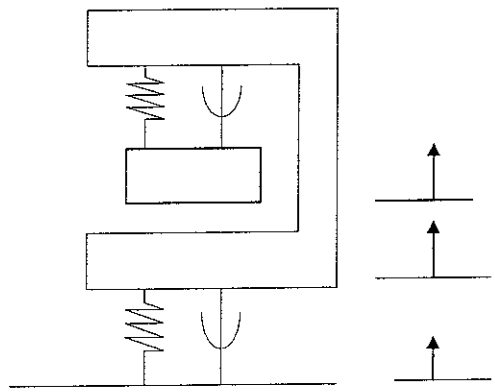

Figure 6 Two degree-of-freedom seat/person system model.

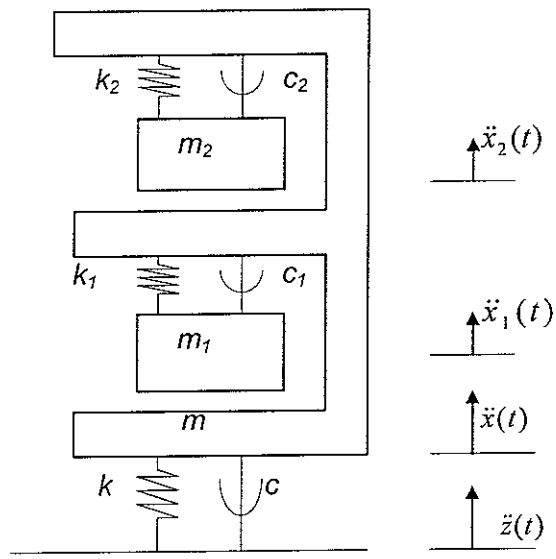

Figure 7. Three degree-of-freedom seat/person system model.

ANNEX A PROGRAMMES TO CALCULATE SEAT STIFFNESS AND DAMPING FROM MEASURED SEAT IMPEDANCE (USING MATLAB)

The purpose of this Section is to calculate seat impedance using recorded experimental data (see Section 8.1, using measured force and displacement) and then calculate seat stiffness, k, and damping, c, using the obtained seat impedance.

(1) *HVLab* routines (calculate seat impedance):

1. Seat dynamic stiffness calculation
2. Seat dynamic stiffness ASCII data output from *HVLab* system.

(2) MATLAB routines (calibrate seat model stiffness, k, and damping, c using obtained seat impedance):

A) Obtain seat stiffness.

Fk.m is a MATLAB program to fit seat stiffness curve and Fk1.m is a subprogram to calculate the least square error. When these programs are used, the only thing needed to do is that change **ascii file name** in the program to real data file name (i.e., the measured ascii data file name).

Fk.m (MATLAB file name to calculate seat stiffness)

```
clc
% Seat stiffness curve fitting
%
%
load ascii file name
% load seat stiffness ascii file


h= ascii file name;
% using h represent seat stiffness ascii file


t=h(2:60,1);
a=h(2:60,2);
b=h(2:60,3);
w=2*pi*t;
y0=a;y=y0;
z0 = [32500];
% z0 - a random estimate value for seat stiffness
```

```
f=fmins('fk1',z0,[0 1.e-4 1.e-4],[],t,y);
k=f(1);

y=k*t./t;

plot(t,y0,'w',t,y,'w*')
title('Road 1')
xlabel('Frequency Hz')
ylabel('Stiffness (N/m)')
k=k
```

fk1.m (MATLAB subprogram file name to calculate the least square error)

```
function  err = fitfun(z, t, y0)
k = z(1);
w=2*pi*t;
y=k*t./t;
N = length(t);
err = sqrt(sum((y - y0).^2)/N);
```

B) Obtain seat damping.

Fc.m is a MATLAB program to fit seat damping curve (imaginary part of measured seat dynamic stiffness) and Fc1.m is a subprogram to calculate the least square error. When these programs are used, the only thing needed to do is that change **ascii file name** in the program to real data file name (i.e., the measured ascii data file name).

.

Fc.m (MATLAB file name to calculate seat damping)*:*

```
clc
% Seat damping curve fitting
%
%
load ascii file name
% load seat stiffness ascii file
```

```
h= ascii file name;
% using h represent seat damping ascii file

t=h(2:90,1);
a=h(2:90,2);
b=h(2:90,3);
w=2*pi*t;
y0=b;y=y0;
z0 = [500];
f=fmins('fc1',z0,[0 1.e-4 1.e-4],[],t,y);
c=f(1);
y=w*c;
plot(t,y0,'w',t,y,'w*')
title('Road 1')
xlabel('Frequency Hz')
ylabel('Damping (Ns/m)')
c
```

fc1.m (MATLAB subprogram file name to calculate the least square error)

```
function  err = fitfun(z, t, y0)
 c = z(1);
w=2*pi*t;
y=w*c;
N = length(t);
err = sqrt(sum((y - y0).^2)/N);
```

ANNEX B PROGRAMMES TO PREDICT SEAT TRANSMISSIBILITY (USING MATLAB)

The purpose of this section is to calculate seat transmissibility using the seat-person model (see Section 10.2.1 as well as Figure 6 and 7). Model parameters of the person are listed in Table 1 (see Section 10.1) and model parameters of seat are obtained in Annex B.

A) Predict seat transmissibility using two degree-of-freedom model (Figure 6) without backrest

```
load Ascii file name
%  Load Ascii file (i.e., measured seat transmissibility)
t= Ascii file name (3:125,1);
e1= Ascii file name (3:125,2);
y0=e1; y=y0;

k=67317;c=172;
% input seat stiffness and damping coming from Annex A

m=6; m1=45.6; k1=44943;  c1=1390;
% input body model parameters (see Table 1)

w=2*pi*t;
h=sqrt((k*k1-(m2*k+c*c1)*w.^2).^2+((k*c1+k1*c-m2*c*w.^2).*w).^2);
i=((k-60*w.^2)*k1+(m1*m2*w.^2-k*m2-c*c1).*w.^2).^2;
j=((k*c1+k1*c-(m1*c1+m2*c+m2*c1)*w.^2).*w).^2;
l=sqrt(i+j);
y=h./l;

plot(t,y0,'o',t,y)
title('Predict seat transmissibility ')
xlabel('Frequency Hz')
ylabel('Transmissibility')
gtext('*  Measured seat transmissibility ')
```

```
gtext('- predict seat transmissibility ')
```

B) Predict seat transmissibility using three degree-of-freedom model (Figure 7) without backrest

```
load Ascii file name
%  Load Ascii file (i.e., measured seat transmissibility)
 t= Ascii file name (3:125,1);
 e1= Ascii file name (3:125,2);

y0=e1; y=y0;

k=67317;c=172;
% input seat stiffness and damping coming from Annex A
m=5.6;m1=36.2;m2=8.9;k1=35007;c1=815;k2=33254;c2=484;
% input body model parameters (see Table 1)

w=2*pi*t;
p1=m1*m2*w.^4-(m1*k2+m2*k1+c1*c2)*w.^2+k1*k2;
p2=(c1*k2+c2*k1)*w-(m1*c2+m2*c1)*w.^3;
p3=k2-m2*w.^2;
p4=k1-m1*w.^2;
p5=k-m*w.^2;
aa=p5.*p1-c*w.*p2-[(m1*k1*w.^2).*p3-m1*c1*c2*w.^4]-[(m2*k2*w.^2).*p4-
m2*c1*c2*w.^4];
bb=(p5.*p2+c*p1.*w)-(m1*c1*p3.*w.^3+m1*c2*k1*w.^3)-
(m2*c2*p4.*w.^3+m2*k2*c1*w.^3);
cc=k*p1-c*w.*p2;
dd=k*p2+c*w.*p1;
h=sqrt(cc.^2+dd.^2);
j=sqrt(aa.^2+bb.^2);

y=h./j;
```

```
plot(t,e1,'w*',t,y,'w-')
title('Predict seat transmissibility ')
xlabel('Frequency Hz')
ylabel('Transmissibility')
gtext('*  Measured seat transmissibility ')
gtext('-  predict seat transmissibility ')
```